Universitat de Girona

DESIGN AND SYNTHESIS OF SHORT ANTIMICROBIAL PEPTIDES FOR PLANT PROTECTION. STUDY OF THEIR MODE OF ACTION

Rafael FERRE MALAGON

Universitat de Girona

PhD Thesis

Design and synthesis of short antimicrobial peptides for plant protection.
Study of their mode of action

Rafael Ferre Malagon

2010

Universitat de Girona

PhD Thesis

Design and synthesis of short antimicrobial peptides for plant protection.
Study of their mode of action

Rafael Ferre Malagon

2010

Programa de Doctorat en Ciències Experimentals i Sostenibilitat

PhD supervisors:

Dra. Marta Planas Grabuleda

Dra. Lidia Feliu Soley

Dr. Eduard Bardají Rodríguez

Memòria presentada per optar al títol de Doctor per la Universitat de Girona

Les doctores Marta Planas Grabuleda, Lidia Feliu Soley i el doctor Eduard Bardají Rodríguez, professors de l'Àrea de Química Òrganica de la Universitat de Girona,

CERTIFIQUEM:

Que aquest treball titulat "Design and synthesis of short antimicrobial peptides for plant proctection. Study of their mode of action", que presenta en Rafael Ferre Malagon per a l'obtenció del títol de Doctor, ha estat realitzat sota la nostra direcció i que compleix els requeriments per poder optar a Menció Europea.

Signatura

Dra. Marta Planas Grabuleda   Dra. Lidia Feliu Soley   Dr. Eduard Bardají Rodríguez

Girona, 7 d'Abril de 2010.

LIST OF PUBLICATIONS

This thesis is based on the following papers:

I.   Ferre, R., E. Badosa, L. Feliu, M. Planas, E. Montesinos, E. Bardají. 2006. Inhibition of plant-pathogenic bacteria by short synthetic cecropin A-melittin hybrid peptides. *Appl. Environ. Microbiol*. 72:3302-3308. (Impact Factor: 3.5)

II. Badosa, E[*]., R. Ferre[*], M. Planas, L. Feliu, E. Besalú, J. Cabrefiga, E. Bardají, E. Montesinos. 2007. A library of linear undecapeptides with bactericidal activity against phytopathogenic bacteria. *Peptides* 28:2276-2285. (Impact Factor: 2.4)

III. Badosa, E., R. Ferre, J. Francés, E. Bardají, L. Feliu, M. Planas, E. Montesinos. 2009. Sporicidal activity of synthetic antifungal undecapeptides and control of Penicillium rot of apples. *Appl. Environ. Microbiol*. 75:5563-5569. (Impact Factor: 3.8)

IV. Ferre, R.[*], M.N. Melo[*], A.D. Correia, L. Feliu, E. Bardají, M. Planas, M. Castanho. 2009. Synergistic effects of the membrane actions of cecropin-melittin antimicrobial hybrid peptide BP100. *Biophys. J*. 96:1815-1827. (Impact Factor: 4.6)

[*]The first and second authors contributed equally to this work

CONTENTS

General abstract

Plant diseases caused by pathogenic microorganisms are one of the major factors limiting worldwide crop production. Their control requires the continued use of pesticides, being mainly based on antibiotics and copper compounds. Although antibiotics are highly efficient in plant disease control, it has been reported the emergence of resistant strains and their use has been banned in some countries, difficulting the plant disease management. Therefore, the search for novel antimicrobial agents has gained importance over the last several years. Antimicrobial peptides (AMPs) are essential compounds of the innate immune system of virtually all organisms and are being considered as a good alternative to conventional antibiotics. Due to their optimal properties, a great deal of scientific effort has been invested in studying their application in human, veterinary and plant disease control.

The present PhD study focused on the development of new sustainable antimicrobial agents derived from the cecropin A-melittin hybrid antimicrobial peptide WKLFKKILKVL-NH$_2$ (Pep3) for use in plant protection. In particular, this work was centered on developing Pep3 analogues active against the economically important plant pathogenic bacteria *Erwinia amylovora*, *Pseudomonas syringae* pv. *syringae*, *Xanthomonas axonopodis* pv. *vesicatoria*, and the phytopathogenic fungi *Fusarium oxysporum*, *Aspergillus niger*, *Rhizopus stolonifer*, and *Penicillium expansum*. Pep3 analogues with high activity against these pathogens while exhibiting low cytotoxicity were obtained through a rational design taking into account some fundamental parameters that have been described to modulate the activity of AMPs, such as the positive charge, the overall hydrophobicity and amphipathicity. The work followed the standard approach in drug discovery which is based on a "hit to lead" stage followed by a "lead optimization" stage. First, we prepared a set of several analogues with the general structure R-X^{1}KLFKKILKX^{10}L-NH$_2$, where X^1 and X^{10} corresponded to amino acids with various degrees of hydrophobicity and hydrophilicity and R included different N-terminal derivatizations. Peptides with improved microbicidal activity and minimized cytotoxicity and sensitivity to protease degradation, compared to Pep3, were identified. Next, we succesfully optimized the best analog using a combinatorial chemistry approach. A 125-member library of synthetic linear undecapeptides was prepared by including 5 variations in each R, X^1 and X^{10} positions. Analogues with the best profile in terms of *in vitro* antimicrobial activity, cytotoxicity and stability to

proteinase K degradation were tested *ex vivo* by evaluating their capacity to prevent infections of *E. amylovora* and *P. expansum* on flowers and fruits, respectively. The peptide KKLFKKILKYL-NH$_2$ (BP100) was highly active to prevent infections of *E. amylovora* in flowers showing efficacies of 63-76% at 100 µM, being only slightly less effective than the antibiotic streptomycin, which is currently used in fire blight control. On the other hand, the peptide Ts-FKLFKKILKVL-NH$_2$ (BP22) was the most effective to prevent *P. expansum* infection in apple fruits, with an average efficacy of 56% disease reduction, being not significantly different than that of a commercial formulation of the reference fungicide imazalil. Therefore, these peptides might be considered as potential agents for use in plant protection either as pesticide ingredients or in some cases expressed in transgenic plants.

Moreover, insights into the mode of action of BP100 were carried out to fully rationalize the biological properties of these peptides and to further improve them. Taking advantage of the intrinsic Tyr fluorescence of BP100, we investigated its binding affinity and damaging effect on phospholipid bilayers modeling the bacterial and mammalian cytoplasmatic membranes using spectroscopic methodologies. Results showed a stronger selectivity of BP100 towards anionic bacterial membrane models as indicated by the high obtained partition constants, being one order of magnitude greater than that for the neutral mammalian membrane models. For the anionic systems, membrane saturation was observed at high peptide/lipid ratios and found to be related with BP100-induced vesicle permeabilization, membrane electroneutrality, and vesicle aggregation. Occurrence of BP100 translocation was unequivocally detected at both high and low peptide/lipid ratios. These findings unravel the relationship among the closely coupled processes of charge neutralization, permeabilization, and translocation in the mechanism of action of antimicrobial peptides. Moreover, it was deduced an equation that correlates the minimum inhibitory concentration (MIC) of an AMP with the partition constant and the threshold concentration in the membrane. This equation provides an easily prediction of *in vivo* antimicrobial activities from simple biophysical parameters.

Resum general

Les malalties de plantes causades per microorganismes són un dels factors limitants més importants en la producció de cultius vegetals. El seu control requereix l'ús continuat de pesticides, els més utilitzats dels quals són els antibiòtics i els compostos de coure. Els antibiòtics són molt efectius per al control de malalties de plantes. Ara bé, s'ha prohibit el seu ús dins la Unió Europea degut a l'aparició de soques microbianes resistents, cosa que dificulta el tractament d'aquestes malalties. Conseqüentment, durant els darrers anys s'ha intensificat la recerca de nous agents antimicrobians. Els pèptids antimicrobians són components essencials del sistema immunològic innat de defensa de pràcticament tots els éssers vius i es consideren com una alternativa als antibiòtics convencionals. Donat que presenten unes excel·lents propietats biològiques, s'ha estudiat de forma exhaustiva la seva potencial aplicació en medicina, agricultura i veterinària.

Aquesta tesi doctoral està basada en el desenvolupament de nous agents antimicrobians derivats del pèptid híbrid cecropina A-melitina WKLFKKILKVL-NH$_2$ (Pep3) que siguin sostenibles i útils per al control de malalties de plantes. Concretament, aquest treball es va centrar en l'obtenció de pèptids anàlegs de Pep3 actius contra les bactèries patògenes *Erwinia amylovora*, *Pseudomonas syringae* pv. *syringae*, i *Xanthomonas axonopodis* pv. *vesicatoria*, i contra els fongs fitopatògens *Fusarium oxysporum*, *Aspergillus niger*, *Rhizopus stolonifer*, i *Penicillium expansum,*responsables de malalties de plantes d'interès econòmic. Aquests pèptids es van dissenyar en base a paràmetres fonamentals que han estat descrits com a moduladors de l'activitat dels pèptids antimicrobians, com són la càrrega catiònica, la hidrofobicitat i l'amfipaticitat. Així, es van obtenir pèptids anàlegs de Pep3 amb una elevada activitat contra els patògens anteriors i que, alhora, presentaven una baixa toxicitat. Per a tal fi es va seguir una metodologia anàloga a la utilitzada per al descobriment de nous fàrmacs basada en una etapa "hit to lead" seguida d'una altra de "lead optimization". En una primera aproximació es van preparar una sèrie d'anàlegs d'estructura general R-X^{1}KLFKKILKX^{10}L-NH$_2$, on X^1 i X^{10} corresponen a aminoàcids amb diferent grau de hidrofobicitat i hidrofilicitat, i R inclou diferents derivatitzacions a l'extrem N-terminal. Es van identificar pèptids que presentaven una major activitat antimicrobiana, una menor citotoxicitat i una major estabilitat proteolítica que Pep3. A continuació, mitjançant química combinatòria, es van optimitzar les propietats

biològiques del millor anàleg obtingut. Es va preparar una quimioteca de 125 undecapèptids lineals per introducció de 5 variacions a cadascuna de les posicions R, X^1 i X^{10}. Per als anàlegs obtinguts amb un millor perfil biològic en quant a activitat antimicrobiana *in vitro*, citotoxicitat i estabilitat a la degradació amb proteïnasa K, es va avaluar la seva capacitat prevenir infeccions causades per *E. amylovora* i *P. expansum* en flors i fruits, respectivament. El pèptid KKLFKKILKYL-NH$_2$ (BP100) va resultar ser molt actiu en la prevenció d'infeccions causades per *E. amylovora* en flors, presentant una eficàcia del 63-76% a una concentració de 100 µM, essent només lleugerament menys efectiu l'estreptomicina, l'antibiòtic actualment usat pel control del foc bacterià. Per altra banda, el pèptid Ts-FKLFKKILKVL-NH$_2$ (BP22) va ser el més efectiu en la prevenció de la infecció causada per *P. expansum* en pomes immadures, mostrant una eficàcia mitjana en la reducció de la malaltia del 56%, similar a la de la formulació comercial de l'antifúngic imazalil. Així doncs, aquests pèptids poden ser considerats potencials agents antimicrobians en la protecció de malalties de plantes bé com ingredients de pesticides o, en alguns casos, expressats en plantes transgèniques.

D'altra banda, amb la intenció de racionalitzar i millorar les propietats biològiques d'aquests pèptids, es va investigar el mecanisme d'acció del pèptid BP100. La fluorescència intrínseca que presenta aquest pèptid pel fet de contenir una Tyr, va permetre investigar la seva afinitat i el seu efecte disruptiu en bicapes fosfolipídiques que modelitzaven membranes citoplasmàtiques bacterianes i de mamífers, mitjançant tècniques espectroscòpiques. Els resultats van mostrar que BP100 presentava una gran selectivitat enfront els models aniònics de membranes bacterianes. De fet, es varen obtenir valors elevats per les constants de partició, essent un ordre de magnitud superior als obtinguts pels models neutres de membrana. Per als models aniònics, també es va observar la saturació de la membrana a proporcions elevades de pèptid/lípid. Aquest fenòmen es va relacionar amb la capacitat de BP100 a induir la permeabilització, la neutralització i l'agregació de les vesícules lipídiques. També es va detectar de forma inequívoca la translocació d'aquest pèptid tant a proporcions de pèptid/lípid elevades com baixes. Aquestes observacions indiquen que en el mecanisme d'acció dels pèptids antimicrobians els processos de neutralització, permeabilització i translocació de membrana estan molt relacionats, i que provablement són sinèrgics. També es va deduir una equació que relaciona la concentració mínima inhibitòria d'un pèptid antimicrobià amb la seva constant de partició i la seva concentració llindar en la membrana. Aquesta

equació facilita la predicció d'activitats antimicrobianes *in vivo* per mitjà de paràmetres biofísics simples.

Chapter I. General introduction

I.1 Plant diseases

Plant diseases caused by phytophatogens are currently one of the major factors limiting worldwide crop production and are mainly induced by environmental factors or by infection with pathogenic organisms, such as bacteria, fungi, viruses, protozoa and nematodes (Agrios 2005). These diseases result in considerable economic losses, aggravating the large-scale starvation estimated in more than 1000 million people with inadequate fed (FAO 2009, Strange 2005). The latter, is still more exacerbated due to the dramatic growth of human population. It is also worth mentioning that in the recent last centuries, phytopathogens have been responsible for important plant epidemics affecting the course of human history and causing, in some occasions, people wave immigration and millions of deaths (Campbell 1990). Despite nowadays plant epidemics are, in general, more stabilized due to the existence of several plant protection strategies, some plant diseases are still far from being completely under control. Although a great amount of research has been undertaken to overcome the damage caused by plant pathogens, a major difficulty encountered is the lack of effective control methods against some severe diseases (Montesinos 2000).

The framework of this thesis is the development of a sustainable and effective strategy to control plant diseases for which no effective methods are available. In particular, this PhD thesis has been mainly focused on the economically important plant pathogenic bacteria *Erwinia amylovora*, *Pseudomonas syringae* pv. *syringae*, and *Xanthomonas axonopodis* pv. *vesicatoria*, and on the fungi *Fusarium oxysporum*, *Aspergillus niger*, *Rhizopus stolonifer*, and *Penicillium expansum*.

Erwinia amylovora is a Gram negative necrogenic bacterium which is the causal agent of fire blight, a devastating bacterial disease that affects several plant species, mainly members of the rosaceous family, e.g. fruit trees such as pear and apple, and ornamental plants (Van der Zwet and Keil 1979, Vanneste 2000, Cabrefiga and Montesinos 2005). Apparently, this disease is believed to be originated in North America, where it was first detected in New York in 1780 (Denning W. 1974), from where it spread around the world affecting about 43 countries (Van der Zwet 2002). The term fire blight describes the appearance of the disease symptoms, since the pathogen blackens, shrinks and cracks the infected leaves, flowers or shoots and even the whole tree, as though burned by fire (Figure I.1).

Figure I.1 Fire blight symptoms in an infected growing pear shoot.
(Photo: Dr. Montesinos)

Pseudomonas syringae pv. *syringae* is a Gram negative bacterium that infects a wide range of deciduous fruit trees, such as pear, cherry, peach and plumb as well as other woody plant species (Agrios 2005). On pear trees, it causes a bacterial blast, disease that limits pear production throughout the world (Moragrega 2003). Symptoms are characterized by the blast of shoots, blossoms, leaves or fruits, which takes place during bloom and post-bloom stages in cool wet weather seasons (Figure I.2).

Figure I.2 Bacterial canker symptoms in an infected growing pear shoot.
(Photo: Dr. Montesinos)

Xanthomonas axonopodis pv. *vesicatoria* is a Gram negative bacterium which is the causal agent of the bacterial spot in tomato and pepper plants (Leyns 1984). This bacterium enters the plant leaves through the stomata, and the fruits through small wounds. On leaves, it produces the so-called water-soaked lesions that later become necrotic (Figure I.3). The disease results in defoliation and in harsh spotted or scalded fruits, causing great yield losses. Bacterial spot disease occurs worldwide, being specially harmful for crops cultivated in warm and damp regions.

Figure I.3 Bacterial spot symptoms in infected pepper leaves.
(Photo: Dr. Montesinos)

Fusarium oxysporum is the responsible of root rot or wilt disease in more than a hundred of different plant species, such as vegetables and ornamental plants (Agrios 2005). This fungus is distributed worldwide, although different special forms often have various degrees of distribution. This fungus persists for a long time in affected fields because it can survive in soils in a dormant form even in the absence of a suitable host plant.

Aspergillus niger is the causal agent of a disease called black mold on various fruits and vegetables, such as onions, tomatoes and grapes, before the harvest and during the postharvest (Agrios 2005). *Aspergillus* is ubiquitous in soils and indoors environments where is a common food contaminant.

Rhizopus stolonifer causes soft rot disease in numerous stone fruits and vegetables, such as sweet potatoes, peaches and cherries, and is also the causal agent of the well known black bread mold. *Rhizopus* soft rot is a worldwide distributed postharvest disease which affects severely during storage, transit and marketing of stone fruits and vegetables limiting their economic value (Bonaterra 2003, Agrios 2005).

Penicillium expansum causes blue mould which is a worldwide important postharvest disease of stone and pome fruits. Apart from substantial economic losses, *P. expansum* has also potential public health significance, due to the production of mycotoxins, such as patulin (Weidenbörner 2001, Sanzani 2009).

I.2 Plant disease management

Plant disease management consists on the application of different strategies to cure (curative strategies) or prevent (preventive strategies) the damage occasioned or that can be occasioned onto plants. These strategies take into account three main important factors (the *disease triangle*) essential for disease development: (1) the presence of the pathogen, (2) the type of host plant, and (3) the environmental conditions. Preventive strategies include avoidance, exclusion, protection and resistance, while curative strategies are essentially based on therapy (eradication).

The use of chemical compounds toxic to the pathogens plays a crucial role in plant protection and therapy, and has been used for centuries in plant disease control. Several hundreds of chemicals have been designed to combat plant diseases by killing or inhibiting the growth of the invading pathogens and may be applied to soil, seed, foliage, flowers or fruits (McManus 2002, Agrios 2005). According to the target pathogen, these chemicals can be termed as bactericides, fungicides, virocides, protocides and nematocides. Only some of them display a therapeutic activity and the vast majority is only effective to protect plants prior to infections and can not cure a disease after it has started (Agrios 2005). Some of the most used chemicals in plant protection comprise copper and sulfur compounds, quinones, and other benzene derivatives as well as heterocyclic compounds and the antibiotics streptomycin, tetracyclines, cycloheximide and griseofulvin. Some of them are toxic for a broad range of pathogens, while others are more specific.

During the last decades, large amounts of chemicals have been used to maintain high crop yields. However, the use of these pesticides has negative effects due to their accumulation in soils and water, affecting the environment and consumer's health (Margni 2002, Karabelas 2009). Moreover, it has been reported that these compounds evoke resistance in some plant-pathogens (Loper 1991, Sundin 1993). Consequently, several countries have undertaken regulatory actions and several pesticides have been banned, which is difficulting plant disease management due to the lack of effective sustainable compounds. Therefore, plant protection has been progressively reoriented to a rational use of pesticides and to the search of new compounds that do not induce phytopathogen resistance and that exhibit low negative effects against the host organism, the environment and public health.

6

I.3 Antimicrobial peptides: emerging candidates for plant protection

Antimicrobial peptides (AMPs) have been found in virtually all forms of life ranging from bacteria to plants, invertebrates and vertebrates, including mammals (Broekaert 1997, Ganz and Lehrer 1998, García Olmedo 1998, Otvos 2000, Zasloff 2002, Brodgen 2003, Bulet 2004). They are an evolutionarily conserved component of the innate immune response, being the main defense system for the majority of species. Several hundreds of natural AMPs have been isolated (see a comprehensive list at http://www.bbcm.univ.trieste.it/~tossi/pag1.htm and http://aps.unmc.edu/AP/main.php) and several thousands have been *de novo* designed and synthetically produced. They display a wide range of biological activities against bacteria, fungi, protozoa, enveloped viruses and even tumour cells (Hancock 2001, Boman 2003, Hancock and Sahl 2006, Jenssen 2006, Zhang and Falla 2006, Montesinos 2007, Zaiou 2007, Hoskin and Ramamoorthy 2008). Moreover, AMPs posses additional immunomodulatory activities essential for the orchestration of the innate immune and inflammatory responses (Hancock 2001, Auvynet and Rosenstein 2009, Lai and Gallo 2009). However, as their name indicates, the most studied feature of AMPs has been their potential antibiotic activity against microbes. During the last decades, AMPs have been widely studied as an alternative to conventional antibiotics, especially for the treatment of drug-resistant infections (Hancock and Patrzykat 2002, Hancock and Sahl 2006, Peschel and Sahl 2006).

I.3.1 Sources of AMPs

Antimicrobial peptides are widely distributed in nature and they have been found in every organism in which that they have been looked for. The main sources of AMPs are categorized below and include microorganisms, plants, invertebrates and vertebrates.

I.3.1.1 AMPs in microorganisms

Since A. Fleming discovery of the potent antibiotic activity of the peptide derivative penicillin produced by the fungus *Penicillium notatum* (Fleming 1929), microorganisms have attracted special attention as a potential source of bioactive compounds. Microorganisms produce a wide range of AMPs that include small bacteriocins and fungal defensins synthesized through ribosomal pathways, and

peptaibols, cyclopeptides and pseudopeptides that are secondary metabolites produced by non-ribosomal synthesis (Ng 2004, Cooter 2005, Montesinos 2007).

Bacteriocins, were among the first AMPs to be isolated and characterized (Mattick and Hirsch 1947). They are produced by bacteria and play an important role in the survival of individual bacterial cells by killing other bacteria that compete for nutrients in the same environment. Bacteriocins constitute a structurally diverse group of peptides, which has been recently divided into two main groups: lanthionine containing (lantibiotics) and non-lanthionine containing peptides, which differ in the presence or the absence of the unusual amino acid lanthionine (Cooter 2005). Nisin, produced by *Lactococcus lactis*, represents the most known and studied lantibiotic and has been used for nearly 50 years as a food preservative without significant development of resistance. Another lantibiotic that should be mentioned is mersacidin, a tetracyclic peptide produced by *Bacillus* spp, which displays similar bactericidal activity than vancomycin towards methicillin-resistant *Staphylococcus aureus*, but without developing microbial resistance (Kruszewska 2004).

I.3.1.2 AMPs in plants

It is widely believed that AMPs play an important and fundamental role in the innate immunity of plants, being part of both permanent and inducible defense barriers (Garcia-Olmedo 1998). According to their defensive role, AMPs have been found in plant sites that are exposed to invading pathogens, such as leaves, flowers, seeds, and tubers. Eight different families of AMPs have been identified in plants, and all of them share a β-sheet globular structure stabilized by 2 to 6 disulfide bridges. Among them, the two major and most studied families are thionins and defensins. Mature thionins are generally 45-47 amino acids in length and can be classified into at least five types (I-V). Thionins are active against bacteria and fungi *in vitro* and transgenic overexpression of their corresponding genes in plants confer protection against plant pathogen challenges (Epple 1997). Plant defensins are generally 45-54 amino acids in length and, based on their sequence, they can be categorized into four different groups or subfamilies (Garcia-Olmedo 1998). Plant defensins display antibacterial and antifungal activities.

I.3.1.3 AMPs in invertebrates

AMPs are also an essential component of the innate immunity of invertebrates (Hancock 2006). Since they lack the adaptive immune system present in vertebrates, their conserved innate immune mechanism (also recognized as an ancient mechanism) represents one of the most extremely effective among the living organisms (Iwanaga and Lee 2005, Hancock 2006). AMPs in invertebrates came into focus in the early eighties when H. Boman and co-workers isolated and purified the insect cecropins (Steiner 1981). Since then, a great number of AMPs hasve been identified in the phagocytic cells of the hemolymph and also in certain epithelial cells of invertebrates (Bulet 1999 and 2004, Otvos Jr 2000, Tincu and Taylor 2004). They can be expressed constitutively or induced as a response to a microbial infection (Iwanaga and Lee 2005). Intense studies in their regulation and expression using the arthropod fruit fly *Drosophila melanogaster* as a model system, led to the successful discovery of pathogen recognition receptors (Toll-like receptors) (Iwanaga and Lee 2005).

Invertebrate AMPs display a broad range of biological activities against invading pathogens (Bulet 1999 and 2004, Tincu and Taylor 2004). The most abundant AMPs group in invertebrates are defensins. They are open-ended cyclic peptides with three to four disulfide bridges and were first isolated from the flesh fly *Sarcophaga peregrina* (Matsuyama and Natori 1988). Moreover, among the AMPs from invertebrates, we also find some of the best studied AMPs, such as the α-helical cecropins, isolated from the hemolymph of the giant silk moth *Hyalophora cecropia*, and melittin, found in the venom of the honey bee *Apis mellifera* (Sato and Feix 2006). It is also worth mentioning that the β-hairpin like peptides tachyplesin and polyphemusin isolated from horseshoe crab hemocytes possess some of the most potent antibacterial and antifungal activities observed (MICs of <2 μg/ml) (Jenssen 2006).

I.3.1.4 AMPs in vertebrates

A large number and variety of AMPs has been isolated from a wide range of vertebrate species, including fish, amphibians and mammals, indicating that, even in the presence of an adaptive immune response, these peptides play an important role in host defense (Jenssen 2006). They have been found in sites that routinely encounter pathogens, such as in mucosal surfaces and skin, within the granules of immune cells or in the crypts of the small intestine.

An impressive number of AMPs (~500) has been isolated from the granular glands of the skin and from the stomach mucosa of various anurans (frogs and toads), which represents a large proportion of the total number of reported AMPs (Bulet 2004). The standard bearer of this group are the α-helical magainins, isolated from the skin secretions of *Xenopus laevi*, and are the typical prototypic amphibian AMPs (Zasloff 1987). Apart from magainins, numerous α-helical AMPs from other amphibians have been reported, such as bombinins, dermaseptins or temporins.

Two other large and diverse group of AMPs from vertebrates include cathelecidins and defensins. Cathelecidins are characterized by a particular well-conserved N-terminal segment (the cathelin domain) of nearly 100 amino acid residues. They have been isolated from many mammalian species, such as pigs, sheeps, horses, rabbits, cattle, mice and even humans. Human and mice produce only one cathelecidin, called hCAT-18/LL-37 and CRAMP, respectively (Bulet 2004). Vertebrate defensins are a family of cyclic AMPs which are classified into three subfamilies: α-defensins, β-defensins, and θ-defensins. The α- and β-defensins are widely distributed in vertebrate species, whereas θ-defensins have been only identified in the neutrophils and monocytes of the Old World monkeys (Jenssen 2006).

I.3.2 Diversity of AMPs

The diversity of AMPs is enormous and arises from their antimicrobial function as well as the different pathogenic microbe challenges that they face in each host organism (Hancock and Sahl 2006). Despite this diversity, AMPs share some common features: (i) they are relatively short (less than 100 amino acids); (ii) have a positive net charge of +2 to +9 due to the presence of Arg, Lys and/or His residues; and (iii) have the ability to assume an amphipathic structure with differentiated hydrophobic and hydrophilic domains. Due to their common net positive charge, they are also referred to as cationic antimicrobial peptides.

The diversity of AMPs difficults their classification. AMPs can be categorized according to their biosynthetic pathway into non-ribosomally or ribosomally synthesized. Moreover, AMPs have been classified according to their source, secondary structural elements, or predominant amino acid residues. One of the most accepted

classifications is based on their secondary structure (Epand and Vogel 1999, van't Hof 2001), being categorized into the four following groups (Figure I.4 and Table I.1).
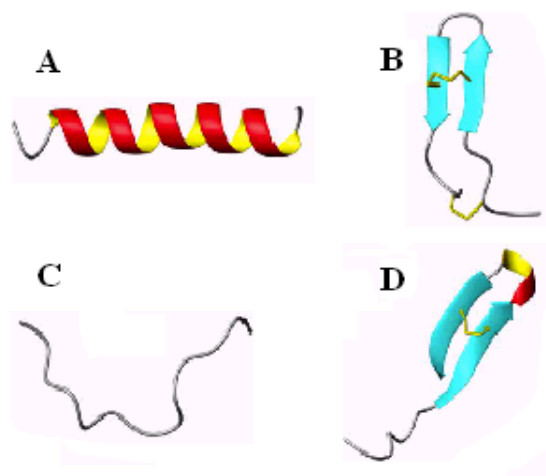
Figure I.4 Structural classes of AMPs. (A) α-helical magainin; (B) β-sheeted polyphemusin; (C) extended indolicidin; (D) looped thanatin. (Adapted from Jenssen 2006).

- *Group I: Linear peptides with an α-helical structure*

This group is mainly composed of linear AMPs such as cecropin A, magainin, LL-37, temporins and of several *de novo* designed peptides. These AMPs tend to be disordered and highly flexible in aqueous solution, whereas all or parts of the peptide fold into an α-helical amphiphatic conformation upon interaction with membranes and membrane-mimicking environments.

- *Group II: β-Sheet structures predominantly stabilized by disulfide bridges*

In contrast to α-helical peptides, β-sheet peptides are conformationally more restrained due to their cyclic structure formed by either disulfide bridges (e.g. tachyplesins, protegrins and defensins, such as HBD-1) or by peptide backbone cyclization (e.g. polymyxin B and gramicidin S). In aqueous solution, they usually adopt a β-sheet conformation which is stabilized upon contact with lipid surfaces.

- *Group III: Linear peptides with an extended structure with predominance of one or more amino acids*

This third group is composed of conformationally extended peptides rich in one or more specific amino acids such as Gly, Trp, Arg and/or His. Similarly to α-helical peptides, they usually are highly flexible in aqueous solution while adopting an amphiphatic structure upon interaction with membranes and membrane-mimicking environments. Indolicidin and bactenecin-5, rich in tryptophan and proline/arginine residues, respectively, belong to this group.

- *Group IV: Peptides with looped structures*

The last group is made up of peptides with a looped structure, such as lantibiotics and peptides with only one sulfide bridge. Lantibiotics are cyclic peptides formed by thioether bridges due to posttranslational dehydratation of the side chains of Ser or Thr residues followed by reaction with cysteine resulting in the formation of the unusual amino acids lanthionine and methyllanthionine, respectively. Nisin and mersacidin constitute the most prominent lantibiotic peptides. Besides, other representative looped peptides are those formed by one disulfide bridge such as thanatin, lactoferricin B and bactenecin-1.

Table I.1 Selected examples of natural antimicrobial peptides categorized according to their secondary structure.

Group	Peptide	Peptide sequence[a]	Source
I α-Helical structure	Cecropin A	KWKLFKKIEKVGQNIRDGIKAGPAVAVVGQATQIAK-NH$_2$	Silk moth
	Magainin	GIGKFLHSAKKFGKAFVGEIMNS	Frog
	LL-37	LLGDFFRKSKEKIGKEFKRIVQRIKDFLRNLVPRTES	Human
	Temporin L	FVQWFSKFLGRIL	Frog
II β-Sheet structure	Tachyplesin I	KWC$_1$FRVC$_2$YRGIC$_2$YRRC$_1$R-NH$_2$	Horseshoe crab
	Protegrin I	RGGRLC$_1$YC$_2$RRRFC$_1$VC$_2$VGR-NH$_2$	Pig
	HBD-1	DHYNC$_1$VSSGGQC$_2$LYSAC$_3$PIFTKIQGTC$_2$YRGKAKC$_1$C$_3$K	Human
III Extended structure	Indolicidin	ILPWKWPWWPWRR-NH$_2$	Bovine
	Bactenecin-5	RFRPPIRRPPIRPPFYPPFRPPIRPPIFPPIRPPFRPPLGPFP	Bovine
IV Looped structure	Lactoferricin B	FKC$_1$RRWQWRMKKLGAPSITC$_1$VRRAF	Bos taurus
	Thanatin	GSKKPVPIIYC$_1$NRRTGKC$_1$QRM	Insect
	Bactenecin-1	RLC$_1$RIVVIRVC$_1$R	Bovine

[a] Subscript numbers represent amino acids joined by disulfide bridges.

I.3.3 Mode of action of AMPs

The biological activity of AMPs has been largely associated with their interaction with membranes. For many of them, is widely believed that the cytoplasmatic membrane disruption is their primary antimicrobial mechanism (Zasloff 2002, Huang 2006). However, there are some evidences that AMPs can inhibit several cellular processes such as nucleic acid and protein synthesis, enzymatic activity, and cell wall synthesis (Yeaman and Yount 2003, Brodgen 2005, Hancock and Sahl 2006, Jenssen 2006, Nicolas 2009). In fact, AMPs that interfere intracellular processes must traverse the cytoplasmatic cell membrane to reach their site of action, which stresses the relevance of peptide-membrane interaction for AMP activity. Among the investigations on the mechanism of action of AMPs with microbes, the vast majority of studies have been centred on bacteria.

The aforementioned common structural features of AMPs are essential for their mode of action. The overall positive charge ensures their electrostatic interactions and accumulation on the polyanionic microbial cell surfaces, while their ability to fold into amphiphatic structures enables their integration into the hydrophobic core of membranes (Tossi 2000, Hancock 2001, Shai 2002, Boman 2003, Yeaman and Yount 2003, Bechinger 2004, Brodgen 2005, Jenssen 2006, Zhang and Falla 2006). Before reaching the cytoplasmatic bacterial membranes, AMPs must traverse the bacterial envelope which is plentiful of negatively charged components such as lipopolisaccharide (LPS) in Gram negative bacteria and wall-associated teichoic acids in Gram positive bacteria. LPS is the main component of the outer leaflet of the outer membrane of Gram negative bacteria and is normally stabilized by divalent cations like Ca^{2+} and Mg^{+}. Cationic peptides posses a higher affinity to LPS than the native divalent cations, and displace them causing a local disturbance in the outer bacterial membrane. This fact facilitates peptides to traverse the outer membrane in a process termed self-promoted uptake (Hancock 2001). Consequently, AMPs reach the cytoplasmatic microbial membranes where they exert their disruptive effect.

Despite the exact mechanism of action has not been clearly unrevealed, several membrane interaction and disruption models have been proposed for AMPs that depend on membrane interference for their antimicrobial activity. The most prominent modes of action are the barrel-stave, the carpet, the toroidal pore, and the disordered toroidal pore

mechanisms (Pouny 1992, Ludtke 1996, Yang 2001, Shai 2002, Brodgen 2005, Huang 2006, Leontiadou 2006). These models account for the morphological changes involved in AMPs-mediated membrane disruption, such as pore formation, cell lysis or peptide translocation to the cytoplasm (Figure I.5). In general, all these models propose that AMPs first interact with the negatively charged lipid-head groups of the microbial cytoplasmatic membrane, they accumulate facing parallel to the lipid bilayer until a critical threshold concentration is reached, after which they self-organize to form a permeation pathway. A description of these models is summarized below.

Barrel-stave model: This mechanism is believed to account for the formation of stable pores by a defined number of peptide molecules (Figure I.5a). Peptides reach the membrane either as monomers or aggregates and binds to its surface. Then, they insert perpendicularly into the lipid core of the membrane recruiting additional monomers and spanning it to form a channel of consistent size. The amphiphylic AMPs which constitute the pore have a well-ordered structure with the hydrophobic patches facing the lipid tails and the hydrophilic patches lining the pore. This model predicts that membrane permeation occurs at low peptide:lipid (P:L) ratios. The cyclic peptide gramicidin S has been proposed to follow this model (Yang 2001, Zhang 2001).

Carpet mechanism: This model foretells the desintegration of the membrane in a detergent-like manner (Figure I.5b). Peptides accumulate lining up parallel on the surface of the membrane in a carpet-like fashion, changing the fluidity and reducing the membrane barrier properties. At a given threshold peptide concentration, the membrane integrity is lost, leading to micellation. This mechanism predicts a high peptide membrane coverage. Dermaseptin S, cecropin, melittin, and ovisporin have been proposed to follow this mechanism (Brodgen 2005, Jenssen 2006).

Toroidal pore model: This model predicts that AMPs form transient and short lived structured pores (Figure I.5c). Initially, peptides lie parallel to the interface of the outer leaflet of the membrane with their polar regions interacting with the lipid-head groups, while their hydrophobic parts are inserted into the membrane (snorkel effect). This interaction causes mechanical stress to the lipid bilayer which becomes thinner with a local lipid tail disorder. Once a threshold peptide concentration is reached, AMPs change their orientation from parallel to perpendicular, forming a cylindrical hydrophilic pore. In toroidal pores, the lipids are curved inwards towards the pore in a

continuous fashion from the surface of the membrane. The lifetime of these transient pores is believed to vary. They open and reseal, and peptides end up in both leaflets of the bilayer. This model accounts for the phospholipid flip-flop and the translocation of the peptide into the cytoplasm, which are not considered in the barrel-stave and the carpet mechanisms. Examples of AMPs that are proposed to exert this mechanism include melittin, magainin, and LL-37 (Brodgen 2005, Jenssen 2006).

Disordered toroidal pore model: This mechanism is a recent modification of the toroidal pore model, and accounts for the formation of transient pores in which peptides adopt a less-rigid conformation and orientation (Figure I.5d). This model, predicted from molecular dynamic simulations, has been proposed for magainin and melittin (Leontiadou 2006, Sengupta 2008), and differs from the classical toroidal pore in the shape of the pore and in the conformation of the peptides that constitute it. While the toroidal model proposes a cylindrical pore with a defined number of helical peptides oriented perpendicular to the plane of the membrane, the disordered toroidal pore possesses a chaotic lumen shape mostly formed by the lipid head-groups and a diffuse distribution of peptides adopting a less-defined conformation. An extrapolation of this model has been proposed for melittin which is called "Droste mechanism". This occours if a high amount of disordered toroidal pores are closely formed leading to the dissolution or micellation of the membrane (Sengupta 2008).
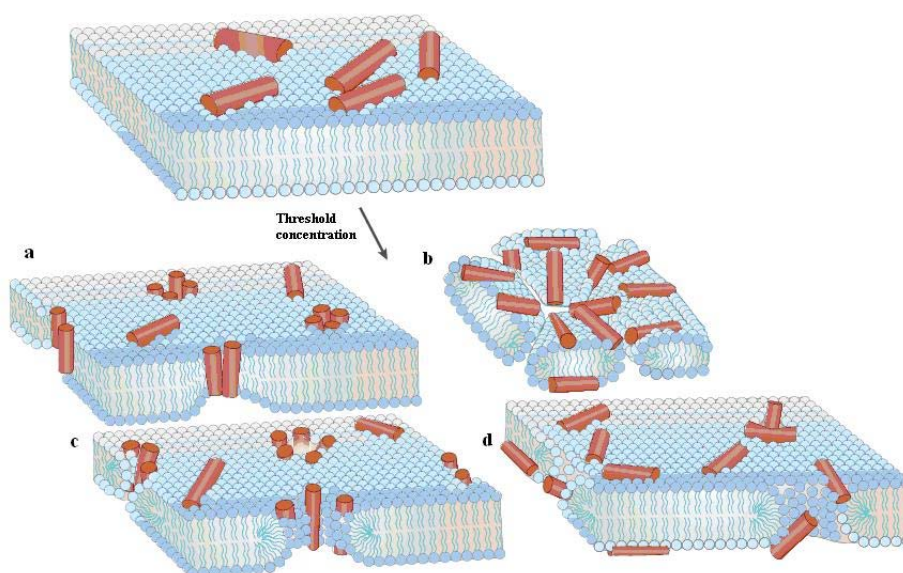
Figure I.5 Mechanisms of AMP-mediated membrane disruption: (**a**) barrel-stave model, (**b**) carpet mechanism, (**c**) toroidal pore model, and (**d**) disordered toroidal pore model. (Taken from Melo 2009)

I.3.4 Peptide-membrane interaction studies

Peptide-membrane interaction studies at the molecular level have been essential for the elucidation of the above mentioned mode of action. Moreover, this knowledge can also help to rationalize the macroscopic properties displayed by AMPs and can contribute to the rational design and development of novel and advanced antibiotics (Melo 2009). Despite the existence of some *in vivo* approaches using intact cells, up to now, most of the knowledge about peptide-lipid interactions emanates from *in vitro* approaches using biophysical studies with model membrane systems (Hancock and Rozek 2002).

I.3.4.1 Model membranes

Biological cytoplasmatic cell membranes are complex structures consisting primarily of a phospholipid bilayer containing functional proteins and other components, such as carbohydrates, interspersed throughout. This complexity difficults the study of peptide-membrane interactions hampering the interpretation of the results due to the multiple variables. Thus, the use of well-defined membrane models has facilitated this study. Evidently, results obtained from membrane model systems are subjected to errors because these models lack biological membrane features such as lipid hetereogeneity, the presence of membrane proteins and polysaccharides, the membrane potential or the efflux pumps (Hancock and Rozek 2002). Morevover, the disruptive effect observed for a given AMP highly depends on the characteristics of the selected model membrane and the experimental conditions.

Among the various membrane-mimicking models, liposomes with different size ($\varnothing$ from < 50 nm to several μm) and with diverse phospholipid compositions represent one of the most succesful approximations. Liposomes are spherical lipid vesicles that can be unilamellar or multilamellar, enclosing a defined volume of aqueous solution inside them (Bangham 1965). They can be constituted either of mixtures of natural lipids or of commercially available synthetic lipids, and can be easily prepared as depicted in Figure I.6. The most representative and used vesicles are multilamellar (MLVs), large unilamellar (LUVs) and small unilamellar (SUVs). Liposome features that have to be taken into account for their use as model membranes include lipid composition, presence of sterols and the addition of membrane probes, which can affect

their stability, charge, curvature, membrane phase and raft formation (Santos and Castanho 2002a).
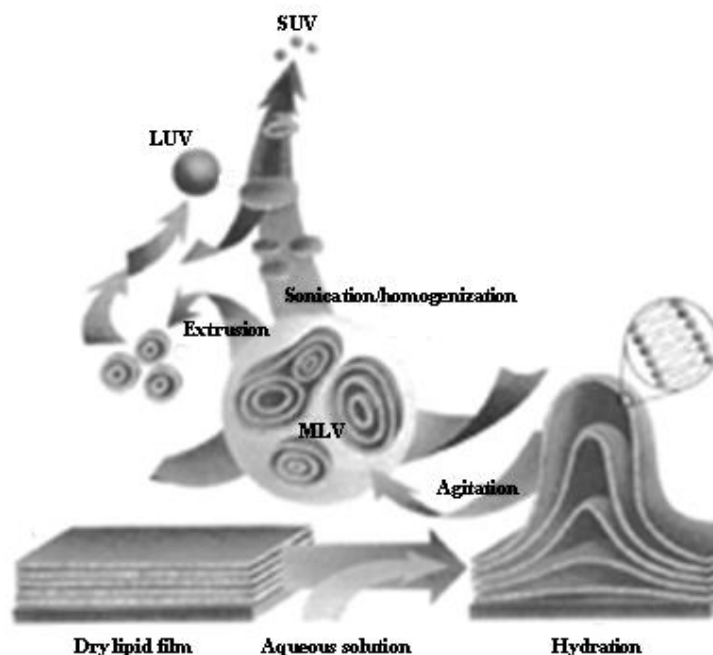
Figure I.6 Schematic representation of the preparation of MLVs, LUVs and SUVs. (Adapted from www.avantilipids.com).

I.3.4.2 Biophysical studies of peptide-membrane interactions

In order to assess the effect of AMPs on membranes, numerous biophysical studies have been carried out to unravel the bases of the peptide-lipid interactions at the molecular level. A large number of experimental techniques has been utilized to gain knowledge of the membrane structure, the peptide conformation and the peptide location upon partitioning with the membrane, as well as of the membrane disruption effect of AMPs. Among them, spectroscopic techniques such as X-ray, nuclear magnetic ressonance (NMR), electron paramagnetic ressonance (EPR), circular dichroism (CD), Fourier transform infrared (FTIR) and fluorescence spectroscopy have been widely used (Epand and Vogel 1999, Bechinger 2004, Brogden 2005).

A key parameter to assess the extent of the peptide-membrane interactions is the Nernst partition constant (K_P), defined as the ratio between the equilibrium membrane-bound and aqueous phase peptide concentrations (Equation. I.1, where L: lipidic phase and W: aqueous phase).

$$K_P = \frac{[Peptide]_L}{[Peptide]_W} \quad \textbf{Equation I.1}$$

Santos et al. have described a partition model to calculate the K_p based on fluorescence spectroscopy. This technique allows the study of the membrane interaction of peptides incorporating intrinsically fluorescent amino acids, such as Trp, Phe or Tyr, avoiding the derivatization with fluorophores. Santos partition model takes advantage of the increase of the fluorescence quantum yield of Trp or Tyr when moving from polar (aqueous phase) to less polar environments (hydrophobic membrane phase). Accordingly, Kp is calculated from fluorescence intensity versus phospholipid concentration plots at a constant peptide concentration.

Fluorescence spectroscopy has also been applied to gain some insight into the in depth membrane localization of peptides by quenching the Trp fluorescence with nitroxide-labelled phospholipids quenchers, such as 5-NS or 16-NS (5- and 16-doxylstearic acids, respectively) (Melo and Castanho 2007).

Other fluorescence experiments using model membranes containing fluorescence probes have allowed the study of functional peptide abilities, such as membrane translocation, membrane pore formation, membrane lysis, phospholipid segregation, and phospholipid flip-flop, which could be closely related with the peptide mode of action (Hancock and Rozek 2002, Henriques and Castanho 2004, Henriques 2007).

I.3.5 Molecular basis of AMP cell selectivity

One of the most interesting properties of AMPs is their cell selectivity for prokaryotic membranes over mammalian and plant membranes. Despite the difficulties encountered to define the precise mechanism of action of AMPs, the main factors that steer this selectivity have been identified and attributed to both peptide and membrane characteristics (Figure I.7) (Yeaman and Yount 2003, Brodgen 2005, Matsuzaki 2009, Melo 2009).

Regarding the peptide structure, two factors have been reported to play an important role in cell selectivity: the net cationic charge and the presence of hydrophobic amino acids. The former leads to a strong interaction with the anionic charged phospholipids present in bacterial membranes. Other anionic components of the

outer bacterial envelope further enhance AMP binding. In contrast, the outer leaflet of mammalian membranes is composed essentially of neutral phospholipids, while acidic phospholipids are only present in the inner leaflet.

On the other hand, despite the presence of hydrophobic amino acids is essential for AMP internalization into the microbial membrane, a high level of hydrophobicity correlates with a strong affinity to the neutral mammalian membranes leading to a high level of toxicity. This is the case of the AMPs melittin, temporin L, and mastoporan which are considered potent toxins.

Concerning the membrane, two features have been described to be involved in AMP selectivity. The presence of membrane-stabilizing sterols protect cells from the disruptive effect of AMPs. Therefore, mammalian membranes which are enriched with sterols are less susceptible to AMPs compared to bacterial membranes which do not incorporate sterols (Mason 2007, Matsuzaki 2009). Moreover the transmembrane potential is usually higher and negative-inside in bacterial bilayers compared to mammalian membranes, which is a driving force for the insertion and translocation of positively charged peptides into bacterial cell membranes (Matsuzaki 2009).
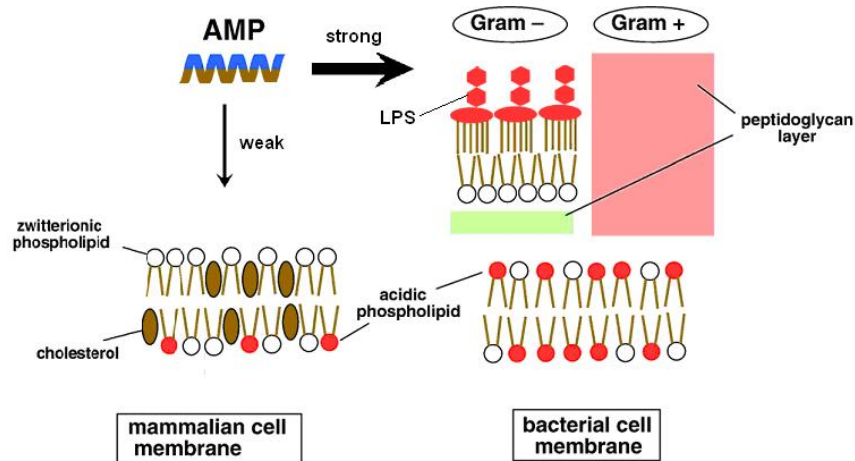
Figure I.7 Molecular basis of AMP cell selectivity. Electrostatic interaction between the positive charge of AMPs (blue) and the negatively charged components (red) is the driving force for cell specificity. (Adapted from Matsuzaki 2009).

I.3.6 Bacterial resistance to AMPs

Based on the modes of action proposed for AMPs, it seems difficult for bacteria to develop resistance to AMPs because this would require dramatic changes in phospholipid membrane composition and/or organization (Zasloff 2002). Moreover, there have been reported several examples of synthethic diasteriomeric AMPs which do not substantially differ in their biological activities, pointing out that the mechanism is not stereospecific (Wade 1990). However, there are some evidences that microbes have been able to develop resistance to AMPs. The following mechanisms have been proposed (Brodgen 2005, Peschel and Sahl 2006):

(i) Proteolytic degradation

Bacterial resistance to AMPs may be developed by the production of peptidases and proteases that degrade peptides. There are different strategies to circumvent this degradation that include the use of constrained cyclic peptides, the incorporation of Pro residues and the amidation of the C-terminus. Alternatively, AMPs can be delivered in the presence of protease inhibitors

(ii) Capturing or extruding

An additional bacterial resistance mechanism consists on the recognition and extracellular capture or extrusion of AMPs by the bacterial cells. Bacteria can produce exoproteins that bind and inactivate AMPs, and also extruding macromolecules which facilitate the ejection of AMPs from bacterial cells. Despite this mechanism has not been completely elucidated, it seems clear that the recognition of certain AMP sequences or structural motifs by these macromolecules is essential. This kind of resistance can be overcome by a suitable amino acid exchange without compromising antimicrobial activity.

(iii) Surface charge alteration

Microbial resistance to AMPs can also be developed by partial reduction of the negative charge of the microbial surfaces. Despite it is unlikely that microbes could replace the essential cell-envelope macromolecules produced by complex biosynthetic processes, they can partially neutralize the anionic cell surface components by incorporating molecules that confer cationic charge, such as D-

Ala in the teichoic acids of the Gram positive cell wall, L-Lys in negative phospholipids or aminoarabinose in the LPS. However, this mechanism is limited by the capacity of bacteria to reduce the anionic net charge, and many AMPs are still active at high concentrations or by increasing their cationic charge.

There are other mechanisms that contribute to the development of bacterial resistance to AMPs such as the formation of biofilms, which confer protection to bacteria, or the alteration of the fluidity of the outer membrane of Gram negative bacteria, which decreases its permeability and enhances bacterial resistance.

Despite these different mechanisms, the presence of many AMP variants in the same environment circumvents the development of resistance of microorganisms (Peschel and Sahl 2006).

I.3.7 Exploiting AMPs in plant disease control

The excellent properties displayed by AMPs, such as a wide spectrum of activity, selectivity towards microbial targets, and a low frequency in developing microbial resistance, have prompted their use in plant protection (Montesinos 2007, Marcos 2008). However, their practical use has been limited by their susceptibility to protease digestion, and their low bioavailability.

In order to overcome these limitations, several strategies have been devised to design shorter, more potent, nontoxic and more stable synthetic AMPs. Thus, numerous synthetic AMPs have been rationally designed and prepared based on either the modification of natural AMPs or on *de novo* design strategies (Montesinos 2007, Marcos 2008).

To date, the synthesis of AMPs obtained by modification of known natural sequences such as ceropins, melittin, magainins, indolicidin or temporins, is one of the most prominent approaches for the discovery of active peptides for plant protection (Montesinos 2007, Marcos 2008, Montesinos and Bardají 2008). These modifications include the addition, deletion or replacement of one or more residues, the truncation of N- or C-terminus, and the assembly of segments from different natural peptides. Interestingly, these peptide analogues showed reduced toxicity compared to their natural

parent sequences, while displaying high activity against phytopathogens. Some representative examples are summarized in Table I.2.

Table I.2 Antimicrobial peptide analogues active against plant pathogens.

Peptide[a]	Sequence	Activity[b]	Reference
Shiva-1 (Cec B)	MPRWRLFRRIDRVGKQIKQGILRAGPAIALVGDARAVG	B	Jaynes 1993
SB-37 (Cec B)	MPKWKVFKKIEKVGRNIRNGIVKAGPAIAVLGEAKALG	B	Nordeen 1992
D4E1 (Cec B)	FKLRAKIKVRLRAKIKL	B + F	DeLucca and Walsh 1999
Pexiganan (Mag II)	GIGKFLKKAKKFGKAFVKILKK-NH$_2$	B	Kamysz 2005
MSI-99 (Mag)	GIGKFLKSAKKFGKAFVKILNS	B + F	Alan and Earle 2002
10R (Ind)	RRPWKWPWWPWRR	B + F	Bhargava 2007
REV4 (Ind)	RRWPWWPWKWPLI	B	Li 2002
MsrA3 (Temporin A)	MASRHMFLPLIGRVLSGIL	B+F	Osusky 2004
MsrA2 (Derm B1)	MAMWKDVLKKIGTVALHAGKAALGAVADTISQ	B + F	Osusky 2005
TPY (Tachyplesin)	KWVFRVNYRGIKYRRQR	F	Rao 1999
CAMEL (Cec A-Mel)	KWKLFKKIGAVLKVL-NH$_2$	B	Kamysz 2005
Pep 1 (Cec A-Mel)	KWKLlKKIGAVLKVL-NH$_2$	F	Cavallarin 1998
Pep 3 (Cec A-Mel)	WKLFKKILKVL-NH$_2$	B + F	Cavallarin1998, Ali 2000
P18 (Cec A-Mag)	KWKLFKKIPKFLHLAKKF	B + F	Lee 2004

[a]Peptide name and its natural parent peptide in parenthesis. Cec: cecropin; Mag: magainin; Ind: indolicidin; Derm: dermaseptin; Mel: melittin. [b]B: antibacterial; F: antifungal.

Chimeric AMPs, which combine the best properties of their natural parent peptides, have attracted considerable attention. In particular, synthetic hybrid AMPs derived from cecropin, melittin, and magainin have been successfully designed (Table I.2). Among them, cecropin-melittin hybrids have been the most studied either in agrosciense or in biomedical fields (Sato and Feix 2006, Marcos 2008, Andreu 2008).

Cecropins were first isolated from the hemolymph of the giant silk moth *Hyalophora cecropia* (Hultmark 1980 and 1982, Steiner 1981). They represent a family of peptides, typically 31-39 amino acids in length, which contain a strong basic N-terminal amphipathic α-helical domain linked by a flexible hinge to a hydrophobic C-terminal α-helical domain. Cecropins display a powerful antibacterial activity against mainly all Gram negative bacteria and some Gram positive bacteria, they do not have cytotoxic effects against human erythrocytes and other eukaryotic cells, but are not stable in plant extracts due to protease degradation (Steiner 1981, Hultmark 1982, Andreu 1983, Mills 1994). On the other hand, melittin, found in the venom of the honey bee *Apis mellifera*, is a 26-amino acid length peptide with an N-terminal hydrophobic domain and a C-terminal hydrophilic domain (Habermann 1972, Raghuraman and Chattopadhyay 2007). Mellitin displays a powerful, broad-spectrum antimicrobial activity, but is also highly hemolytic (Boman 1989, Andreu 1992, Raghuraman and Chattopadhyay 2007). In an effort to improve the biological properties of cecropins and mellitin, several short cecropin-mellitin hybrid peptides were designed and synthesized (Boman 1989, Andreu 1992, Wade 1992, Piers and Hancock 1994, Lee 1997). These chimeric peptides displayed an antimicrobial activity comparable to that of the parent peptides, with a broader spectrum of activity against Gram positive bacteria than cecropins, showed less hemolytic activity than mellitin, and were less susceptible to protease degradation (Boman 1989, Andreu 1992, Wade 1992). In particular, the undecapeptide WKLFKKILKVL-NH$_2$ (Pep 3), derived from the well-known cecropin A(1-7)-mellitin(2-9) hybrid peptide (CAMEL) (Andreu 1992), was found to be sufficient for antifungal and antibacterial activities against plant pathogens, displaying also low cytotoxicity (Figure I.8) (Cavallarin 1998, Aliand Reddy 2000).

Cecropin A	KWKLFKKIEKMGRNIRDGIVKAGPAIEVIGSAKAI-NH$_2$
Melittin	GIGAVLKVLTTGLPALISWIKRKRQQ
CAMEL	KWKLFKKIGAVLKVL-NH$_2$
Pep 3	WKLFKKILKVL-NH$_2$
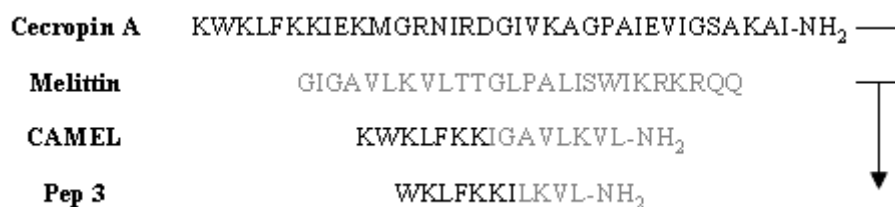
Figure I.8 Design of the chimeric peptide Pep 3.

I.4 Synthesis of antimicrobial peptides

Over the past decades there have been important advances in the field of peptide synthesis which have greatly facilitated the discovery of novel bioactive peptides with improved properties.

I.4.1 Solid-phase peptide synthesis

The brilliant solid-phase peptide synthesis (SPPS) procedure developed by R. B. Merrifield in 1963 is nowadays the most applied methodology for the preparation of peptides (Merrifield 1963 and 1986). For this genius discovery, R. B. Merrifield was awarded with the Nobel Prize in 1984. SPPS essentially consists on the covalent attachment of the C-terminal growing peptide chain onto an insoluble solid support (Scheme I.1). SPPS offers several advantages over the traditionally solution-phase procedures, such as high efficiency and straightforward purification steps. It is suitable for the synthesis of peptides up to 50 amino acids, with acceptable yields and high purity. Moreover, the simplicity of the SPPS procedures facilitates their automation allowing the production of large collections of peptides in a short period of time. SPPS represented an inflection point in the field of combinatorial and high-throughput chemistry for the synthesis of not only peptides and small proteins, but also of oligosaccharides, oligonucleotides and a huge number of diverse organic compounds.

Briefly, the main steps of SPPS consist on (Scheme I.1):

(i)   Attachment of the first amino acid, conveniently protected, onto the solid support which incorporates a linker or spacer to facilitate the final release of the peptide.

(ii)   Selective N^α-deprotection of the previously incorporated amino acid.

(iii)   Cycles of coupling and N^α-deprotection steps of the corresponding protected amino acids until the desired peptide sequence is achieved.

(iv)   Deprotection and release of the peptide from the support to obtain the final product.
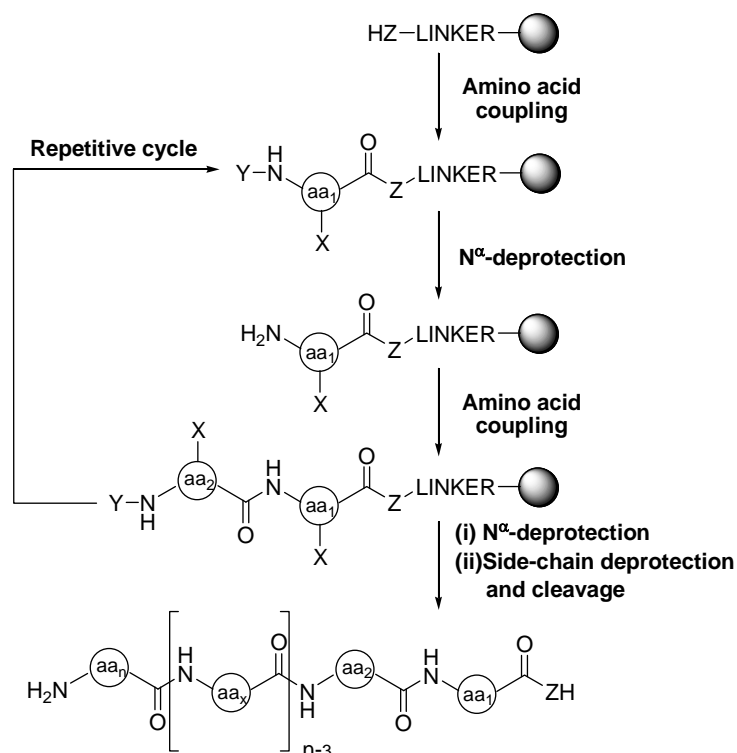
Scheme I.1 General strategy of SPPS. X: amino acid side-chain protecting groups; Y: N^{α}-protecting group; Z: O, NH.

An appropriate solid-phase strategy is crucial for a successful peptide synthesis and requires the suitable election of the solid support, the linker, the α-amino and side-chain protecting groups, and the coupling reagents.

(i)   The solid support
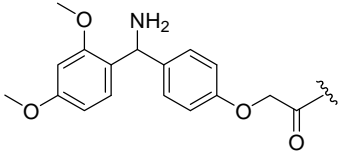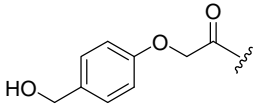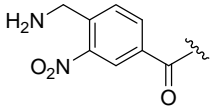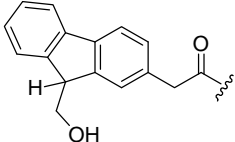
The solid support consists on an insoluble filterable polymer which should fulfill the following properties: (a) it must be composed of particles of consistent and convenient shape and size that are mechanically robust; (b) it must be inert to all reagents and reaction conditions; (c) it must allow fast solvent and reagent diffusion and access to all reactive sites; and (d) it must contain functionality to enable efficient anchoring of the linker or the first amino acid (Miranda and Alewood 2000).

Nowadays, a large number of solid supports for peptide synthesis are available. Among them, the most widely used are resin beads made from cross-linked polystyrene (PS), polyacrylamide, and polyethylene glycol (PEG) grafted onto a cross-linked polystyrene (Kates and Albericio 2000).

(ii) The linker

The linker is a bifunctional molecule which is bounded to both the solid support and the first amino acid of the peptide sequence. One side of the linker is irreversibly anchored to the solid support, while the other side serves for the attachment of the first amino acid and behaves as a cleavable protecting group for the final release of the peptide (Kates and Albericio 2000). They are commonly categorized according to their cleavage conditions. Some representative linkers are shown in Table I.3.

Table I.3 Some representative linkers used in SPPS.
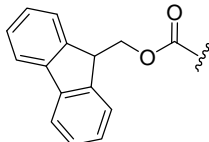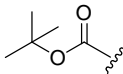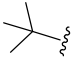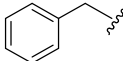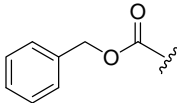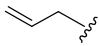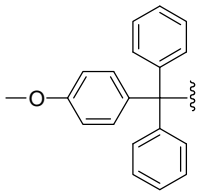
Structure	Name	Cleavage conditions	Resulting C-terminus
	Rink	TFA	Amide
	PAC	TFA	Acid
	Nonb	hν (350 nm)	Amide
	HMFA	Piperidine	Acid

(iii) Protecting groups

In order to control the formation of the desired peptide amide bond, protecting groups are essential for masking the functional groups which are not involved in the the reaction. Therefore, the amino acids are conveniently protected. The main features associated with a protecting group are: (a) it must be easily introduced into the functional group; (b) it must be stable to the reaction conditions; (c) it must not add any additional reactivity; and (d) it must be safely removed at the end of the synthetic process (permanent protecting groups) or when the functional group requires manipulation (temporary protecting groups) (Isidro-Llobet 2009). The most common

orthogonal strategies for SPPS are the 9-fluorenylmethoxycarbonyl (Fmoc) / *tert*-butyl (^{t}Bu) (Carpino and Han 1970) and the *tert*-butyloxycarbonyl (Boc) / benzyl (Bn) (Merrifield 1963 and 1986). Some representative protecting groups are shown in Table I.4.

Table I.4 Some representative protecting groups and removal conditions

Structure	Name	Removal
	9-Fluorenylmethoxycarbonyl (**Fmoc**)	Piperidine DBU
	tert-Butyloxycarbonyl (**Boc**)	Concentrated TFA
	tert-Butyl (**^{t}Bu**)	Concentrated TFA
	Benzyl (**Bn**)	HF H$_2$
	Benzyloxycarbonyl (**Z**)	HF H$_2$
	Allyl (**Al**)	Pd(PPh$_3$)$_4$
	4-Methoxytrityl (**Mtt**)	Diluted TFA

(iv) Coupling reagents

Coupling reagents are essential for formation of the the peptide amide bond under mild conditions. During the peptide chain elongation, they activate the carboxyl group of the amino acid to be incorporated facilitating its reaction with the N^{α}-amino

group of the residue anchored onto the solid suport. A good coupling method should fulfill the following main requirements: (a) it should assure maximum efficiency provinding quantitative coupling yields (high conversion); (b) it should keep the stereochemical integrity of the incorporated amino acid (avoiding epimerization); and (c) it should not cause side-chain reactions (limited by-products). Nowadays, the most common coupling reagents for SPPS are carbodiimides, aminium/uronium, and phosphonium salts (Valeur and Bradley 2009). Some representative examples are shown in Figure I.9.
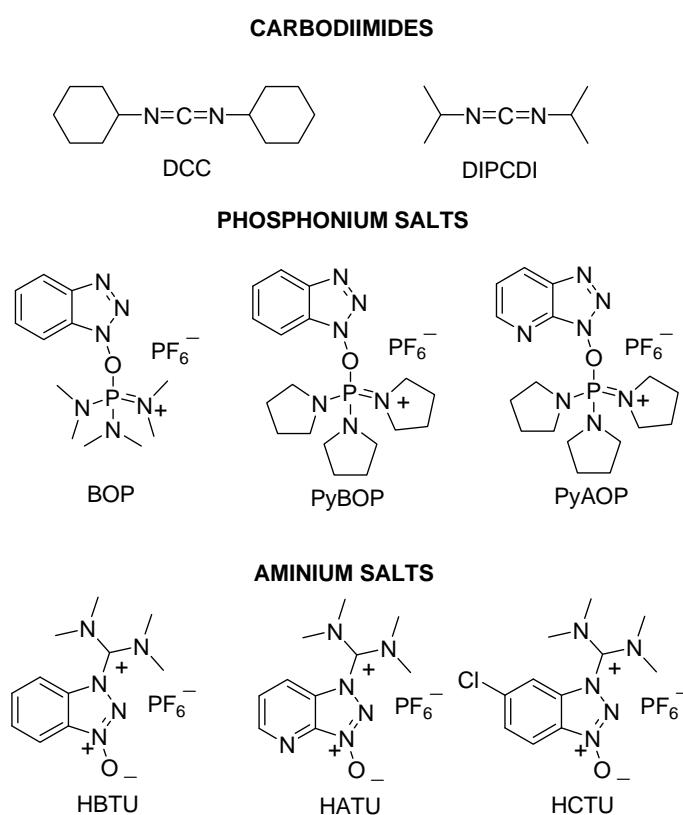
Figure I.9 Some representative coupling reagents.

I.4.2 Combinatorial chemistry

The process involved in the development of lead candidates is time consuming and limited by the number of individual compounds that can be synthesized. Combinatorial chemistry procedures have emerged as an useful tool in drug discovery, specially for lead finding and lead optimization (Figure I.10) (Lazo and Wipf 2000). However, despite the existence of numerous examples of combinatorial libraries

addressed to biomedical fields, there are only few examples focused on agroscience (Marcos 2008).
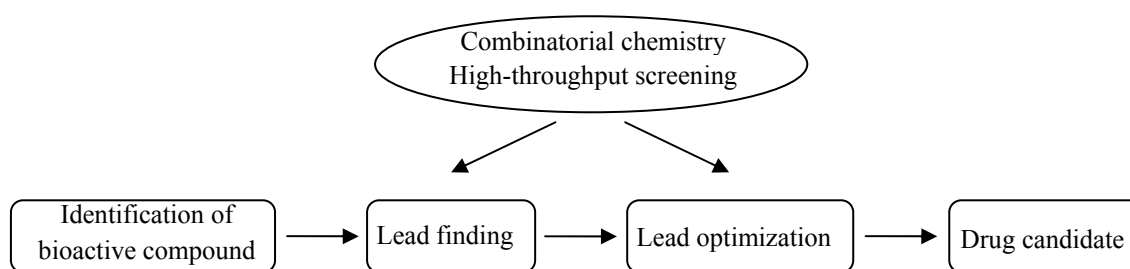
Figure I.10 Drug discovery process.

Combinatorial chemistry covers a diversity of techniques that allow the easy, rapid and efficient production of large collections of compounds (libraries), which can then be rapidly screened (Bannwarth and Hinzen 2006). Two kinds of libraries are mainly produced: the so-called "defined" and "non-defined" synthetic libraries.

The "defined" libraries are obtained using parallel synthetic methods that provide final pure samples of single peptides, which facilitates the interpretation of the biological results. Parallel strategies are not convenient for the synthesis of large peptide libraries. However, this approach is useful for the lead optimization of a previously identified active compound. For instance, LIPPSO group recently reported a 66-membered defined library of cyclic decapeptides with general structure c($X^1X^2X^3X^4X^5$Phe$X^7X^8X^9$Gln), being X = Lys or Leu, which was screened against the plant pathogenic bacteria *E. amylovora*, *P. syringae*, and *X. vesicatoria* (Monroc 2006). The most active peptides, c(LysLysLeuLysLysPheLysLysLeuGln) (BPC194) and c(LysLeuLysLysLysPheLysLysLeuGln) (BPC198) were comparable in terms of activity to the antibiotic streptomycin (Monroc 2006). Other examples of AMPs active against phytopathogens obtained from defined libraries are the heptapeptides 77-3 and 77-12 (Gonzalez 2002) and PAF26 derivatives (Muñoz 2007).

The "non-defined" libraries are prepared using iterative or positional scanning strategies where multiple sequences are produced fixing the amino acids in selected positions and randomizing the amino acids of the other sites. These strategies allow the production of large libraries and peptides are obtained as mixtures. Therefore, deconvolution procedures are required to identify the most important amino acid at each positionin terms of activity. As a matter of example, the peptide PAF26 (Ac-rkkwfw-

NH_2), obtained through positional scanning, displayed antifungal activity against *Penicillium digitatum*. The library consisted of 6 sublibraries, each one containing 19 mixtures of 19^5 peptides (Figure I.11) (López-García 2002). Other examples of AMP active against phytopathogens obtained by means of "non-defined" libraries are the pentapetide PPD1 and the hexapeptide 66-10 (Reed 1997).
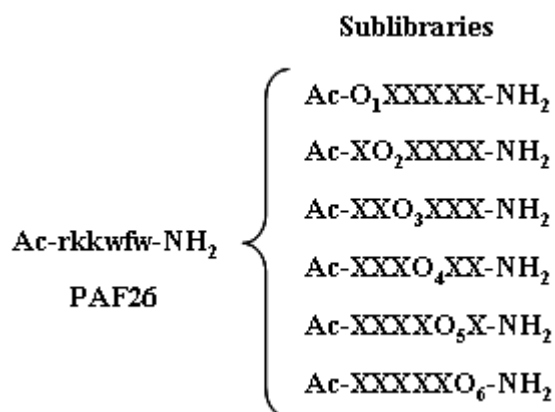
Figure I.11 Schematic representation of the positional scanning approach for PAF26. O is defined by one of the 19 D-amino acids; X, close-to-equimolar mixture of the 19 D-amino acids; Cys was omitted.

Chapter II. General objectives

The present PhD dissertation is centred on the development of new short antimicrobial peptides for their potential application in the control of plant diseases caused by the economically important plant pathogenic bacteria *Erwinia amylovora*, *Pseudomonas syringae* pv. *syringae*, *Xanthomonas axonopodis* pv. *vesicatoria*, and the plant pathogenic fungi *Fusarium oxysporum*, *Aspergillus niger*, *Rhizopus stolonifer*, and *Penicillium expansum*, for which the available methods are neither sufficiently effective nor sustainable.

In particular, the main objectives of this thesis can be summarized as follows:

a) Solid-phase synthesis of short antimicrobial peptides derived from the cecropin A-melittin hybrid undecapetide Pep3 and evaluation of their biological activity against the above phytopathogens.

b) Improvement of the biological properties displayed by the most effective peptide through a combinatorial chemistry approach.

c) Study of the mode of action of the best peptide by investigating its interaction with different model membrane systems using spectroscopic methodologies.

Chapter III. Design and synthesis of short antimicrobial peptides for plant protection

Chapter III.1. Inhibition of plant-pathogenic bacteria by short synthetic cecropin A-melittin hybrid peptides

Short peptides of 11 residues were synthesized and tested against the economically important plant pathogenic bacteria *Erwinia amylovora*, *Pseudomonas syringae*, and *Xanthomonas vesicatoria* and compared to the previously described peptide Pep3 (WKLFKKILKVL-NH$_2$). The antimicrobial activity of Pep3 and 22 analogues was evaluated in terms of the MIC and the 50% effective dose (ED$_{50}$) for growth. Peptide cytotoxicity against human red blood cells and peptide stability toward protease degradation were also determined. Pep3 and several analogues inhibited growth of the three pathogens and had a bactericidal effect at low micromolar concentrations (ED$_{50}$ of 1.3 to 7.3 µM). One of the analogues consisting of a replacement of both Trp and Val with Lys and Phe, respectively, resulted in a peptide with improved bactericidal activity and minimized cytotoxicity and susceptibility to protease degradation compared to Pep3. The best analogues can be considered as potential lead compounds for the development of new antimicrobial agents for use in plant protection either as components of pesticides or expressed in transgenic plants.

Inhibition of Plant-Pathogenic Bacteria by Short Synthetic Cecropin A-Melittin Hybrid Peptides

Rafael Ferre,[1] Esther Badosa,[2] Lidia Feliu,[1] Marta Planas,[1] Emili Montesinos,[2]* and Eduard Bardají[1]

*Laboratori d'Innovació en Processos i Productes de Síntesi Orgànica (LIPPSO), Departament de Química,[1] and
Laboratori de Patologia Vegetal, Institut de Tecnologia Agroalimentària, CIDSAV-CeRTA,[2]
Universitat de Girona, Campus Montilivi, 17071 Girona, Spain*

Short peptides of 11 residues were synthesized and tested against the economically important plant pathogenic bacteria *Erwinia amylovora*, *Pseudomonas syringae*, and *Xanthomonas vesicatoria* and compared to the previously described peptide Pep3 (WKLFKKILKVL-NH₂). The antimicrobial activity of Pep3 and 22 analogues was evaluated in terms of the MIC and the 50% effective dose (ED$_{50}$) for growth. Peptide cytotoxicity against human red blood cells and peptide stability toward protease degradation were also determined. Pep3 and several analogues inhibited growth of the three pathogens and had a bactericidal effect at low micromolar concentrations (ED$_{50}$ of 1.3 to 7.3 μM). One of the analogues consisting of a replacement of both Trp and Val with Lys and Phe, respectively, resulted in a peptide with improved bactericidal activity and minimized cytotoxicity and susceptibility to protease degradation compared to Pep3. The best analogues can be considered as potential lead compounds for the development of new antimicrobial agents for use in plant protection either as components of pesticides or expressed in transgenic plants.

Phytopathogenic bacteria are responsible for great losses in economically important crops such as vegetables and fruit (1). Although a great amount of research has been undertaken to overcome the damage caused by this type of bacteria, a major difficulty encountered is the lack of effective control against some severe diseases (37). Plant protection against these pathogens is mainly based on copper derivatives and antibiotics. However, these compounds are regarded as environmental contaminants, and resistant strains of plant-pathogenic bacteria have been reported in several crops (34, 48).

In recent years, much attention has been paid to searching for new classes of antibiotics to which bacteria cannot develop resistance. Endogenous antimicrobial peptides have emerged as good candidates (26, 27, 51). These peptides have been found in a variety of sources, including mammals, amphibians, insects, and plants, and they are known to play important roles in the host defense system and innate immunity (12–14, 21, 22, 43).

Most antimicrobial peptides are cationic and have the ability to adopt an amphipathic conformation in which positively charged and hydrophobic groups segregate onto opposing faces of an α-helix, a β-sheet, or other tertiary structures (7, 9, 11, 25, 29, 46, 49, 51). Natural antimicrobial peptides exhibit a broad spectrum of activity against bacteria, fungi, enveloped viruses, parasites, and tumor cells. They are lytic, have a synergistic activity with conventional antibiotics, neutralize endotoxins, and have very few reported side effects (7, 9, 11, 25, 29, 46, 49). Their mechanism of action has been studied mainly in bacteria. Amphiphilicity is thought to be a key requisite for these peptides to interact with their primary target, the cell membrane. They do not interact with a specific receptor but, rather, disturb bilayer integrity, either by disruption or pore formation, probably by direct peptide-lipid interactions (7, 9, 11, 25, 29, 46, 49). This unique mode of action makes the induction of resistance difficult, because it requires dramatic changes in phospholipid membrane composition and/or organization (51).

Cecropins are some of the best studied cationic antimicrobial peptides, representing a family of highly basic α-helical peptides first found in the hemolymph of the giant silk moth *Hyalophora cecropia* as a response to a bacterial infection (32, 47). In particular, cecropin A is a 37-amino-acid linear peptide, which consists of a strongly basic N-terminal amphipathic α-helical domain connected to a hydrophobic C-terminal α-helix by a flexible hinge. Cecropin A displays powerful lytic activity against gram-positive and gram-negative bacteria but has no cytotoxic effects against human erythrocytes and other eukaryotic cells (6, 32, 47). The basis of this selectivity has been attributed to the absence of acidic phospholipids and presence of sterols in eukaryotic cells (18). However, major concerns about the use of cecropin A as a pesticide in plant protection are the high production cost of such a long peptide and its sensitivity to protease degradation. Searches for shorter, more potent, nontoxic, and more stable peptides have led to the identification of synthetic peptides with broader and higher activity than their natural counterparts (3, 5, 6, 8, 16, 17, 19, 23, 33, 41, 50). In particular, the 11-residue sequence WKLFKKI LKVL-NH₂ (Pep3), derived from the well-known cecropin A(1-7)-melittin(2-9) hybrid peptide (8, 17, 23), is sufficient for antifungal and antibacterial activities (4, 16).

Reports on the activity of short synthetic cecropin A-melittin hybrid peptides concerning plant-pathogenic microorganisms have been focused mainly on fungal plant pathogens (4, 16). Studies involving plant-pathogenic bacteria are practically limited to *Erwinia carotovora* (4). Our current research is oriented

TABLE 1. Sequences and α-helicity of synthetic peptides

Peptide	Sequence[a]											$[\theta]_{222}$[b]	α-Helix (%)
Pep3	W	K	L	F	K	K	I	L	K	V	L-NH$_2$	−9,048	23.5
BP01	W	K	L	F	K	K	I	L	K	V	**L-OH**	ND[c]	ND
BP02		K	L	F	K	K	I	L	K	**K**	L-NH$_2$	ND	ND
BP03		K	L	F	K	K	I	L		**K-NH$_2$**		ND	ND
BP04	W	K	L	F	**K-NH$_2$**							ND	ND
BP05	W	K	L	F	**K-OH**							ND	ND
BP06						K	I	L	K	V	L-NH$_2$	ND	ND
BP07						K	I	L	K	V	**L-OH**	ND	ND
BP08	Ac-W	K	L	F	K	K	I	L	K	V	L-NH$_2$	−10,851	29.5
BP09	Ts-W	K	L	F	K	K	I	L	K	V	L-NH$_2$	−13,341	37.8
BP10	Bz-W	K	L	F	K	K	I	L	K	V	L-NH$_2$	−13,119	37.1
BP11	Bn-W	K	L	F	K	K	I	L	K	V	L-NH$_2$	−10,665	28.9
BP12	Pam-W	K	L	F	K	K	I	L	K	V	L-NH$_2$	ND	ND
BP13	**F**	K	L	F	K	K	I	L	K	V	L-NH$_2$	ND	ND
BP14	**Y**	K	L	F	K	K	I	L	K	V	L-NH$_2$	ND	ND
BP33	**L**	K	L	F	K	K	I	L	K	V	L-NH$_2$	−8,918	23.1
BP15	**K**	K	L	F	K	K	I	L	K	V	L-NH$_2$	−9,892	26.3
BP16	**K**	K	L	F	K	K	I	L	K	**K**	L-NH$_2$	ND	ND
BP76	**K**	K	L	F	K	K	I	L	K	**F**	L-NH$_2$	−9,188	24.0
BP17	W	K	L	F	K	K	I	L	K	**K**	L-NH$_2$	ND	ND
BP18	W	K	L	F	K	K	I	L	K	**W**	L-NH$_2$	−8,922	23.1
BP19	W	K	L	F	K	K	I	L	K	**F**	L-NH$_2$	−9,950	26.5
BP20	W	K	L	F	K	K	I	L	K	**Y**	L-NH$_2$	−10,316	27.7

[a] Boldfaced letters indicate the modifications introduced into the Pep3 sequence. Ac, acetyl; Ts, tosyl; Bz, benzoyl; Bn, benzyl; Pam, palmitoyl.
[b] Determined in 50% trifluoroethanol in 10 mM sodium phosphate buffer (pH 7.4).
[c] ND, not determined.

to develop new control methods against economically important plant pathogenic bacteria, such as *Erwinia amylovora*, the causal agent of fire blight of rosaceous plants; *Xanthomonas vesicatoria*, the cause of bacterial spot of tomato and pepper; and *Pseudomonas syringae*, the cause of several blight diseases (15, 38, 40). To date, apart from the antibiotics streptomycin and tetracycline registered in certain countries, no effective method to treat these plant diseases has been described.

The production of antimicrobial peptides by self-defending genetically improved plants constitutes an effective means for improving crop protection against bacterial diseases (42). However, the use of genetically modified crops is governed by several restrictions in some countries. Therefore, peptide synthesis has been regarded as a useful alternative, but a major concern is the high production cost associated with the preparation of large peptides. Within this context, we were interested in the identification of short synthetic peptides (≤11 residues) with specific activity against *E. amylovora*, *X. vesicatoria*, and *P. syringae*. In particular, our study was centered on the sequence of Pep3, which shows interesting antibacterial activities, but it has not been tested against the above plant-pathogenic bacteria.

In the present study we report the activity of Pep3 and 22 new analogues against the phytopathogenic bacteria *E. amylovora*, *X. vesicatoria*, and *P. syringae*. Analogues were designed based on the α-helical wheel diagram of Pep3 and synthesized by the solid-phase method. Circular dichroism (CD) spectroscopy was employed to investigate the secondary structure of the peptides. The main objective was to obtain new peptides with higher bactericidal activity and lower cytotoxic effects and sensitivity to protease degradation than Pep3.

MATERIALS AND METHODS

Peptide synthesis. All peptides listed in Table 1 were synthesized by the solid-phase method using 9-fluorenylmethoxycarbonyl (Fmoc)-type chemistry, *tert*-butyloxycarbonyl side chain protection for Lys and Trp, and *tert*-butyl for Tyr. All the Fmoc acid derivatives, reagents, and solvents were obtained from Senn Chemicals International (Gentilly, France). Fmoc-Rink-4-methylbenzhydrylamine resin (0.64 mmol/g; Novabiochem, Darmstadt, Germany) was used as solid support to obtain C-terminal peptide amides and 4-hydroxymethylphenoxypropionic acid polyethylene glycol-polystyrene resin (0.23 mmol/g; Perspective Biosystems, Framingham, Mass.) to synthesize C-terminal peptide acids BP01, BP05, and BP07. Peptides were obtained with >90% purity by high-performance liquid chromatography (HPLC). Electrospray ionization mass spectrometry was used to confirm peptide identity.

Bacterial strains and growth medium. The following plant-pathogenic bacterial strains were used: *E. amylovora* PMV6076 (Institut National de la Recherche Agronomique, Angers, France), *P. syringae* pv. *syringae* EPS94 (Institut de Tecnologia Agroalimentària, Universitat de Girona, Spain) and *X. vesicatoria* 2133-2 (Instituto Valenciano de Investigaciones Agrarias, Valencia, Spain). All bacteria were stored in liquid LB medium supplemented with glycerol (20%) and maintained at −80°C. *E. amylovora* PMV6076 and *P. syringae* pv. *syringae* EPS94 were scraped from LB agar after growth for 24 h and *X. vesicatoria* 2133-2 was scraped after 48 h at 25°C. The cell material was suspended in sterile water to obtain a suspension of 10^8 CFU ml^{-1}.

Antimicrobial activity. Lyophilized peptides were solubilized in sterile Milli-Q water to a final concentration of 1,000 μM and filter sterilized through a 0.22-μm-pore-size filter. For MIC assessment, dilutions of the synthetic peptides were made to obtain final concentrations of 750, 500, 250, 200, 150, 125, 100, 75, 50, and 25 μM. For cecropin A, the concentrations were 250, 200, 150, 125, 100, 75, 50, 25, 12.5, 6.25, and 3.12 μM. Twenty microliters of each dilution was mixed in each well of a microtiter plate with 20 μl of the corresponding suspension of the bacterial indicator, 160 μl of tryptic soy broth (BioMèrieux, France), to a total volume of 200 μl. Two replicates for each strain, peptide, and concentration were used. Positive controls contained water instead of peptide, and negative controls contained peptides without bacterial suspension. Microbial growth was automatically determined by optical density measurement at 600 nm (Bioscreen C; Labsystem, Helsinki, Finland). Microplates were incubated at 25°C with 20 s of shaking before hourly absorbance measurements for 48 h. The experiment was repeated twice.

The MIC was defined as the lowest peptide concentration with no growth at the end of the experiment. Since it may be that certain compounds have the same MIC but different inhibition-dose relationships, an additional parameter, the 50% effective dose (ED_{50}), was determined for the measurement of activity. Growth was measured as the area under the curve. Inhibition of growth (I) was calculated as a percentage of the positive control using the following equation: $I = 100 \times [(AC - AS)/AC]$, where AC is the area under the curve of the control, and AS is the area under the curve of a given peptide concentration.

The ED_{50} is the concentration required to obtain 50% inhibition of growth and was calculated from the inhibition-dose data for each peptide. Inhibition data were fitted to the probit-dose model (20, 36). The equation of the probit-dose model is as follows: $y = \phi\{[\log_{10}(x) - \lambda]/\tau\}$, where y is the proportion of inhibition, x is the peptide concentration, ϕ denotes the cumulative distribution function for the standard normal, λ is a parameter equivalent to ED_{50}, and τ is the peptide efficiency.

Regression and parameter estimation were performed by a nonlinear least-squares method using the NLIN procedure of the PC-Statistical Analysis System, version 8.2 (SAS Institute Inc., Cary, NC).

Analysis of bactericidal activity. The bactericidal activity of peptides was determined for the reference peptide Pep3 and the analogues BP11, BP15, BP33, and BP76. LB broth-grown cultures of *E. amylovora*, *P. syringae*, and *X. vesicatoria* inoculated at 4×10^6 CFU ml^{-1} were incubated in a 5 μM concentration of the corresponding peptide. Aliquots of 500 μl were removed at 30-min intervals during 3 h and diluted 10-fold, and the dilutions were plated on LB agar plates. The CFU were counted after a 48-h incubation at 25°C. Values were expressed as percentages of survival from the start of the experiment.

Hemolytic activity. The hemolytic activity of the peptides was evaluated by determining hemoglobin release from erythrocyte suspensions of fresh human blood (5%, vol/vol). Blood was aseptically collected using a BD Vacutainer K2E system with EDTA (Belliver Industrial State, Plymouth, United Kingdom) and stored for less than 2 h at 4°C. Blood was centrifuged at $6,000 \times g$ for 5 min, washed three times with Tris buffer (10 mM Tris, 150 mM NaCl, pH 7.2) and diluted with Tris buffer. Peptides were solubilized in Tris buffer to final concentrations of 800, 400, 200, 100, 50, 25, and 12.5 μM. Fifty microliters of human red blood cells was mixed with 50 μl of the peptide solution and incubated under continuous shaking for 1 h at 37°C. Then, the tubes were centrifuged at $3,500 \times g$ for 10 min. Eighty-microliter aliquots of the supernatant were transferred to 100-well microplates (Bioscreen) and diluted with 80 μl of Milli-Q water. Hemolysis was measured as the absorbance at 540 nm with a Bioscreen plate reader. Complete hemolysis was determined in TRIS buffer plus melittin (Sigma-Aldrich Corporation, Madrid, Spain) as a positive control. The percentage of hemolysis (H) was calculated using the following equation: $H = 100 \times [(O_p - O_b)/(O_m - O_b)]$, where O_p is the density for a given peptide concentration, O_b is the density for the buffer, and O_m is the density for the melittin positive control.

To analyze dose-response relationships in hemolysis, the 50% hemolytic dose (HD_{50}) was determined following the procedure previously described for the analysis of antibacterial activity.

Susceptibility to protease degradation. Digestion of Pep3, BP08, BP09, BP10, BP15, BP20, BP33, and BP76 by proteinase K (Sigma-Aldrich Corp., Madrid, Spain) was carried out by treating 50 μg/ml peptide with 1 μg/ml proteinase K in 100 mM Tris buffer, pH 7.6, at room temperature. The peptide cleavage after 5, 10, 15, 30, and 45 min was monitored by HPLC using a Kromasil (4.6- by 40-mm column; 3.5-μm particle size) C_{18} reverse-phase column. Linear gradients of 0.1% aqueous trifluoroacetic acid and 0.1% trifluoroacetic acid in CH$_3$CN were run from 0.98:0.02 to 0:1 over 7 min with UV detection at 220 nm. Digestion was estimated as the percentage of degraded peptide calculated from the decrease of the HPLC peak area of the native peptide.

CD spectroscopy. CD measurements were obtained using a Jasco spectropolarimeter (J-810; Easton, MD) at 25°C. Spectra were obtained in a fused quartz cell with 1-mm path length over a wavelength range of 190 to 250 nm at 0.1-nm intervals, 50 nm/min speed, 0.5-s response time, and 1-nm bandwidth. Peptides were dissolved to a 100 μM concentration in 50% (vol/vol) trifluoroethanol in 10 mM sodium phosphate buffer at pH 7.4. A baseline correction was made with only solvent in the cell. Data were expressed in terms of mean residue ellipticity [θ] (degrees × cm² dmol^{-1}), calculated per mol of total amide groups present in the different peptides. The percent helicity of the peptide was calculated as follows: α-helix (%) = $([\Theta]_{222} - [\Theta]_{222}^0)/[\Theta]_{222}^{100}$, where $[\Theta]_{222}$ is the experimentally observed absolute mean residue ellipticity at 222 nm. Values for $[\Theta]_{222}^0$ and $[\Theta]_{222}^{100}$, corresponding to 0 and 100% helix content at 222 nm, were estimated to be −2,000 and −30,000 (degrees × cm² dmol^{-1}), respectively (33).
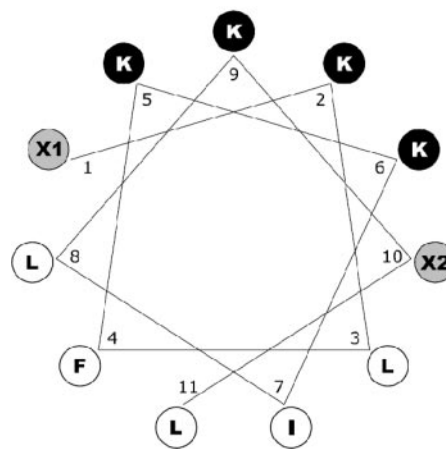
FIG. 1. Edmunson wheel projection of the 11-mer peptides that were synthesized. Black background, hydrophilic amino acids (Lys); white background, hydrophobic amino acids; gray background, residues that can be either hydrophilic (Lys) or hydrophobic (Leu, Trp, Tyr, and Phe), depending on the sequence as shown in Table 1.

RESULTS

Design of peptides. Primary structures of Pep3 analogues reported here are shown in Table 1. All peptides were prepared as C-terminal amides except BP01, BP05, and BP07. Analogues BP08 to BP12 were blocked at the N termini with an acetyl, tosyl, benzoyl, benzyl, or palmitoyl group, respectively. To examine whether the entire sequence of Pep3 is necessary for its full antibacterial activity, N- and C-terminal deletion analogues (BP02 to BP07) were synthesized. Analogues BP13 to BP20, BP33, and BP76 were designed based on the ideal α-helical wheel diagram of Pep3 (Fig. 1). We investigated the effect of individually replacing tryptophan and valine residues with amino acids possessing various degrees of hydrophobicity and hydrophilicity. Thus, tryptophan was replaced with Phe (BP13), Tyr (BP14), Lys (BP15), or Leu (BP33). Valine was replaced with Lys (BP17), Trp (BP18), Phe (BP19), or Tyr (BP20). Tryptophan and valine were replaced with Lys and Phe, respectively (BP76). The hydrophilic surface area of Pep3 was further increased by replacing both tryptophan and valine residues with Lys (BP16).

Antibacterial activity. The peptides synthesized were tested for antibacterial activity against *E. amylovora*, *P. syringae*, and *X. vesicatoria*. Results obtained are shown in Table 2. Pep3, which has not been previously tested against these bacteria, inhibited the growth of all three pathogens. The ED_{50} values of the peptide were in the range of 3.6 to 5.5 μM. The C-terminal peptide acid derivative BP01 was significantly less active than Pep3, and the N- and C-terminal deletion analogues (BP02 to BP07) were inactive against these pathogens (data not shown).

Except for the *N*-palmitoylated peptide BP12, derivatization of the N terminus of Pep3 produced peptides (BP08 to BP11) with significant biological activity, with ED_{50} values ranging from 2 μM to 15.1 μM. The *N*-benzylated analogue BP11 was the most inhibitory peptide within this group and slightly better than Pep3 (ED_{50} of 2.5 to 5.0 μM).

Replacement of Trp in Pep3 with Lys (BP15) or Leu (BP33)

TABLE 2. Antimicrobial activity against three plant-pathogenic bacteria and cytotoxicity of selected peptides

Peptide	MIC (μM)			ED$_{50}$ (μM)			HD$_{50}$ (μM)
	E. amylovora	P. syringae	X. vesicatoria	E. amylovora	P. syringae	X. vesicatoria	
Pep3	7–10	7–10	7–10	5.5	5.5	3.6	104
BP08	10–12	7–10	2–5	9.0	4.3	2.0	17
BP09	12–15	12–15	<2	11.2	6.9	ND[a]	10
BP10	15–20	15–20	<2	15.1	9.5	ND	11
BP11	7–10	5–7	2–5	5.0	3.8	2.5	30
BP12	50–100	50–100	25–50	60.0	56.8	14.7	6
BP15	5–7	2–5	12–15	4.3	1.6	7.3	334
BP18	5–7	5–7	<2	3.0	2.5	ND	26
BP19	5–7	5–7	<2	1.3	1.9	ND	32
BP20	2–5	2–5	2–5	3.2	2.7	2.3	42
BP33	5–7	5–7	10–12	4.3	3.2	4.1	190
BP76	2–5	2–5	2–5	2.5	2.1	1.9	203
Cecropin A[b]	<1	<1	<1	<0.3[c]	<0.3	<0.3	ND

[a] ND, not determined.
[b] Cecropin A was included for comparison purposes.
[c] Estimated visually from graphs; lowest concentration tested.

induced a slight increase in the overall activity (ED$_{50}$ values of 1.6 to 7.3 μM and 3.2 to 4.3 μM, respectively). In contrast, replacement of Trp with Phe (BP13) or Tyr (BP14) resulted in analogues with poor antibacterial activity (data not shown).

Analogues BP18, BP19 and BP20, which have Trp, Phe, or Tyr instead of Val, were considerably more active than the parent peptide Pep3 (ED$_{50}$ of 1.3 to 3.2 μM). In contrast, BP17, which has Lys instead of Val, did not show antibacterial activity (data not shown).

Double replacement of Trp and Val with Lys and Phe (BP76), respectively, also led to a significant increase of the antibacterial activity compared to Pep3 (ED$_{50}$ of 1.9 to 2.5 mM). In contrast, BP16, which possesses two Lys residues instead of Trp and Val residues, was not active (data not shown).

MICs of these cecropin A-derived peptides were also determined (Table 2) and were in good agreement with the ED$_{50}$ values. In general, X. vesicatoria was more sensitive to each of the peptides than were the other two bacteria. Complete inhibition of X. vesicatoria was observed at 2 μM for peptides BP09, BP10, BP18, and BP19. On the basis of MICs, BP15, BP20, and BP76 were the most potent peptides against P. syringae (MIC of 2 to 5 μM), and the MICs of BP20 and BP76 were the lowest against E. amylovora (MIC of 2 to 5 μM).

Since some of the analogues synthesized showed similar antibacterial activity against the bacterial strains tested, we evaluated their bactericidal activity by comparing the time course to kill mid-logarithmic-phase culture suspensions of E. amylovora, P. syringae, and X. vesicatoria. As shown in Fig. 2, at the concentration tested, all the peptides had a slower bactericidal effect against P. syringae than against the other two pathogens, except for BP11, which had no effect on E. amylovora. BP15 showed higher bactericidal activity against E. amylovora than Pep3 and similar bactericidal activity against P. syringae and X. vesicatoria. Notably, BP76 was the peptide with the highest bactericidal effect against E. amylovora and X. vesicatoria. Its activity against X. vesicatoria was
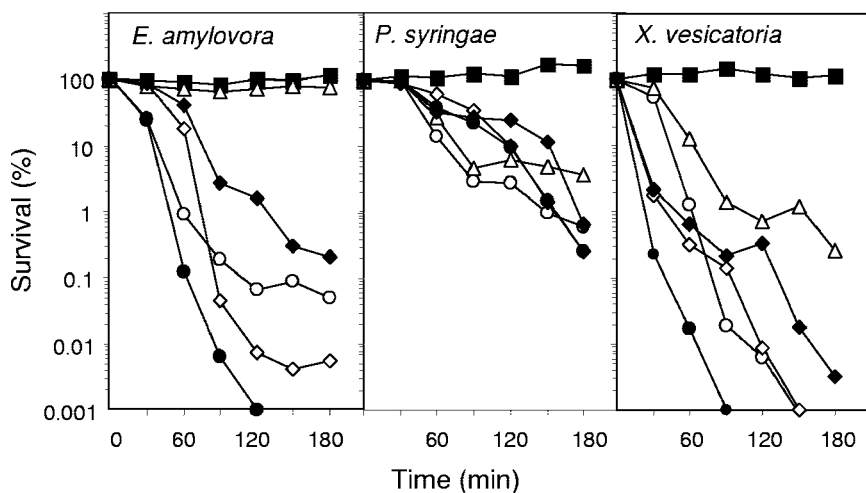

FIG. 2. Kinetics of survival of P. syringae, X. vesicatoria, and E. amylovora in the presence of Pep3 (○) or selected analogues. Bacterial suspensions were untreated (■) or treated with 5 μM concentrations of BP11 (△), BP15 (◇), BP33 (◆), or BP76 (●), and viable cells were determined at different time intervals.
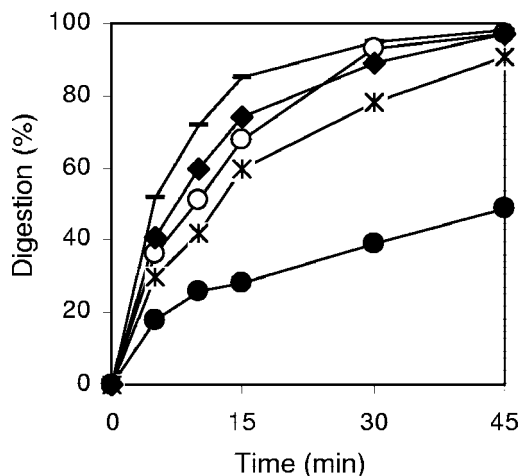
FIG. 3. Kinetics of digestion of Pep3 (○) and selected analogues BP08 (⊢), BP20 (∗), BP33 (◆), and BP76 (●) by proteinase K.

nearly complete after a 90-min exposure period at a concentration of 5 μM.

Hemolytic activity. The toxicity of the peptides to eukaryotic cells was tested by their ability to lyse human red blood cells, and results were compared to melittin as a standard. Results are shown in Table 2. The HD_{50} values of the peptides ranged from 6 to 334 μM. Pep3 showed moderate hemolytic activity (HD_{50} of 104 μM). Derivatization of the N terminus of Pep3 (BP08 to BP12) caused a significant increase in hemolytic activity (HD_{50} of 6 to 30 μM). The *N*-palmitoylated analogue, BP12, was the most hemolytic peptide (HD_{50} of 6 μM). BP33, which has a Leu instead of a Trp residue, was twofold less hemolytic than Pep3 (HD_{50} of 190 μM), and BP15, containing a Lys instead of a Trp residue, was more than threefold less hemolytic than Pep3 (HD_{50} of 334 μM). The replacement of Val in Pep3 with Trp, Phe, or Tyr resulted in peptides (BP18 to BP20) with a high level of hemolytic activity (HD_{50} of 26 to 42 μM). Replacement of Trp and Val with Lys and Phe (BP76), respectively, led to a twofold decrease of hemolytic activity (HD_{50} of 203 μM).

Susceptibility to proteolysis. The susceptibility of some peptides to proteolysis was studied by exposure to proteinase K and monitoring the degradation by reverse-phase HPLC over time (Fig. 3). Pep3, BP15, BP33, and the N-terminal derivatized peptides BP08 to BP10 showed similar stabilities. Interestingly, BP76 turned out to be twofold more stable than Pep3. While Pep3 was completely degraded after 45 min of incubation with the enzyme, BP76 underwent only a 50% degradation.

α-Helical structures determined by CD. We investigated the secondary structures of the 11-residue peptides which showed the highest biological activity by analyzing their CD spectra in 50% (vol/vol) trifluoroethanol in 10 mM sodium phosphate buffer at pH 7.4. The α-helical contents obtained are listed in Table 1. The spectra of all peptides were characteristic of a typical α-helical conformation with two negative minimum bands at 208 and 222 nm. Results showed that Pep3 and its analogues have a moderate α-helical content (23.1 to 37.8%).

DISCUSSION

Despite the existence of natural potent antimicrobial peptides (e.g., magainins and cecropins), a search for more potent and shorter peptides with a broader spectrum of activity has led to the identification of highly potent synthetic peptides. Several design strategies have been devised in order to develop new compounds with maximum antimicrobial activity and minimum cytotoxicity. For instance, juxtaposition of the N-terminal sections of cecropin A and melittin has resulted in hybrids with better antimicrobial spectra than the parent peptide cecropin A and less hemolytic activity than melittin. In particular, Pep3, an 11-mer peptide corresponding to cecropin A(2-8)-melittin(6-9), is effective as a bactericidal and fungicidal (4, 16) agent.

In the present work, we have evaluated the biological activity of Pep3 against *E. amylovora*, *X. vesicatoria*, and *P. syringae*. Although antimicrobial peptides have been tested against these pathogens (2, 39), to the best of our knowledge, inhibition of these bacteria by Pep3 or short synthetic peptides (≤11 residues) has not been previously reported. Our results showed that Pep3 inhibits growth of these plant-pathogenic bacteria at low micromolar concentrations (MIC of <10 μM).

Using Pep3 as a template, we have synthesized new analogues with improved biological properties. Inhibitory concentrations of peptides for the different bacteria varied significantly, with *X. vesicatoria* being the most susceptible pathogen. These results are in agreement with previous reports, which showed that *X. vesicatoria* was more susceptible than *P. syringae* and *E. carotovora* to peptides such as MII, MSI-99, and cecropin B (2). These different levels of susceptibility of bacteria to peptides with different amino acid sequences have been attributed to variation in the components of the plasma membranes of the target microorganism, e.g., charge and lipid composition, which would influence rates of binding of cationic peptides to the membranes (31).

The mechanism of action of antimicrobial peptides against gram-negative bacteria is thought to involve first the so-called "self-promoted uptake" pathway across the outer membrane (45). Then, cationic peptides interact with the negatively charged phospholipids of the inner membrane, followed by either channel formation or simple membrane disruption (7, 9, 11, 25, 29, 46, 49). Since the 11-residue hybrid peptide Pep3 is not long enough to span the entire width of the membrane, a "carpet-like" mechanism seems more plausible. In such a mechanism, peptides first lie parallel to the surface of the phospholipid bilayer with their hydrophobic sides facing the membranes and their cationic sides facing outside, and this is followed by membrane permeation/disintegration once a threshold concentration is reached (46). Therefore, it appears that the ability to adopt an amphipathic structure is important for activity of this type of peptide. Other parameters that modulate the activity are the degree of structure formation, the net positive charge, and the overall hydrophobicity. It has been shown that the accomplishment of these structural parameters is not stringently necessary for activity against several gram-negative bacteria, but rather a good balance between them is required. In the design of short peptides, a fine-tuning of charge, helix-forming propensity, an adequate hydrophobicity,

and, in particular, the number of aliphatic residues, is even more important (24).

The design of the peptides in the present work was based on the above-mentioned rationale. The amphipathic character of Pep3 becomes evident when it is represented as an ideal α-helix by means of an Edmunson wheel plot. Accordingly, analogues BP13 to BP20, BP33, and BP76 were designed based on this ideal α-helical wheel diagram. Replacement of amino acids located at the interface, e.g., Trp and Val, with residues with various degrees of hydrophilicity and hydrophobicity, resulted in great changes in antibacterial activity. Replacement of Trp in Pep3 with Phe or Tyr and acetylation, benzoylation, or tosylation of the N terminus of Pep3 decreased antibacterial activity, whereas replacement of Trp with Leu or Lys or benzylation induced a slight increase in the overall activity. Replacement of Val with hydrophobic aromatic residues afforded peptides considerably more active than Pep3 (BP18 to BP20), but when a Lys was incorporated, no activity was observed (BP17). Double replacement of both Trp and Val with Lys and Phe (BP76), respectively, induced a significant increase of antibacterial activity, whereas an increase in the size of the hydrophilic face by incorporation of two Lys residues (BP16) resulted in complete loss of activity. Consequently, structural features that seem to be important for the antibacterial activity are a basic N terminus and a hydrophobic C terminus. In contrast to antibacterial activity that was dramatically influenced by single- or double-residue replacement, the α-helical content of peptides was not significantly affected.

As previously described with other cationic peptides (25, 28) and unlike conventional antibiotics that in many cases are bacteriostatic, Pep3, BP11, BP15, BP33, and BP76 showed a bactericidal effect against the three bacteria tested at concentrations around the MIC.

Peptide cytotoxicity was also strongly influenced by the nature of the amino acid replacement in Pep3. Replacement of Trp in Pep3 with a cationic residue such as Lys produced the less hemolytic peptides BP15 and BP76. In contrast, derivatization of the N terminus of Pep3 or replacement of Val with more hydrophobic residues resulted in peptides with higher cytotoxicity. This result is in accordance with previous studies on antimicrobial peptides reporting that an increase in the peptide hydrophobicity is shown to be related to an increase in cytotoxicity (41). This selectivity has been attributed to the differences in membrane lipid composition between bacteria and mammalian cells. The absence of acidic phospholipids and presence of sterols reduce the susceptibility of eukaryotic cells to lytic peptides (35). Moreover, replacement of Trp with an aliphatic amino acid such as Leu (BP33) also led to a decrease in hemolytic activity. Peptides containing tryptophan residues have been previously reported to display high hemolytic activity, which has been attributed to the ability of tryptophan to assume a defined orientation when binding to cholesterol (10).

The peptides reported here are comparable in terms of activity to antibiotics, such as streptomycin, used in agriculture for bacterial disease control with an in vitro activity of 2 to 9 μM and operational doses for field treatment of around 100 μM. In the case of the best peptides described here, these concentrations are not expected to present toxic effects in regard to the HD_{50}.

Protease digestion stability is a desired property in antimicrobial peptides to assure a reasonable half-life of the molecules in the plant environment. Proteases from epiphytic microorganisms or intrinsic to the plant in internal tissues may degrade antimicrobial peptides (4, 16). Again, certain replacements of amino acids in Pep3 had a strong influence in susceptibility to protease digestion. N-terminal derivatization or single residue replacement did not improve the stability of Pep3. In contrast, double replacement of both Trp and Val with Lys and Phe, respectively, was associated with an important increase in peptide stability. The double replacement for natural amino acids were equivalent to methods commonly used to increase peptide stability such as replacement of a natural amino acid with a D-amino acid or peptide cyclization (30, 44).

In conclusion, we have obtained peptides effective against *E. amylovora*, *X. vesicatoria*, and *P. syringae*. Moreover, we have improved the bactericidal activity and minimized cytotoxic effects and sensitivity to protease degradation of the previously described antimicrobial peptide Pep3. Therefore, these peptides might be considered as potential lead compounds for the development of antimicrobial agents for use in plant protection either as pesticide ingredients or as agents expressed in transgenic plants. Optimization of their antimicrobial properties by combinatorial chemistry and ex vivo and in vivo studies are currently in progress.

REFERENCES

1. **Agrios, G. N.** 1998. Plant pathology, 4th ed. Academic Press, San Diego, Calif.
2. **Alan, A. R., and E. Earle.** 2002. Sensitivity of bacterial and fungal plant pathogens to the lytic peptides, MSI-99, magainin II, and cecropin B. Mol. Plant-Microbe Interact. **15:**701–708.
3. **Alberola, J., A. Rodríguez, O. Francino, X. Roura, L. Rivas, and D. Andreu.** 2004. Safety and efficacy of antimicrobial peptides against naturally acquired leishmaniasis. Antimicrob. Agents Chemother. **48:**641–643.
4. **Ali, G. S., and A. S. N. Reddy.** 2000. Inhibition of fungal and bacterial plant pathogens by synthetic peptides: in vitro growth inhibition, interaction between peptides, and inhibition of disease progression. Mol. Plant-Microbe Interact. **13:**847–859.
5. **Andreu, D., and R. B. Merrifield.** 1985. N-terminal analogues of cecropin A: synthesis, antibacterial activity, and conformational properties. Biochemistry **24:**1683–1688.
6. **Andreu, D., R. B. Merrifield, H. Steiner, and H. G. Boman.** 1983. Solid-phase synthesis of cecropin A and related peptides. Proc. Natl. Acad. Sci. USA **80:**6475–6479.
7. **Andreu, D., and L. Rivas.** 1998. Animal antimicrobial peptides: an overview. Biopolymers **47:**415–433.
8. **Andreu, D., J. Ubach, A. Boman, B. Wåhlin, D. Wade, R. B. Merrifield, and H. G. Boman.** 1992. Shortened cecropin A-melittin hybrids. Significant size reduction retains potent antibiotic activity. FEBS Lett. **296:**190–194.
9. **Bechinger, B.** 2004. Structure and function of membrane-lytic peptides. Crit. Rev. Plant Sci. **23:**271–292.
10. **Blondelle, S. E., and K. Lohner.** 2000. Combinatorial libraries: a tool to design antimicrobial and antifungal peptide analogues having lytic specificities for structure-activity relationship studies. Biopolymers **55:**74–87.
11. **Boman, H. G.** 2003. Antibacterial peptides: basic facts and emerging concepts. J. Intern. Med. **254:**197–215.
12. **Brodgen, K. A., M. Ackermann, P. B. McCray, Jr., and B. F. Tack.** 2003. Antimicrobial peptides in animals and their role in host defences. Int. J. Antimicrob. Agents **22:**465–478.
13. **Broekaert, W. F., B. P. A. Cammue, M. F. C. DeBolle, K. Thevissen, G. W. De Samblanx, and R. W. Osborn.** 1997. Antimicrobial peptides from plants. Crit. Rev. Plant Sci. **16:**297–323.

14. **Bulet, P., R. Stöcklin, and L. Menin.** 2004. Antimicrobial peptides: from invertebrates to vertebrates. Immunol. Rev. **198:**169–184.

15. **Cabrefiga, J., and E. Montesinos.** 2005. Analysis of aggressiveness of *Erwinia amylovora* using disease-dose and time relationships. Phytopathology **95:** 1430–1437.

16. **Cavallarin, L., D. Andreu, and B. San Segundo.** 1998. Cecropin A-derived peptides are potent inhibitors of fungal plant pathogens. Mol. Plant-Microbe Interact. **11:**218–227.

17. **Chicharro, C., C. Granata, R. Lozano, D. Andreu, and L. Rivas.** 2001. N-terminal fatty acid substitution increases the leishmanicidal activity of CA(1-7)M(2-9), a cecropin-melittin hybrid peptide. Antimicrob. Agents Chemother. **45:**2441–2449.

18. **Christensen, B., J. Fink, R. B. Merrifield, and D. Mauzerall.** 1988. Channel-forming peptides of cecropins and related model compounds incorporated into planar lipid membranes. Proc. Natl. Acad. Sci. USA **85:**5072–5076.

19. **Fink, J., R. B. Merrifield, A. Boman, and H. G. Boman.** 1989. The chemical synthesis of cecropin D and an analogue with enhanced antibacterial activity. J. Biol. Chem. **264:**6260–6267.

20. **Finney, D. J.** 1971. Probit analysis, 3rd ed. Cambridge University Press, Cambridge, United Kingdom.

21. **Ganz, T., and R. I. Lehrer.** 1998. Antimicrobial peptides of vertebrates. Curr. Opin. Immunol. **10:**41–44.

22. **García-Olmedo, F., A. Molina, J. M. Alamillo, and P. Rodríguez-Palenzuela.** 1998. Plant defense peptides. Biopolymers **47:**479–491.

23. **Giacometti, A., O. Cirioni, W. Kamysz, G. D'Amato, C. Silvestri, M. S. Del Prete, J. Lukasiak, and G. Scalise.** 2004. In vitro activity and killing effect of the synthetic hybrid cecropin A-melittin peptide CA(1-7)M(2-9)NH$_2$ on methicillin-resistant nosocomial isolates of *Staphylococcus aureus* and interactions with clinically used antibiotics. Diagn. Microbiol. Infect. Dis. **49:**197–200.

24. **Giangaspero, A., L. Sandri, and A. Tossi.** 2001. Amphipathic α helical antimicrobial peptides: a systematic study of the effects of structural and physical properties on biological activity. Eur. J. Biochem. **268:**5589–5600.

25. **Hancock, R. E. W.** 2001. Cationic peptides: effectors in innate immunity and novel antimicrobials. Lancet Infect. Dis. **1:**156–164.

26. **Hancock, R. E. W., and R. Lehrer.** 1998. Cationic peptides: a new source of antibiotics. Trends Biotechnol. **16:**82–88.

27. **Hancock, R. E. W., and A. Patrzykat.** 2002. Clinical development of cationic antimicrobial peptides: from natural to novel antibiotics. Curr. Drug Targets Infect. Disord. **2:**79–83.

28. **Hancock, R. E. W., and A. Rozek.** 2002. Role of membranes in the activities of antimicrobial cationic peptides. FEMS Microbiol. Lett. **206:**143–149.

29. **Hancock, R. E. W., and M. G. Scott.** 2000. The role of antimicrobial peptides in animal defenses. Proc. Natl. Acad. Sci. USA **97:**8856–8861.

30. **Hong, S. Y., J. E. Oh, and K.-H. Lee.** 1999. Effect of D-amino acid substitution on the stability, the secondary structure and the activity of membrane-active peptide. Biochem. Pharmacol. **58:**1775–1780.

31. **Huang, H. W.** 2000. Action of antimicrobial peptides: two-state model. Biochemistry **39:**8347–8352.

32. **Hultmark, D., A. Engstrom, H. Bennich, R. Kapur, and H. G. Boman.** 1982. Insect immunity: isolation and structure of cecropin D and four minor antibacterial components from *Cecropia pupae*. Eur. J. Biochem. **127:**207–217.

33. **Lee, D. G., Y. Park, I. Jin, K.-S. Hahm, H.-H. Lee, Y.-H. Moon, and E.-R. Woo.** 2004. Structure-antiviral activity relationships of cecropin A-magainin 2 hybrid peptide and its analogues. J. Pept. Sci. **10:**298–303.

34. **Loper, J. E., M. D. Henkels, R. G. Roberts, G. G. Grove, M. J. Willet, and T. J. Smith.** 1991. Evaluation of streptomycin, oxytetracycline and copper resistance of *Erwinia amylovora* isolated from pear orchards in Washington state. Plant Dis. **75:**287–290.

35. **Matsuzaki, K., K. Sugishita, N. Fujii, and K. Miyajima.** 1995. Molecular basis for membrane selectivity of antimicrobial peptide, magainin 2. Biochemistry **34:**3421–3429.

36. **Montesinos, E., and A. Bonaterra.** 1996. Dose-response models in biological control of plant pathogens: an empirical verification. Phytopathology **86:**856–863.

37. **Montesinos, E., P. Melgarejo, M. A. Cambra, and J. Pinochet (ed.).** 2000. Enfermedades de los frutales de pepita y hueso. Ediciones Mundi Prensa, Barcelona, Spain.

38. **Montesinos, E., and P. Vilardell.** 2001. Effect of bactericides, phosphonates and nutrient amendments on blast of dormant flower buds of pear: a field evaluation for disease control. Eur. J. Plant Pathol. **107:**787–794.

39. **Mourgues, F., M. Brisset, and E. Chevreau.** 1998. Activity of different antibacterial peptides on *Erwinia amylovora* growth, and evaluation of the phytotoxicity and stability of cecropins. Plant Sci. **139:**83–91.

40. **Ninot, A., N. Aletà, C. Moragrega, and E. Montesinos.** 2002. Evaluation of a reduced copper spraying program to control bacterial blight of walnut. Plant Dis. **86:**583–587.

41. **Oh, D., S. Y. Shin, S. Lee, J. H. Kang, S. D. Kim, P. D. Ryu, K.-S. Hahm, and Y. Kim.** 2000. Role of the hinge region and the tryptophan residue in the synthetic antimicrobial peptides, cecropin A(1-8)-magainin 2(1-12) and its analogues, on their antibiotic activities and structures. Biochemistry **39:** 11855–11864.

42. **Osuky, M., G. Zhou, L. Osuska, R. E. Hancock, W. W. Kay, and S. Misra.** 2000. Transgenic plants expressing cationic peptide chimeras exhibit broad-spectrum resistance to phytopathogens. Nat. Biotechnol. **18:**1162–1166.

43. **Otvos, L., Jr.** 2000. Antibacterial peptides isolated from insects. J. Pept. Sci. **6:**497–511.

44. **Rozek, A., J.-P. S. Powers, C. L. Friedrich, and R. E. W. Hancock.** 2003. Structure-based design of an indolicidin peptide analogue with increased protease stability. Biochemistry **42:**14130–14138.

45. **Sawyer, J. G., N. L. Martin, and R. E. W. Hancock.** 1988. Interaction of macrophage cationic proteins with the outer membrane of *Pseudomonas aeruginosa*. Infect. Immun. **56:**693–698.

46. **Shai, Y.** 2002. Mode of action of membrane active antimicrobial peptides. Biopolymers **66:**236–248.

47. **Steiner, H., D. Hultmark, A. Engstrom, H. Bennich, and H. G. Boman.** 1981. Sequence and specificity of two antibacterial proteins involved in insect immunity. Nature **292:**246–248.

48. **Sundin, G. W., and C. L. Bender.** 1993. Ecological and genetic analysis of copper and streptomycin resistance in *Pseudomonas syringae* pv. *syringae*. Appl. Environ. Microbiol. **59:**1018–1024.

49. **Tossi, A., L. Sandri, and A. Giangaspero.** 2000. Amphipathic, α-helical antimicrobial peptides. Biopolymers **55:**4–30.

50. **Wade, D., D. Andreu, S. A. Mitchell, A. M. V. Silveira, A. Boman, H. G. Boman, and R. B. Merrifield.** 1992. Antibacterial peptides designed as analogues or hybrids of cecropins and melittin. Int. J. Pept. Protein Res. **40:**429–436.

51. **Zasloff, M.** 2002. Antimicrobial peptides of multicellular organisms. Nature **415:**389–395.

Chapter III.2. A library of linear undecapeptides with bactericidal activity against phytopathogenic bacteria

A 125-member library of synthetic linear undecapeptides was prepared based on a previously described peptide K^{1}KLFKKILKF^{10}L-NH$_2$ (BP76) that inhibited *in vitro* growth of the plant pathogenic bacteria *Erwinia amylovora*, *Xanthomonas axonopodis* pv. *vesicatoria*, and *Pseudomonas syringae* pv. *syringae* at low micromolar concentrations. Peptides were designed using a combinatorial chemistry approach by incorporating amino acids possessing various degrees of hydrophobicity and hydrophilicity at positions 1 and 10 and by varying the N-terminus. Library screening for *in vitro* growth inhibition identified 27, 40 and 113 sequences with MIC values below 7.5 μM against *E. amylovora*, *P. syringae* and *X. vesicatoria*, respectively. Cytotoxicity, bactericidal activity and stability towards protease degradation of the most active peptides were also determined. Seven peptides with a good balance between antibacterial and hemolytic activities were identified. Several analogues displayed a bactericidal effect and low susceptibility to protease degradation. The most promising peptides were tested *in vivo* by evaluating their preventive effect of inhibition of *E. amylovora* infection in detached apple and pear flowers. The peptide KKLFKKILKYL-NH$_2$ (BP100) showed efficacies in flowers of 63–76% at 100 μM, being more potent than BP76 and only less effective than streptomycin, currently used for fire blight control.

Badosa, E., R. Ferre, M. Planas, L. Feliu, E. Besalú, J. Cabrefiga, E. Bardají,
E. Montesinos. 2007. A library of linear undecapeptides with bactericidal
activity against phytopathogenic bacteria. *Peptides* 28:2276-2285. (Impact
Factor: 2.4)

http://www.sciencedirect.com/science/journal/01969781

http://dx.doi.org/10.1016/j.peptides.2007.09.010

Chapter III.3. Sporicidal activity of synthetic undecapeptides and control of *Penicillium* rot of apples

The antifungal activity of cecropin A(2-8)-melittin(6-9) hybrid undecapeptides, previously reported as active against plant pathogenic bacteria, was studied. A set of 15 sequences was screened *in vitro* against *Fusarium oxysporum*, *Penicillium expansum*, *Aspergillus niger*, and *Rhizopus stolonifer*. Most compounds were highly active against *F. oxysporum* (MIC < 2.5 μM) but were less active against the other fungi. The best peptides were studied for their sporicidal activity and for Sytox green uptake in *F. oxysporum* microconidia. A significant inverse linear relationship was observed between survival and fluorescence, indicating membrane disruption. Next, we evaluated the *in vitro* activity against *P. expansum* of a 125-member peptide library with the general structure R-X^1KLFKKILKX^{10}L-NH$_2$, where X^1 and X^{10} corresponded to amino acids with various degrees of hydrophobicity and hydrophilicity and R included different N-terminal derivatizations. Fifteen sequences with MICs below 12.5 μM were identified. The most active compounds were BP21 {Ac,F,V} and BP34 {Ac,L,V} (MIC < 6.25 μM), where the braces denote R, X^1, and X^{10} positions and where Ac is an acetyl group. The peptides had sporicidal activity against *P. expansum* conidia. Seven of these peptides were tested *in vivo* by evaluating their preventative effect of inhibition of *P. expansum* infection in apple fruits. The peptide Ts-FKLFKKILKVL-NH$_2$ (BP22), where Ts is a tosyl group, was the most active with an average efficacy of 56% disease reduction, which was slightly lower than that of a commercial formulation of the fungicide imazalil.

Sporicidal Activity of Synthetic Antifungal Undecapeptides and Control of *Penicillium* Rot of Apples[▽]

Esther Badosa,[1] Rafael Ferré,[2] Jesús Francés,[1] Eduard Bardají,[2] Lidia Feliu,[2]
Marta Planas,[2] and Emilio Montesinos[1]*

Laboratory of Plant Pathology, Institute of Food and Agricultural Technology-CIDSAV-XaRTA,[1] and LIPPSO, Department of Chemistry,[2] University of Girona, Campus Montilivi, 17071 Girona, Spain

The antifungal activity of cecropin A(2-8)-melittin(6-9) hybrid undecapeptides, previously reported as active against plant pathogenic bacteria, was studied. A set of 15 sequences was screened in vitro against *Fusarium oxysporum*, *Penicillium expansum*, *Aspergillus niger*, and *Rhizopus stolonifer*. Most compounds were highly active against *F. oxysporum* (MIC < 2.5 μM) but were less active against the other fungi. The best peptides were studied for their sporicidal activity and for Sytox green uptake in *F. oxysporum* microconidia. A significant inverse linear relationship was observed between survival and fluorescence, indicating membrane disruption. Next, we evaluated the in vitro activity against *P. expansum* of a 125-member peptide library with the general structure R-X^{1}KLFKKILKX^{10}L-NH$_2$, where X^1 and X^{10} corresponded to amino acids with various degrees of hydrophobicity and hydrophilicity and R included different N-terminal derivatizations. Fifteen sequences with MICs below 12.5 μM were identified. The most active compounds were BP21 {Ac,F,V} and BP34 {Ac,L,V} (MIC < 6.25 μM), where the braces denote R, X^1, and X^{10} positions and where Ac is an acetyl group. The peptides had sporicidal activity against *P. expansum* conidia. Seven of these peptides were tested in vivo by evaluating their preventative effect of inhibition of *P. expansum* infection in apple fruits. The peptide Ts-FK LFKKILKVL-NH$_2$ (BP22), where Ts is a tosyl group, was the most active with an average efficacy of 56% disease reduction, which was slightly lower than that of a commercial formulation of the fungicide imazalil.

The discovery of antimicrobial compounds to treat plant diseases of economical importance in agriculture remains a major scientific challenge (1). Antimicrobial peptides are being considered as a good alternative to current fungicides and a great deal of scientific effort has been invested in studying their application in plant disease control (29, 34, 35).

Antimicrobial peptides have been reported to display interesting activities against pathogenic microbes that are resistant to conventional antibiotics and to exhibit a broad spectrum of activity against bacteria, fungi, enveloped viruses, parasites, and tumor cells (7–10, 19, 20, 40, 49). The mechanism of action of these peptides against fungi consists of cell lysis by binding to the membrane surface and disrupting its structure, interference with the synthesis of essential cell wall components, or interaction with specific internal targets (12, 13, 15, 23, 29).

Despite their good lytic activity, major concerns about the use of antimicrobial peptides as pesticides in plant protection are the high production cost associated with synthetic procedures and their low stability toward protease degradation. Several design strategies have been devised in order to find shorter and more stable peptides, while maintaining or increasing the activity with a low cytotoxicity. These strategies include the juxtaposition of fragments of natural antimicrobial peptides, the modification of natural peptides, and the de novo design of sequences maintaining the crucial features of native antimicro-bial peptides (2, 3, 11, 24, 32, 38, 42). However, the process involved in the development of lead candidates is time consuming and limited by the number of individual compounds that can be synthesized. Combinatorial chemistry has allowed the rapid preparation of synthetic libraries and their screening has led to the identification of peptides with high activity against selected phytopathogenic bacteria and fungi (4, 26, 27, 33).

During our current research oriented to the development of new antimicrobial agents for use in plant protection, we designed linear undecapeptides (CECMEL11) derived from the cecropin A-melittin hybrid peptide WKLFKKILKVL-NH$_2$ (Pep3) (5, 17). Using a combinatorial approach, we identified peptides with high activity against plant pathogenic bacteria, such as *Erwinia amylovora*, *Xanthomonas vesicatoria*, and *Pseudomonas syringae*, and with low susceptibility to protease degradation (4, 5).

In order to broaden the study, we decided to test the CECMEL11 peptides against the plant pathogenic fungi *Fusarium oxysporum*, *Aspergillus niger*, *Rhizopus stolonifer*, and *Penicillium expansum*. The fungus *F. oxysporum* causes *Fusarium* wilt in more than a hundred species of plants, and it is an important pathogen in horticultural crops (44). Several *Rhizopus* and *Penicillium* species cause soft rot and blue mold rot, respectively, which are important postharvest diseases in stone and pome fruits (6, 18, 22, 39). Apart from the economic losses, *Aspergillus* and *Penicillium* species are also of interest from a public health point of view due to the production of mycotoxins (45, 47). The importance of *Penicillium* species in the postharvest of fruits emphasizes the interest to develop antimicrobial peptides to control this fungus.

* Corresponding author. Mailing address: Laboratory of Plant Pathology, Institute of Food and Agricultural Technology-CIDSAV-XaRTA, University of Girona, Campus Montilivi, 17071 Girona, Spain. Phone: 34-972-418427. Fax: 34-972-418399. E-mail: emonte @intea.udg.edu.

TABLE 1. Antifungal activity and hemolytic activity of selected linear undecapeptides

Peptide	Sequence	MIC (μM)				% Hemolysis[a]
		F. oxysporum	*P. expansum*	*A. niger*	*R. stolonifer*	
Pep3	WKLFKKILKVL-NH$_2$	2.5–5.0	15–20	5.0–7.5	10–12.5	56 ± 4.7
BP1	WKLFKKILKVL-OH	20–25	>100	20–25	>100	0.0
BP8	Ac–WKLFKKILKVL-NH$_2$	1.2–2.5	7.5–10	15–20	>100	96 ± 5.2
BP9	Ts-WKLFKKILKVL-NH$_2$	1.2–2.5	15–20	20–25	50–100	76 ± 3.5
BP10	Bz-WKLFKKILKVL-NH$_2$	5.0–7.5	20–25	20–25	>100	73 ± 3.4
BP11	Bn-WKLFKKILKVL-NH$_2$	1.2–2.5	25–50	20–25	>100	90 ± 1.8
BP13	FKLFKKILKVL-NH$_2$	1.2–2.5	25–50	20–25	50–100	15 ± 3.9
BP14	YKLFKKILKVL-NH$_2$	1.2–2.5	25–50	15–20	50–100	30 ± 3.0
BP15	KKLFKKILKVL-NH$_2$	0.6–1.2	12.5–15	5.0–7.5	7.5–10	16 ± 2.9
BP16	KKLFKKILKKL-NH$_2$	0.6–1.2	>100	20–25	50–100	0
BP17	WKLFKKILKKL-NH$_2$	1.2–2.5	50–100	20–25	25–50	25 ± 2.2
BP18	WKLFKKILKWL-NH$_2$	1.2–2.5	20–25	20–25	25–50	68 ± 6.3
BP19	WKLFKKILKFL-NH$_2$	1.2–2.5	20–25	20–25	25–50	95 ± 3.3
BP20	WKLFKKILKYL-NH$_2$	0.6–1.2	20–25	15–20	25–50	77 ± 1.3
BP33	LKLFKKILKVL-NH$_2$	0.3–0.6	25–50	20–25	25–50	37 ± 2.7
BP76	KKLFKKILKFL-NH$_2$	0.6–1.2	25–50	20–25	25–50	34 ± 2.1

[a] Percent hemolysis at 150 μM. The confidence interval for the mean is included.

Taking into account the relevance of these pathogens, the aim of the present study was the analysis of the antifungal activity profile of the CECMEL11 peptides in order to identify sporicidal sequences against the above fungi. As a proof of concept, the feasibility of using such peptides to protect fruits from fungal spoilage was evaluated using a *P. expansum*/apple model.

MATERIALS AND METHODS

Peptide synthesis. All peptides were synthesized as previously described by the solid-phase method using 9-fluorenylmethoxycarbonyl (Fmoc)-type chemistry, *tert*-butyloxycarbonyl side chain protection for Lys and Trp, and *tert*-butyl for Tyr (4, 5, 17). Fmoc-Rink-4-methylbenzhydrylamine resin (0.64 mmol/g) was used as solid support to obtain C-terminal peptide amides and 4-hydroxymethylphenoxypropionic acid polyethylene glycol-polystyrene resin (0.23 mmol/g) to synthesize the C-terminal peptide acid. Couplings of the Fmoc amino acids (3 eq) were mediated by *N*-[(1*H*-benzotriazol-1-yl)(dimethylamino)methylene]-*N*-methylmethanaminium hexafluorophosphate *N*-oxide (HBTU) (3 eq) and *N,N*-diisopropylethylamine (DIEA) (3 eq) in *N,N*-dimethylformamide (DMF) and monitored by a ninhydrin test. The Fmoc group was removed by treating the resin with a mixture of piperidine-DMF (3:7). Acetylation was performed by treatment with acetic anhydride-pyridine-CH$_2$Cl$_2$ (1:1:1). Tosylation was carried out by treatment with *p*-toluenesulphonyl chloride (40 eq) and DIEA (80 eq) in CH$_2$Cl$_2$–*N*-methyl-2-pyrrolidinone (CH$_2$Cl$_2$-NMP) (9:1). Benzoylation was performed by treatment with benzoyl chloride (40 eq) and DIEA (80 eq) in CH$_2$Cl$_2$-NMP (9:1). Benzylation was achieved by treatment with benzyl bromide (40 eq) and DIEA (80 eq) in CH$_2$Cl$_2$-NMP (9:1). Peptides were cleaved from the resin with trifluoroacetic acid-H$_2$O-triisopropylsilane (95:2.5:2.5) and were obtained with >90% high-performance liquid chromatography purity. Electrospray ionization mass spectrometry was used to confirm peptide identity.

Fungal strains and growth media. The following plant pathogenic fungal strains were used: *Penicillium expansum* EPS 26 (INTEA, University of Girona), *Fusarium oxysporum* f. sp. *lycopersici* FOL 3 race 2 (ATCC 201829; American Type Culture Collection), *Aspergillus niger* (CECT 2694; Colección Española de Cultivos Tipo), and *Rhizopus stolonifer* (CECT 2344). The strains were cultured on potato dextrose agar (PDA) plates (Difco) using aseptic procedures to avoid contamination. Conidia from fungal mycelium (except for *F. oxysporum*) were obtained from 5-day-old PDA cultures of the fungus incubated at 25°C. The inoculum was prepared by scraping spore material from the culture surfaces with a wet cotton swab and resuspending it in distilled water containing 0.5% of Tween 80. Microconidia of *F. oxysporum* were obtained from 1-week-old potato dextrose broth (PDB) cultures (Oxoid) of the fungus incubated at 25°C in the dark in a rotary shaker at 125 rpm. After incubation, the culture was filtered through several layers of sterile cheesecloth to eliminate macroconidia and mycelial growth of the fungus. Then, the effluent was centrifuged at 8,000 × *g* for 20 min at 4°C, and the pellet was resuspended in sterile water. The concentration of conidia was determined using a hemacytometer and adjusted to 10^4 conidia ml^{-1} for *F. oxysporum*, 10^3 conidia ml^{-1} for *P. expansum* and *A. niger*, and 10^2 conidia ml^{-1} for *R. stolonifer*.

Antifungal activity. The lyophilized peptides listed in Table 1 were solubilized in sterile Milli-Q water to a final concentration of 1 mM and filter sterilized through a 0.22-μm-pore filter (Sartorius). For MIC assessment, stock solutions of peptides were prepared at different concentrations. Antifungal activity was tested on *F. oxysporum*, *P. expansum*, *A. niger*, and *R. stolonifer*. Twenty microliters of each stock solution was mixed in a microtiter plate well with 80 μl of the corresponding suspension of the fungal pathogen and 100 μl of double-concentrated PDB to a total volume of 200 μl containing 0.003% (wt/vol) of chloramphenicol. The final peptide concentrations assayed were 100, 50, 25, 20, 15, 12.5, 10, 7.5, 5, 2.5, 1.2, 0.6, and 0.3 μM. Three replicates for each strain, peptide, and concentration combination were used. Positive controls contained water instead of peptide, and negative controls contained peptides without the fungal pathogen. Microbial growth was automatically determined by optical density measurement at 600 nm (Bioscreen C; Labsystems, Helsinki, Finland). Microplates were incubated at 20°C with 1 min/9 min on/off shaking cycles, and the measurements were done every 2 h for 6 days. The MIC was taken as the lowest peptide concentration without growth at the end of the experiment.

The 125-member peptide library was tested for antifungal activity on *P. expansum* at final concentrations of 25, 12.5, and 6.25 μM, as described above.

Fungicidal activity against nongerminated *F. oxysporum* and *P. expansum* conidia. Stock solutions of peptides were prepared at different concentrations. Microconidial suspensions of *F. oxysporum* and *P. expansum* were adjusted to 8 × 10^6 conidia ml^{-1}, as described above. The test tubes contained 190 μl of the conidial suspension, 100 μl of the corresponding peptide concentration, and 710 μl of 50-fold diluted PDB. The final peptide concentrations assayed were 20, 15, 10, 5, and 2.5 μM for *F. oxysporum* and 25, 12.5, and 6.25 μM for *P. expansum*. After mixing, the test tubes were incubated for 35 min (*F. oxysporum*) or 180 min (*P. expansum*) at 25°C and 10-fold serially diluted, and aliquots of 100 μl from suitable dilutions were spread in triplicate on PDA plates. The sample dilution and additional dilution into the total amount of medium contained on the PDA plate were sufficient to prevent residual activity of the peptide. Viable colonies were counted after incubation for 3 days at 25°C. Values were expressed as percentages of survival from the start of the experiment.

Effect of peptides on Sytox green uptake by *F. oxysporum* conidia. A suspension of *F. oxysporum* conidia in 20-fold-diluted PDB (180 μl, 5 × 10^5 conidia ml^{-1}) was dispensed into microtiter plate wells. Subsequently, 20 μl of the corresponding peptide stock solution, as described above for fungicidal activity, was added, and the plates were incubated for 24 h at 25°C. Then, Sytox green was added to a final concentration of 0.2 μM, and the plates were incubated for 1 h at 25°C to stabilize the fluorescence. Sytox green uptake was determined by fluorometric measurement with a microplate reader (Varioskan, Ascent FL; Labsystems, Finland), recording the fluorescence spectra between 510 and 580 nm. The controls were prepared with water instead of peptide. Three replicates for each

treatment were prepared. The fluorescence increase with respect to that of the control was calculated at 528 nm. Dose-response curves for each peptide were generated by plotting the fluorescence increase against the peptide concentration.

Hemolytic activity. The hemolytic activity of peptides was evaluated at 150 μM. Hemoglobin release from erythrocyte suspensions of fresh human blood (5%, vol/vol) was determined using the absorbance at 540 nm, as previously described (17).

Inhibition of *P. expansum* infections in apple fruits. Golden apples were collected at harvest time from a commercial orchard near Girona, Spain, washed, surface-disinfected by immersion for 1 min in a diluted solution of sodium hypochlorite (1% active chlorine), and washed two times by immersion in distilled water. The excess of water was subsequently removed under airflow. The fruits were wounded with a cork borer, making six wounds per fruit of approximately 5 mm^2 and a 10-mm depth.

Preliminary tests were performed to evaluate the phytotoxicity and effective concentrations, using treated-uninoculated, nontreated-inoculated, and treated-inoculated treatments. The tests were carried out at 200 and 500 μM peptide concentrations.

For the main trial, peptide treatments were applied by depositing 50 μl of a 300 μM solution in each wound. Appropriate controls consisted of nontreated fruits and of fruits treated with the reference fungicide imazalil at the recommended concentration (375 μM Fungaflor [20%, wt/vol]; Janssen Pharmaceutica NV, Berse, Belgium). After the peptide or fungicide was completely absorbed, the wounds were inoculated with 20 μl of a *P. expansum* EPS26 spore suspension at 10^3 conidia ml^{-1}. Three replicates of three fruits per replicate were prepared for each treatment. The apples were placed in polystyrene tray packs that were fit into boxes and maintained at 20°C. The lesion diameter was measured after 11 days of pathogen inoculation. The experiment was repeated twice. The data were analyzed using the general linear model procedure of the Statistical Analysis System (SAS version 9.1.2, 2009). To correct variance heterogeneity, the values were arcsine transformed before the analysis. A Tukey multiple range test (*P* = 0.05) was conducted to separate the means of the lesion diameter values for individual treatments in both experiments.

RESULTS

Evaluation of the antifungal activity of a set of CECMEL11 undecapeptides. In a first screening, a set of 15 peptides was studied (Table 1). They are C-terminal amide 11-residue sequences except for BP1, which is a C-terminal acid peptide. Peptides BP8 to BP11 are derivatized at the N termini with an acetyl (Ac), tosyl (Ts), benzoyl (Bz), or benzyl (Bn) group, respectively. Analogues BP13 to BP20, BP33, and BP76 differ on the residues at positions 1 and 10, including amino acids with various degrees of hydrophobicity and hydrophilicity.

These peptides were screened in vitro for antifungal activity against *F. oxysporum*, *P. expansum*, *A. niger*, and *R. stolonifer* (Table 1). All sequences exhibited antifungal activity (MIC < 25 μM) against at least two pathogens. *F. oxysporum* was particularly sensitive to the peptides. Thirteen out of 15 sequences were more active against *F. oxysporum* than Pep3 with MICs below 2.5 μM. BP33 was the most active peptide (MIC of 0.3 to 0.6 μM), four sequences (BP15, BP16, BP20, and BP76) displayed antifungal activity within 0.6 and 1.2 μM, and eight peptides showed MICs ranging from 1.2 to 2.5 μM. The benzoylated peptide BP10 was slightly less active (MIC of 5.0 to 7.5 μM), while the C-terminal acid peptide BP1 displayed the lowest activity (MIC of 20 to 25 μM).

In the case of *P. expansum*, three peptides exhibited antifungal activity with MICs below 20 μM. Among them, analogues BP8 and BP15 were the most active (MIC of 7.5 to 10 and 12.5 to 15 μM, respectively), displaying higher activity than Pep3 (MIC of 15 to 20 μM). Peptides BP1 and BP16 were inactive up to a concentration of 100 μM. Among the peptides active against *A. niger*, four sequences showed antifungal ac-
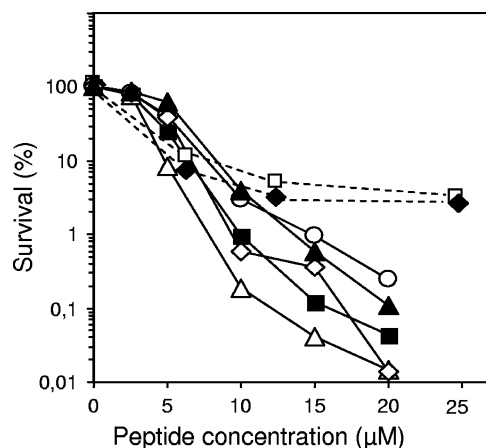

FIG. 1. Sporicidal activity of peptides Pep3 (▲), BP15 (○), BP20 (■), BP33 (△), and BP76 (◇) on *F. oxysporum* conidia (solid lines) and of peptides BP21 (□) and BP22 (◆) on *P. expansum* conidia (dashed lines). Conidial suspensions were treated with peptides and incubated for 35 min (*F. oxysporum*) or 180 min (*P. expansum*) at 25°C. Viable spores were counted after dilution and plating in PDA. Values are expressed as percentages of survival from the start of the experiment.

tivity below 20 μM. The best activity was observed for peptide BP15, being as active as Pep3 (MIC of 5.0 to 7.5 μM). *R. stolonifer* was the least sensitive fungi. Only BP15 exhibited an antifungal activity below 20 μM, being more active (MIC of 7.5 to 10 μM) than Pep3 (MIC of 10 to 12.5 μM). Four sequences were not active against this fungus (MIC > 100 μM), including the C-terminal acid peptide BP1 and the N-terminal-derivatized peptides BP8, BP10, and BP11.

The toxicity of this peptide set to red blood cells is included in Table 1. When tested at 150 μM, two of these peptides (BP1 and BP16) were not hemolytic, six sequences showed a low to moderate level of hemolysis (<50%), and seven were more hemolytic (>50%). Interestingly, BP15, which displayed a high activity against all fungi tested, exhibited a low hemolysis (16%).

The fungicidal activities of the most active peptides, BP15, BP20, BP33, and BP76, were evaluated against *F. oxysporum* by comparing the survival of the conidia after 35 min of exposure at different peptide concentrations (Fig. 1). Pep3 was included for comparison purposes. At concentrations around the MIC (<5.0 μM), all peptides exhibited a similar behavior, whereas an increase of peptide concentration led to a different logarithmic pattern for each sequence. BP76, BP33, and BP20 were more potent than Pep3. Notably, BP33 was the most sporicidal, causing a 3- to 4-log survival reduction at 10 to 20 μM in 35 min.

The membrane permeation of *F. oxysporum* conidia by peptides Pep3, BP15, BP20, BP33, and BP76 was studied by determining the fluorescence increase observed on suspensions of the conidia after treatment with different peptide concentrations and Sytox green (Fig. 2). In all cases, fluorescence increased rapidly with peptide concentration, following a dose-response saturation relationship. The maximum values of fluorescence were achieved at 10 to 20 μM. BP20 was the most potent peptide in terms of the fluorescence-increase response, displaying a higher value than Pep3. Moreover, conidia sur-
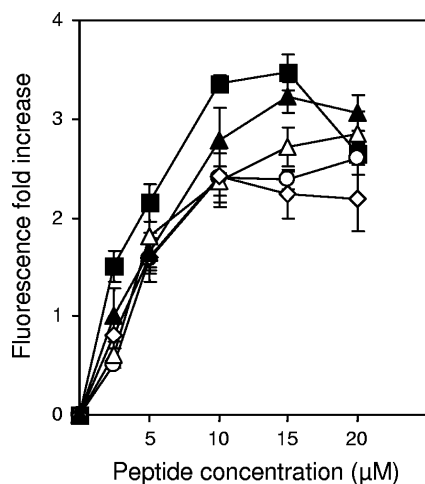
FIG. 2. Effect of peptides Pep3 (▲), BP20 (■), BP33 (△), BP15 (○) or BP76 (◇) on Sytox green uptake by *F. oxysporum* conidia. Conidia were incubated with peptides in 20-fold-diluted PDB at 25°C for 24 h; then, Sytox green was added and incubated for an additional h at 25°C and fluorescence determined at 528 nm. Values are expressed as fluorescence increases and are the means of three replicates. Bars represent the confidence intervals for the means.

vival was plotted against fluorescence increase (Fig. 3). Interestingly, survival percentage correlated significantly with Sytox green uptake ($y = 100.3 - 35.46x$; $R^2 = 0.88$), indicating that probably membrane disruption is the primary mechanism of action.

Evaluation of a 125-member peptide library against *P. expansum*. The general structure of the peptide library was R-X^{1}KLFKKILKX^{10}L-NH$_2$, where X^1 and X^{10} corresponded to amino acids with various degrees of hydrophobicity and hydrophilicity and R included different N-terminal derivatizations. The library was designed by combining five variations at each R, X^1, and X^{10} position as follows: at the R position, H, Ac, Ts, Bz, or Bn; at the X^1 position, Lys, Leu, Trp, Tyr, or Phe; and at the X^{10} position, Lys, Val, Trp, Tyr, or Phe (4). Library members are denoted using braces, such as {R,X^1,X^{10}}, which define the variations at each R, X^1, and X^{10} position. This library was screened in vitro for antifungal activity against *P. expansum* (Fig. 4). Fifty-four sequences displayed activity below 25 μM. In general, peptides with Ac at
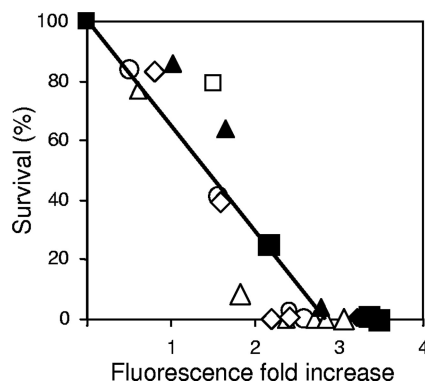

FIG. 3. Relationship between sporicidal activity and Sytox green uptake in *F. oxysporum* conidia treated with peptides Pep3 (▲), BP20 (■), BP33 (△), BP15 (○), or BP76 (◇).
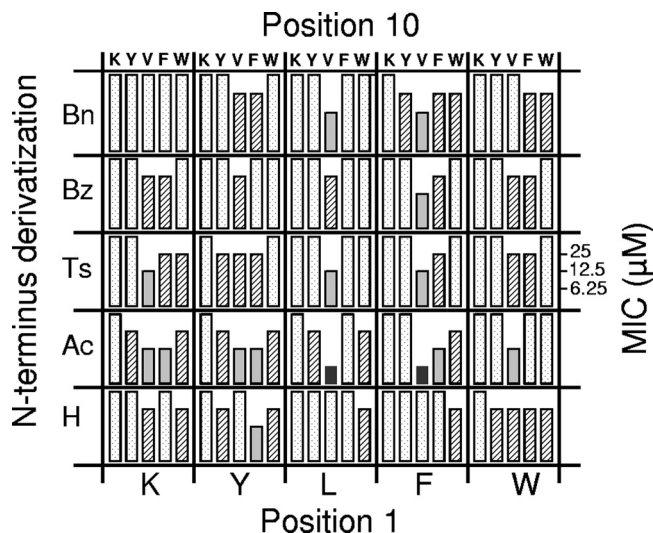

FIG. 4. MICs of the 125-member peptide library against *P. expansum* in full-strength PDB. Amino acids with various degrees of hydrophilicity and hydrophobicity (X^1 and X^{10}) and N-terminal derivatizations (R) were introduced in the sequence R-X^{1}KLFKKILKX^{10}L-NH$_2$. Derivatization corresponds to acetylation (Ac), tosylation (Ts), benzoylation (Bz), and benzylation (Bn). Solid black bars stand for a MIC of <6.5 μM, shaded bars for a MIC of 6.25 to 12.5 μM, striped bars for a MIC of 12.5 to 25 μM, and dotted bars for a MIC of >25 μM.

the R position and Val at the X^{10} position were associated with high activity. Peptides BP21 {Ac,F,V} and BP34 {Ac,L,V} were the most active with MICs below 6.25 μM. Thirteen sequences showed moderate activity (MICs of 6.25 to 12.5 μM), and 39 peptides displayed low activity (MICs of 12.5 to 25 μM). The fungicidal activities of BP21 and BP22 {Ts,F,V} against *P. expansum* were evaluated (Fig. 1). These peptides were sporicidal, but a longer exposure (180 min) was necessary to kill the conidia, compared to that for *F. oxysporum* (35 min). The hemolysis of the peptides with a MIC of <25 μM ranged from 35 to 96% at 150 μM. Peptides BP21, BP22, and BP34, which exhibited high antifungal activity, showed 85, 73, and 45% hemolysis at this concentration, respectively. Although these hemolytic activities are significant, they are similar to that observed for the reference fungicide imazalil, which ranges from 53 to 77% at 150 μM.

Inhibition of *P. expansum* infection in apple fruits. First, the influence of the sequence of peptide application and pathogen inoculation on the inhibition of *P. expansum* infections in apple fruits was evaluated. The following three protocols were compared: (i) peptide BP76 was preventatively applied to the wound before spore inoculation, (ii) it was mixed with spores and immediately applied, or (iii) it was mixed with spores, preincubated, and subsequently applied (Fig. 5). The results showed that the protocol used had a significant effect on the inhibition of infection. BP76 was highly effective when mixed with spores and preincubated, whereas it was ineffective when applied preventatively. Despite these results, the preventative strategy was chosen because it mimics the treatments used for field control of plant diseases.

Next, the most active peptides were tested at 200 and 500 μM using the preventative treatment. The results showed that even
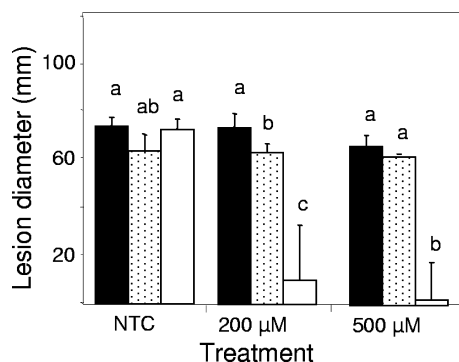
FIG. 5. Effect of the strategy of peptide application and pathogen inoculation on infection by *P. expansum* in apple wounds. The peptide BP76 was assayed following three protocols: (i) applied to wounds 1 h before pathogen inoculation (preventative, black bars); (ii) mixed with spores of the pathogen and immediately applied to wounds (simultaneous, dotted bars); or (iii) mixed with spores and preincubated for 10 h before treatment (simultaneous with preincubation, white bars). The confidence intervals for the means are indicated at the tops of the bars. Letters over the bars for a given treatment indicate significant differences according to the mean separation test.
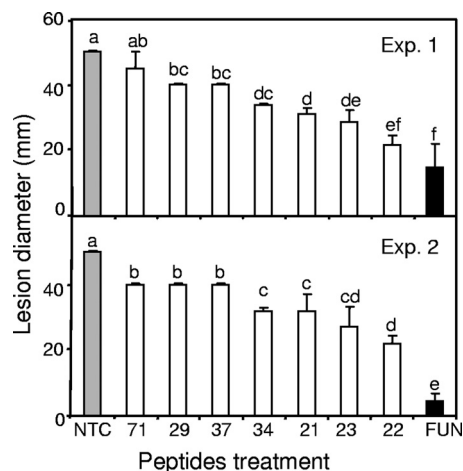

FIG. 6. Effect of the preventative application of peptides in wounds of apple fruits on *P. expansum* infection. Wounds were treated with peptides at 300 μM and inoculated with conidia, and rot lesion diameter was determined after 11 days of incubation at 20°C. Two experiments were performed. A nontreated control (NTC) and a reference treatment with the fungicide imazalil (FUN) (375 μM) were used. The confidence intervals for the means are indicated at the tops of the bars. Letters over the bars for a given treatment indicate significant differences according to the mean separation test.

though peptides were effective at both concentrations, they were not sufficiently discriminated (data not shown). Therefore, a peptide concentration of 300 μM and a preventative strategy were used in the following assays. Notably, peptides did not produce symptoms of phytotoxicity when applied to apple wounds at the above concentrations.

Finally, the inhibitory activity of the peptides against *P. expansum* infection was evaluated. Two experiments were performed. All peptides tested (BP21 {Ac,F,V}, BP22 {Ts,F,V}, BP23 {Bz,F,V}, BP29 {Ac,K,V}, BP34 {Ac,L,V}, BP37 {Bn,L,V}, and BP71 {H,Y,F}) significantly decreased apple rot lesion size at 300 μM compared to that of the nontreated control, except for BP71 in the first experiment (Fig. 6). The most active peptide in both experiments was BP22 with an average efficacy of 56% disease reduction. This efficacy was not significantly different than that of a commercial formulation of the reference fungicide imazalil in the first experiment, but it was lower in the second experiment.

DISCUSSION

Synthetic cecropin A (2-8)-melittin (6-9) hybrid undecapeptides (CECMEL11) with the general structure R-X^{1}KLFKKILKX^{10}L-NH$_2$ were evaluated against *Fusarium oxysporum*, *Penicillium expansum*, *Aspergillus niger*, and *Rhizopus stolonifer*. Sequences highly active in vitro against *F. oxysporum* (MIC < 2.5 μM) and *P. expansum* (MIC < 12.5 μM) were found. To compare the potency of these peptides with other reported antifungal sequences, it has to be taken into account that the type of culture medium influences the MICs. For example, the hexapeptide PAF26 exhibited a MIC of 4 to 6 μM when tested against *Penicillium digitatum* in 10- to 20-fold-diluted PDB (36–38), whereas the MIC increased to 20 to 40 μM when using undiluted broth (27). Using the latter conditions, other synthetic hexapeptides (26) and the antimicrobial peptide MSI99 (2) showed MICs of 20 to 80 μM against the fungal species *P. digitatum*, *Botrytis cinerea*, and *F. oxysporum*. The

best CECMEL11 peptides were highly active against *P. expansum* in spite of the fact that the assays were performed using undiluted broth. This is in agreement with the reported activity for two of our peptides against *P. digitatum* (37).

Spores are resting structures of fungi with high survival capacity under adverse conditions and are the most difficult stages to control (43). Therefore, the sporicidal activity of antifungal peptides is critical for efficient control of fungal diseases. Several CECMEL11 antifungal peptides have been found to be sporicidal against *F. oxysporum* and *P. expansum* at concentrations around the MIC. Notably, the best peptides killed 99 to 99.9% of the *F. oxysporum* spores in 35 min at 20 μM. These results correspond to decimal reduction times of 10 to 15 min, which are comparable with the ones reported for currently used antiseptics and disinfectants (30). Moreover, the correlation observed between sporicidal activity and Sytox green uptake suggests that fungal membrane disruption could be the primary mode of action. A similar behavior has been described for other antifungal peptides such as tetralipopeptides (28), the hexapeptide PAF26 (36), and several cecropin-derived peptides (11, 14). However, a correlation between cell permeation and antimicrobial activity is not always observed, because some antimicrobial peptides do not disrupt bacterial membranes or have additional modes of action, including intracellular targets (16, 31, 46, 48).

Antimicrobial peptides derived from natural compounds or de novo designed have been reported to be antibacterial, antifungal, or both (29, 34). The screening of the CECMEL11 library against plant pathogenic bacteria and fungi led to the identification of peptides covering all possibilities. When the library was tested against plant pathogenic bacteria, a set of 15 peptides with high antibacterial activity was identified (4). The evaluation of the library for activity against *P. expansum* led to the identification of another set of 15 peptides displaying high

antifungal activity. The two sets had four peptides in common, with both high antibacterial and antifungal activities. As a matter of example, peptide BP100 was strongly antibacterial but poorly antifungal, BP21 displayed strong antifungal activity but poor antibacterial activity, and BP15 was both antibacterial and antifungal.

Our results confirm previous data on how subtle changes in a peptide sequence influence antimicrobial activity (4, 27, 33). The specificity observed for antimicrobial peptides has been reported to depend on both the peptide and the microorganism tested (41). Among the parameters that modulate peptide activity are the ability to adopt an amphipathic structure, the net positive charge, and the overall hydrophobicity (21). In particular, we previously found that the CECMEL11 peptides with the highest antibacterial activity shared the following structural features: a net charge of $+4$ to $+6$, a Lys at position 1, and an aromatic residue at position 10. Moreover, N-terminal derivatization led to less active peptides (4). In contrast, different structural requirements were associated with high antifungal activity against *P. expansum*. The best peptides bear a charge of $+4$ or $+5$ and a valine at position 10 and were N-terminal acetylated. On the other hand, the features of the target membrane that may influence peptide specificity are the structure, the length, and the complexity of the hydrophilic polysaccharide in its outer layer. Based on the results obtained in this study, it is tempting to speculate that subtle lipid composition differences of fungal membranes (or conidial walls) are responsible for the different activity and specificity profiles of the CECMEL11 peptides.

Among the sequences with highest in vitro antifungal activity against *P. expansum*, peptide Ts-FKLFKKILKVL-NH$_2$ (BP22), when applied preventatively to apple wounds, showed an efficacy slightly lower than that of a commercial fungicide formulation of imazalil. This lower efficacy could be attributed to the inactivation of the peptide and to not being formulated. A certain degree of peptide inactivation by intracellular fluids or cell compounds is expected. In fact, it has been reported that plant protein extracts or intracellular fluids of tomato or tobacco strongly decrease the activity of antimicrobial peptides (11). On the other hand, in many reports, the in vivo tests are performed by inoculating a mixture of fungal spores and the peptide into a wound made into the plant material. In contrast, CECMEL11 peptides were applied into the wound and absorbed by fruit tissues, and subsequently, the pathogen was inoculated into the treated site. Obviously, in the first approach, the peptide has more chance to interact with the target, leading to a dramatic decrease of the number of live cells that are inoculated and, thus, giving disease overcontrol. This could explain that, in our case, a higher peptide concentration (300 µM) was necessary to control apple infections than that reported for peptides inoculated as a mixture with spores (100 to 200 µM) (37). However, a preventative strategy is more realistic because it mimics the standard application of commercial fungicides, such as imazalil, in postharvest rot control. Moreover, it has been described that formulation can greatly improve the antimicrobial activity of pesticides (25). In this study, unlike imazalil, which was used as a commercial formulation, CECMEL11 peptides were applied as aqueous solutions.

Toxicity to animal or plant cells is always a problem with

antimicrobial peptides targeted to bacteria or fungi when the mechanism of action is based on the interaction with cell membranes. Even though the hemolytic activity of CECMEL11 peptides was significant at 150 µM, this concentration is around 30 times the MIC, and it is of the same order as that of the reference fungicide imazalil.

In conclusion, the reported technology seems to be feasible because the effective doses of the CECMEL11 peptides are of the same order as those of current fungicides, and despite being unformulated, their level of efficacy is only slightly lower. The major challenge of this research is to meet the requirement of a low production cost for these antimicrobial peptides for food and agricultural use. Molecular farming of these peptides is currently under development and evaluation.

REFERENCES

1. **Agrios, G. N.** 1998. Plant pathology, 4th ed. Academic Press, San Diego, CA.
2. **Alan, A. R., and E. Earle.** 2002. Sensitivity of bacterial and fungal plant pathogens to the lytic peptides, MSI-99, magainin II, and cecropin B. Mol. Plant-Microbe Interact. **15:**701–708.
3. **Ali, G. S., and A. S. N. Reddy.** 2000. Inhibition of fungal and bacterial plant pathogens by synthetic peptides: in vitro growth inhibition, interaction between peptides, and inhibition of disease progression. Mol. Plant-Microbe Interact. **13:**847–859.
4. **Badosa, E., R. Ferre, M. Planas, L. Feliu, E. Besalú, J. Cabrefiga, E. Bardají, and E. Montesinos.** 2007. A library of linear undecapeptides with bactericidal activity against phytopathogenic bacteria. Peptides **28:**2276–2285.
5. **Bardají, E., E. Montesinos, E. Badosa, L. Feliu, M. Planas, and R. Ferre.** April 2006. Antimicrobial linear peptides. Patent WO/2007/125142 A1.
6. **Bonaterra, A., M. Mari, L. Casallini, and E. Montesinos.** 2003. Biological control of *Monilinia laxa* and *Rhizopus stolonifer* in postharvest stone fruit by *Pantoea agglomerans EPS125* and putative mechanisms of antagonism. Int. J. Food Microbiol. **84:**93–104.
7. **Broekaert, W. F., B. P. A. Cammue, M. F. C. DeBolle, K. Thevissen, G. W. De Samblanx, and R. W. Osborn.** 1997. Antimicrobial peptides from plants. Crit. Rev. Plant Sci. **16:**297–323.
8. **Brogden, K. A.** 2005. Antimicrobial peptides: pore formers or metabolic inhibitors in bacteria? Nat. Rev. Microbiol. **3:**238–250.
9. **Brogden, K. A., M. Ackermann, P. B. McCray, Jr., and B. F. Tack.** 2003. Antimicrobial peptides in animals and their role in host defences. Int. J. Antimicrob. Agents **22:**465–478.
10. **Bulet, P., R. Stöcklin, and L. Menin.** 2004. Antimicrobial peptides: from invertebrates to vertebrates. Immunol. Rev. **198:**169–184.
11. **Cavallarin, L., D. Andreu, and B. San Segundo.** 1998. Cecropin A-derived peptides are potent inhibitors of fungal plant pathogens. Mol. Plant-Microbe Interact. **11:**218–227.
12. **De Lucca, A. J., and T. J. Walsh.** 1999. Antifungal peptides: novel therapeutic compounds against emerging pathogens. Antimicrob. Agents Chemother. **43:**1–11.
13. **De Lucca, A. J., and T. J. Walsh.** 2000. Antifungal peptides: origin, activity and therapeutic potential. Rev. Iberoam. Micol. **17:**116–120.
14. **DeLucca, A. J., J. M. Bland, T. J. Jacks, C. Grimm, T. E. Cleveland, and T. J. Walsh.** 1997. Fungicidal activity of cecropin A. Antimicrob. Agents Chemother. **41:**481–483.
15. **Deshayes, S., M. C. Morris, G. Divita, and F. Heitz.** 2005. Cell-penetrating peptides: tools for intracellular delivery of therapeutics. Cell. Mol. Life Sci. **62:**1839–1849.
16. **Epand, R. M., and H. J. Vogel.** 1999. Diversity of antimicrobial peptides and their mechanisms of action. Biochim. Biophys. Acta **1462:**11–28.
17. **Ferre, R., E. Badosa, L. Feliu, M. Planas, E. Montesinos, and E. Bardají.** 2006. Inhibition of plant-pathogenic bacteria by short synthetic cecropin A-melittin hybrid peptides. Appl. Environ. Microbiol. **72:**3302–3308.
18. **Francés, J., A. Bonaterra, M. C. Moreno, J. Cabrefiga, E. Badosa, and E. Montesinos.** 2006. Pathogen aggressiveness and postharvest biocontrol efficiency in *Pantoea agglomerans*. Postharvest Biol. Technol. **39:**299–307.
19. **Ganz, T., and R. I. Lehrer.** 1998. Antimicrobial peptides of vertebrates. Curr. Opin. Immunol. **10:**41–44.

20. **García-Olmedo, F., A. Molina, J. M. Alamillo, and P. Rodríguez-Palenzuela.** 1998. Plant defense peptides. Biopolymers **47:**479–491.

21. **Giangaspero, A., L. Sandri, and A. Tossi.** 2001. Amphipathic alpha-helical antimicrobial peptides: a systematic study of the effects of structural and physical properties on biological activity. Eur. J. Biochem. **268:**5589–5600.

22. **Hernández-Lauzardo, A. N., S. Baustista-Baños, M. G. Velázquez-del Valle, M. G. Méndez-Montealvo, M. M. Sánchez-Rivera, and L. A. Bello-Pérez.** 2008. Antifungal effects of chitosan with molecular weights on in vitro development of *Rhizopus stolonifer* (Ehrenb.:Fr.) Vuill. Carbohydr. Polym. **73:**541–547.

23. **Jenssen, H., P. Hamill, and R. E. W. Hancock.** 2006. Peptide antimicrobial agents. Clin. Microbiol. Rev. **19:**491–511.

24. **Kamysz, W., A. Krolicka, K. Bogucka, T. Ossowski, J. Lukasiak, and E. Lojkowska.** 2005. Antibacterial activity of synthetic peptides against plant pathogenic *Pectobacterium* species. J. Phytopathol. **153:**313–317.

25. **Knowles, D. A.** 1998. Chemistry and technology of agricultural formulations. Kluwer Academic, London, United Kingdom.

26. **López-García, B., L. González-Candelas, E. Pérez-Payá, and J. F. Marcos.** 2000. Identification and characterization of a hexapeptide with activity against phytopathogenic fungi that cause postharvest decay in fruits. Mol. Plant-Microbe Interact. **13:**837–846.

27. **López-García, B., E. Pérez-Payá, and J. F. Marcos.** 2002. Identification of novel hexapeptides bioactive against phytopathogenic fungi through screening of a synthetic peptide combinatorial library. Appl. Environ. Microbiol. **68:**2453–2460.

28. **Makovitzki, A., D. Avrahami, and Y. Shai.** 2006. Ultrashort antibacterial and antifungal lipopeptides. Proc. Natl. Acad. Sci. USA **103:**15997–16002.

29. **Marcos, J., A. Muñoz, E. Pérez-Payá, S. Misra, and B. López-García.** 2008. Identification and rational design of novel antimicrobial peptides for plant protection. Annu. Rev. Phytopathol. **46:**271–301.

30. **Mazzola, P. G., T. C. Vessoni, and A. M. Martins.** 2003. Determination of decimal reduction time (D value) of chemical agents used in hospitals for disinfection purposes. BMC Infect. Dis. **3:**24.

31. **McPhee, J. B., M. G. Scott, and R. E. W. Hancock.** 2005. Design of host defence peptides for antimicrobial and immunity enhancing activities. Comb. Chem. High Throughput Screen. **8:**257–272.

32. **Monroc, S., E. Badosa, L. Feliu, M. Planas, E. Montesinos, and E. Bardají.** 2006. De novo designed cyclic peptides as inhibitors of plant pathogenic bacteria. Peptides **27:**2567–2574.

33. **Monroc, S., E. Badosa, E. Besalú, M. Planas, E. Bardají, E. Montesinos, and L. Feliu.** 2006. Improvement of cyclic decapeptides against plant pathogenic bacteria using a combinatorial chemistry approach. Peptides **27:**2575–2584.

34. **Montesinos, E.** 2007. Antimicrobial peptides and plant disease control. FEMS Microbiol. Lett. **270:**1–11.

35. **Montesinos, E., and E. Bardají.** 2008. Synthetic antimicrobial peptides as agricultural pesticides for plant-disease control. Chem. Biodivers. **5:**1225–1237.

36. **Muñoz, A., B. López-García, and J. F. Marcos.** 2006. Studies on the mode of action of the antifungal hexapeptide PAF 26. Antimicrob. Agents Chemother. **50:**3847–3855.

37. **Muñoz, A., B. López-García, and J. F. Marcos.** 2007. Comparative study of antimicrobial peptides to control citrus postharvest decay caused by *Penicillium digitatum*. J. Agr. Food Chem. **55:**8170–8176.

38. **Muñoz, A., and J. F. Marcos.** 2006. Activity and mode of action against fungal phytopathogens of bovine lactoferricin-derived peptides. J. Appl. Bacteriol. **101:**1–9.

39. **Ogawa, J. M., E. I. Zehr, G. W. Bird, D. F. Ritchie, K. Uriu, and J. K. Uyemoto (ed.).** 1995. Compendium of stone fruit diseases. APS Press, St. Paul, MN.

40. **Otvos, L., Jr.** 2000. Antibacterial peptides isolated from insects. J. Pept. Sci. **6:**497–511.

41. **Papo, N., and Y. Shai.** 2003. Exploring peptide membrane interaction using surface plasmon resonance: differentiation between pore formation versus membrane disruption by lytic peptides. Biochemistry **42:**458–466.

42. **Powell, W. A., C. M. Catranis, and C. A. Maynard.** 1995. Synthetic antimicrobial peptide design. Mol. Plant-Microbe Interact. **8:**792–794.

43. **Russell, A. D., W. D. Hugo, and G. A. J. Ayliffe (ed.).** 1982. Principles and practice of disinfection, preservation and sterilization. Blackwell Science, Oxford, United Kingdom.

44. **Scheffknecht, S., R. Mammerler, S. Steinkellner, and H. Vierheilig.** 2006. Root exudates of mycorrhizal tomato plants exhibit a different effect on microconidia germination of *Fusarium oxysporum f. sp. lycopersici* than root exudates from nonmycorrhizal tomato plants. Mycorrhiza **6:**365–370.

45. **Sholberg, P. L., and W. S. Conway.** 2004. Postharvest pathology. *In* K. C. Gross, C. Y. Wang, and M. Saltveit (ed.), Agriculture handbook number 66: the commercial storage of fruits, vegetables, and florist and nursery stocks. U.S. Department of Agriculture (USDA), Agricultural Research Service (ARS), Washington, DC. http://www.ba.ars.usda.gov/hb66/contents.html.

46. **Steffen, H., S. Rieg, I. Wiedemann, H. Kalbacher, A. Deeg, H. G. Sahl, A. Peschel, F. Götz, C. Garbe, and B. Schittek.** 2006. Naturally processed dermcidin-derived peptides do not permeabilize bacterial membranes and kill microorganisms irrespective of their charge. Antimicrob. Agents Chemother. **50:**2608–2620.

47. **Weidenbörner, M.** 2001. Encyclopedia of food mycotoxins. Springer, Berlin, Germany.

48. **Yount, N. Y., and M. R. Yeaman.** 2005. Immunocontinuum: perspectives in antimicrobial peptide mechanisms of action and resistance. Protein Pept. Lett. **12:**49–67.

49. **Zasloff, M.** 2002. Antimicrobial peptides of multicellular organisms. Nature **415:**389–395.

Chapter IV. Study of the mode of action of the antimicrobial peptide BP100

Chapter IV.1. Synergistic effects of the membrane actions of cecropin-melittin antimicrobial hybrid peptide BP100

BP100 (KKLFKKILKYL-NH$_2$) is a short cecropin A-melittin hybrid peptide, obtained through a combinatorial chemistry approach, which is highly effective in inhibiting both the *in vitro* and *in vivo* growth of economically important plant pathogenic Gram-negatives. The intrinsic Tyr fluorescence of BP100 was taken advantage of to study the peptide's binding affinity and damaging effect on phospholipid bilayers modeling the bacterial and mammalian cytoplasmic membranes. *In vitro* cytotoxic effects of this peptide were also studied on mammalian fibroblast cells. Results show a stronger selectivity of BP100 toward anionic bacterial membrane models as indicated by the high obtained partition constants, one order of magnitude greater than for the neutral mammalian membrane models. For the anionic systems, membrane saturation was observed at high peptide/lipid ratios and found to be related with BP100-induced vesicle permeabilization, membrane electroneutrality, and vesicle aggregation. Occurrence of BP100 translocation was unequivocally detected at both high and low peptide/lipid ratios using a novel and extremely simple method. Moreover, cytotoxicity against mammalian models was reached at a concentration considerably higher than the minimum inhibitory concentration. Our findings unravel the relationships among the closely coupled processes of charge neutralization, permeabilization, and translocation in the mechanism of action of antimicrobial peptides.

Synergistic Effects of the Membrane Actions of Cecropin-Melittin Antimicrobial Hybrid Peptide BP100

Rafael Ferre,[†] Manuel N. Melo,[‡] Ana D. Correia,[‡] Lidia Feliu,[†] Eduard Bardají,[†] Marta Planas,[†] and Miguel Castanho[‡*]

[†]Laboratori d'Innovació en Processos i Productes de Síntesi Orgànica, Departament de Química, Universitat de Girona, Girona, Spain; and [‡]Instituto de Medicina Molecular, Faculdade de Medicina, Universidade de Lisboa, Lisbon, Portugal

ABSTRACT   BP100 (KKLFKKILKYL-NH$_2$) is a short cecropin A-melittin hybrid peptide, obtained through a combinatorial chemistry approach, which is highly effective in inhibiting both the in vitro and in vivo growth of economically important plant pathogenic Gram-negatives. The intrinsic Tyr fluorescence of BP100 was taken advantage of to study the peptide's binding affinity and damaging effect on phospholipid bilayers modeling the bacterial and mammalian cytoplasmic membranes. In vitro cytotoxic effects of this peptide were also studied on mammalian fibroblast cells. Results show a stronger selectivity of BP100 toward anionic bacterial membrane models as indicated by the high obtained partition constants, one order of magnitude greater than for the neutral mammalian membrane models. For the anionic systems, membrane saturation was observed at high peptide/lipid ratios and found to be related with BP100-induced vesicle permeabilization, membrane electroneutrality, and vesicle aggregation. Occurrence of BP100 translocation was unequivocally detected at both high and low peptide/lipid ratios using a novel and extremely simple method. Moreover, cytotoxicity against mammalian models was reached at a concentration considerably higher than the minimum inhibitory concentration. Our findings unravel the relationships among the closely coupled processes of charge neutralization, permeabilization, and translocation in the mechanism of action of antimicrobial peptides.

INTRODUCTION

Antimicrobial peptides (AMPs) form an essential part of the innate immune system of virtually all forms of life (1–7). During the last decades, AMPs have been widely studied, as they may become an alternative to conventional antibiotics, especially for the treatment of drug-resistant infections (8, 9). Hundreds of AMPs have been isolated (see a comprehensive list at http://www.bbcm.univ.trieste.it/~tossi/pag1.htm) and several thousands have been de novo designed and synthetically produced. They display a wide range of biological activities against bacteria, fungi, protozoa, enveloped viruses, and even tumor cells (9–14). Interestingly, they retain activity against antibiotic-resistant strains and do not readily elicit resistance (15–17).

Despite displaying extensive sequence heterogeneity, most AMPs share two functionally important features: a net positive charge and the ability to assume an amphipathic structure. These structural characteristics are essential for the mode of action of most AMPs, which target the microbial membrane. The net positive charge promotes their binding to the anionic microbial surface, while the amphipathic structure favors peptide insertion into the membrane (10–12,15,16,18–20). Despite extensive studies, the precise mechanism of peptide-membrane interaction and cell killing has not been firmly established for many AMPs. Several models have been proposed to account for the morphological

changes involved in AMPs-mediated membrane disruption, such as pore formation (21), cell lysis (22), or peptide translocation into the cytoplasm (23). Recently, some studies have shown that, apart from membrane damage, other mechanisms may be involved including intracellular targets (9,15,16). However, in such mechanisms, peptides still must traverse the cell membrane to reach their site of action, which stresses the relevance of peptide-membrane interactions for AMP activity.

Cecropins, first isolated from the hemolymph of the giant silk moth *Hyalophora cecropia*, are some of the best studied AMPs (24–26). They represent a family of peptides composed of 31–39 amino acids with antibacterial activity against both Gram-negative and Gram-positive bacteria. Cecropins do not exhibit cytotoxic effects against human erythrocytes and other eukaryotic cells, but are susceptible to protease degradation (24,27,28). In an effort to overcome the high production costs of such long peptides and to improve their biological properties, short peptide analogs have been designed and synthesized. These studies have led to the identification of nontoxic and more stable peptide sequences displaying a broader and higher activity than their natural counterparts (29–36). In particular, the undecapeptide WKLFKKILKVL-NH$_2$ (Pep3), derived from the well-known cecropin A(1–7)-melittin(2–9) hybrid (30,33,34), has been found to be sufficient for antifungal and antibacterial activities, while displaying low cytotoxicity (32,37–40).

Recently, we have identified cecropin A-melittin hybrid undecapeptides derived from Pep3 which inhibit in vitro growth of economically important plant pathogenic bacteria such as *Erwinia amylovora*, *Pseudomonas syringae*

pv. *syringae*, and *Xanthomonas axonopodis* pv. *vesicatoria* (38–40). In particular, KKLFKKILKYL-NH$_2$ (BP100), obtained through a combinatorial chemistry approach, displays a bactericidal effect against these bacteria as well as minimized cytotoxicity and low susceptibility to proteinase K degradation (38). Moreover, BP100 is highly effective to prevent infections of *E. amylovora* in pear and apple flowers, being only slightly less potent than streptomycin, which is the most active compound currently used in fire blight control (38).

Although it has been proposed that the mode of action of cecropins and melittin depends on the peptide concentration and membrane composition (41–45), the mechanisms involved in the action of cecropin-melittin hybrid peptides, and especially that of short undecapeptides, are very far from being completely understood. Insights into the mode of action of BP100 are essential for the full rationalization of the biological properties of this peptide as well as for their further improvement. In this study, we investigated the interaction of BP100 with different model membranes using spectroscopic methodologies, which can afford valuable information about peptide-membrane interaction. A comprehensive study was carried out to ascertain the conditions under which BP100 disrupts membranes or, alternatively, translocates across them to reach the lumen of vesicles. Moreover, the in vitro cytotoxic effects of this peptide were also studied on mammalian fibroblast cells.

MATERIALS AND METHODS

Reagents and apparatus

The ultraviolet-visible absorption and steady-state fluorescence emission assays were performed at room temperature in a model No. V-560 UV-Vis spectrophotometer (JASCO, Hachioji, Japan) and in a model No. IBH FL3-22-time-correlated single photon-counting (TCSPC) spectrofluorometer (Horiba Jobin Yvon, Longjumeau, France), equipped with a 450 W Xe lamp and double monochromators, or in a Cary Eclipse Thermo Spectronic spectrofluorometer (Varian, Palo Alto, CA), equipped with a 75 kW pulsed Xe lamp. Multiwell absorption measurements were performed in a Multiskan RC plate reader (Labsystems, Helsinki, Finland). Time-resolved fluorescence decays were collected in the FL3-22-TCSPC spectrofluorometer using a time-correlated single photon counting (TCSPC) technique with a 279-nm nanoLED source (IBH, Glasgow, UK); reduction of scattered light contribution to the decays was achieved by horizontally polarizing the excitation light with a Glan-Thompson polarizer; lifetimes were calculated from time-resolved fluorescence intensity decays using at least 10 K counts in the peak channel; fluorescence intensity decay curves were deconvoluted with the software package DAS 6.1 from IBH.

Dynamic light scattering and ζ-potential measurements were taken in a Zetasizer Nano-ZS (Malvern Instruments, Worcestershire, UK), equipped with a 633-nm HeNe laser.

We used 2-(4-(2-hydroxyethyl)-1-piperazinyl)-ethanesulfonic acid (HEPES), sodium chloride, chloroform, ethanol (spectroscopic grade), acrylamide, dimethyl sulfoxide, and trypan blue (Merck, Darmstadt, Germany). Phospholipids 1-palmitoyl-2-oleoyl-*sn*-glycero-3-phosphocholine (POPC) and 1-palmitoyl-2-oleoyl-*sn*-glycero-3-(phosphor-rac-(1-glycerol)) (POPG) were from Avanti Polar Lipids (Alabaster, AL). Cholesterol, cell culture media, serum, antimicrobials, trypsin/versine, 3-(4,5-dimethylthiazol-2-yl)-2,5-diphenyl-2*H*-tetrazolium bromide (MTT), and crystal violet stain were from Sigma (St. Louis, MO). Lipophilic quenchers 5- and 16-NS (5- and 16-doxylstearic acids, respectively) were from Aldrich Chemical (Milwaukee, WI).

All the 9-fluorenylmethoxycarbonyl (Fmoc)-amino acid derivatives, reagents, and solvents used in the peptide synthesis were obtained from Senn Chemicals International (Gentilly, France). Fmoc-Rink-4-methylbenzhydrylamine resin (0.64 mmol/g) was purchased from Novabiochem (Darmstadt, Germany). Trifluoroacetic acid, *N*-methyl-2-pyrrolidinone, and triisopropylsilane were from Sigma-Aldrich (Madrid, Spain). Piperidine and *N*,*N*-diisopropylethylamine were purchased from Fluka (Buchs, Switzerland). Solvents for high-performance liquid chromatography (HPLC) were obtained from J.T. Baker (Deventer, Holland).

Solutions were prepared in a 10 mM HEPES buffer at pH 7.4, containing 150 mM NaCl (the so-called physiologic ionic strength). All BP100 fluorescence measurements were recorded at an excitation wavelength of 275 nm, except for the experiments involving acrylamide in which the peptide was excited at 285 nm to minimize the relative quencher/fluorophore light absorption ratio.

Peptide synthesis

BP100 was synthesized as a C-terminal carboxamide on a Rink *p*-methylbenzhydrylamine resin by the solid-phase synthesis method using standard 9-fluorenylmethoxycarbonyl (Fmoc) chemistry (38). The peptide was purified by reverse-phase semipreparative HPLC on a 5 μm, 1.0 × 25 cm C18 Tracer column (Teknokroma, Barcelona, Spain) using a linear gradient from 10 to 60% acetonitrile in water with 0.1% trifluoroacetic acid over 50 min. The peptide was obtained with >95% HPLC purity. Electrospray ionization mass spectrometry was used to confirm peptide identity.

Preparation of model membrane vesicles

Large unilamellar vesicles (LUVs) of 100-nm diameter and multilamellar vesicles (MLVs) of different phospholipid composition were used as biological membrane models. MLVs were obtained by hydration of dried phospholipid films under vortex agitation; when required, multilamellarity was enhanced by first hydrating the films in a fraction of the final volume. LUVs were prepared by freezing-thawing and extruding MLVs, as described elsewhere (46). Sonication of vesicles, when needed, was carried out in an Ultrasound Technology UP200S power sonicator (Hielscher Ultrasonics, Teltow, Germany). Mammalian model systems included 100% POPC LUVs and 2:1 POPC/cholesterol LUVs. Bacterial model systems included 2:1 and 4:1 POPG/POPC LUVs.

Photophysical characterization of BP100 in aqueous solution

The linear dependence of the absorbance and fluorescence intensity of BP100 on its concentration was tested over the 0–140 μM range. To check whether peptide aggregation occurs in the aqueous phase, the Tyr fluorescence was quenched by sequentially adding aliquots of a 4 M acrylamide solution to a 15 μM peptide sample, while recording both the absorbance and fluorescence intensity. Quenching assays data were analyzed according to the Stern-Volmer formalism (47) and were corrected for simultaneous light absorption of fluorophore and quencher (48).

Peptide-membrane incorporation studies

The extent of the partition of BP100 to each model membrane was evaluated by titrating a 15 μM peptide solution with the corresponding LUVs suspension and recording the fluorescence emission. Samples were incubated for 10 min after each addition of lipid suspension. The molar ratio partition constants, K_p, were calculated by fitting the experimental data with Eq. 1, as described elsewhere (49). The quantities I_W and I_L are the fluorescence intensities the mixture would display if all the peptide is in the aqueous or

the lipidic phase, respectively; γ_L is the phospholipid molar volume, which is considered to be 0.763 M^{-1}, corresponding to the typical value for liquid crystalline lipid bilayers (50); and [L] is the phospholipid concentration. Fluorescence data were corrected both for dilution and scattered light (51),

$$\frac{I}{I_W} = \frac{1 + K_p \gamma_L \frac{I_L}{I_W}[L]}{1 + K_p \gamma_L [L]}, \tag{1}$$

$$K_p = \frac{[BP100]_L}{[BP100]_W}, \tag{2}$$

where $[BP100]_L$ and $[BP100]_W$ are the peptide concentrations in the lipid volume or in the aqueous phase, respectively. It should be noted that because K_p implicitly includes electrostatic contributions that may be dependent upon the global peptide concentration, it should be taken as an apparent partition constant (52).

Membrane saturation studies were carried out with 2:1 POPG/POPC LUVs. Saturation points were determined by adding small aliquots of a 750 μM stock peptide solution to an LUV suspension (phospholipid concentrations of 0, 40, 75, 125, 175, and 250 μM) containing 100 mM acrylamide. The fluorescence emission was recorded after 10 min of each peptide addition. To prevent dilution of acrylamide, the stock peptide solution also contained 100 mM of this aqueous phase quencher. The peptide/lipid (P/L) ratio at saturation (σ) and K_p were calculated by fitting the obtained saturation points with Eq. 3, as described elsewhere (53):

$$[P] = \frac{\sigma}{K_p \gamma_L} + \sigma[L]. \tag{3}$$

In-depth membrane localization studies

Differential quenching studies were carried out by sequentially adding aliquots of a lipophilic quencher—either 5-NS or 16-NS—to a LUV suspension previously equilibrated with 10 μM BP100; two different LUV concentrations—125 and 250 μM—were used so as to set either saturation or nonsaturation states and quencher concentration was increased or reduced accordingly; time-resolved fluorescence measurements of the Tyr in BP100 were taken. To prevent bilayer alterations while adding the 5- and 16-NS quencher aliquots, prepared in ethanol, care was taken to keep final ethanol concentrations below 2% (v/v) (54). Results were analyzed with a methodology based on the knowledge of the quenchers' in-depth distributions in the membrane (55), modified to implement a least-squares fitting to the data.

Vesicle permeabilization studies

The kinetics of BP100-induced vesicle leakage was monitored by Co^{2+} quenching of the fluorescence of 1% N-NBD-PE (56) incorporated into 125 μM 2:1 POPG/POPC vesicles, at BP100 concentrations ranging from 0 to 25 μM. Briefly, experiments were carried out by adding aliquots of BP100 to a suspension of vesicles in the presence of 20 mM CoCl$_2$. The CoCl$_2$, which is unable to permeate phospholipid membranes, was added to the vesicles shortly before the measurement, quenching the outer leaflet N-NBD-PE fluorescence. The kinetics were started with the addition of BP100. Permeabilization of the membrane to the Co^{2+} ions results in further quenching of the inner leaflet N-NBD-PE population. The decrease of NBD fluorescence emission intensity at 515 nm was monitored with excitation at 460 nm. The percentage of leakage at time t after peptide addition was determined from Eqs. 4–6,

$$\% \ leakage \ (t) = [Co^{2+}]_{in}(t) / [Co^{2+}]_{out}(t)$$
$$\approx [Co^{2+}]_{in}(t) / [Co^{2+}]_{TOTAL}, \tag{4}$$

where $[Co^{2+}]_{TOTAL}$, $[Co^{2+}]_{in}$, and $[Co^{2+}]_{out}$ correspond to the global, luminal, and external quencher concentrations, respectively. The approxima-

tion of $[Co^{2+}]_{out}(t)$ as $[Co^{2+}]_{TOTAL}$ can be made because no significant decrease of external quencher concentration is expected upon leakage: at these lipid concentrations, the total internal vesicle volume can be calculated to be <0.005% of the sample volume (57). From the collisional quenching Stern-Volmer formulation (58), quencher concentrations can be related with fluorescence intensities,

$$\% \ leakage \ (t) = \frac{-\Delta I_{in}(t)}{I_{in}(t) \times K_{SV}} \div \frac{-\Delta I_{max}}{I_c \times K_{SV}} = \frac{I_c \times \Delta I_{in}(t)}{I_{in}(t) \times \Delta I_{max}} \tag{5}$$

where K_{SV} is the Stern-Volmer quenching constant, I_{in} is the contribution of inner leaflet fluorophores to the global fluorescence intensity, ΔI_{in} is the change in I_{in} after peptide addition, ΔI_{max} is the maximum change in global fluorescence from before quencher addition to complete leakage, and I_c corresponds to the minimum fluorescence intensity at 100% leakage, obtained by vesicle sonication. There are two populations contributing to the global fluorescence: the inner and outer leaflet fluorophores; because the external quencher concentration remains virtually constant, the fluorescence intensity of the outer fluorophore fraction will also be approximately constant and $\Delta I = \Delta I_{in}$, where ΔI is the change in global intensity upon peptide addition. In addition, from the moment of quencher addition, the external fraction decreases to its minimum possible fluorescence intensity which, given the large size of a vesicle, is roughly one-half of I_c. This allows the substitution of $I_{in}(t)$ as $I(t) - 0.5 \times I_c$,

$$\% \ leakage \ (t) = \frac{I_c \times \Delta I(t)}{(I(t) - 0.5I_c) \times (I_c - I_{pre})}, \tag{6}$$

where I_{pre} is the global fluorescence intensity before quencher addition.

Leakage kinetics were tentatively fitted with the system of ordinary differential equations described in Gregory et al. (59).

Membrane translocation studies

To determine the occurrence and extent of peptide translocation across the membrane a novel method was devised: the increase of BP100 fluorescence upon membrane interaction was followed after MLV addition. A control experiment was performed in which the interaction kinetic was instead initiated with LUVs produced from the same suspension of MLVs. In the occurrence of translocation, the interaction kinetic with the MLVs would be slowed down with respect to LUV interaction due to the multiple membrane crossing steps. In the absence of translocation, although the lipid concentration is the same in MLV and LUV suspensions, the peptide would sense an apparently lower concentration of lipid in an MLV suspension, as only the outer lipid shell is accessible; as such, fluorescence would never increase as much with MLVs as with LUVs (see Fig. 1 for details). A quantity of 40 μM 2:1 POPG/POPC LUVs and MLVs were used. The sensitivity in the detection of peptide-lipid interaction was improved by adding aliquots of 200 mM of acrylamide to increase the fluorescence change upon binding. Potential artifactual increases of BP100 emission due to scattered light contribution were controlled by monitoring the ratio of fluorescence intensities at 303 and 330 nm.

Vesicle aggregation and charge studies

Turbidity studies were carried out by monitoring the changes induced by BP100 in the optical density (OD) of a vesicle suspension. Briefly, aliquots of a 1 mM BP100 stock solution were added to 125 μM 2:1 POPG/POPC vesicle suspensions. Peptide concentrations tested ranged from 0 to 21 μM. The OD was recorded at 450 nm every 2 s for 30 min after peptide addition.

Dynamic light scattering measurements were carried out in similar conditions as the OD measurements. BP100 concentrations ranged from 0 to 16.5 μM. The ζ-potential measurements were performed at 250 μM lipid and at BP100 concentrations up to membrane saturation.
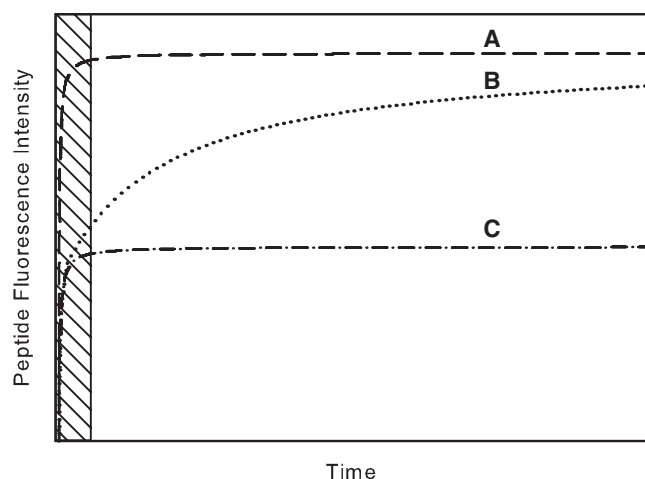
FIGURE 1 Expected fluorescence increase kinetics of BP100 in interaction with LUVs or MLVs. (*A*) LUVs with or without the occurrence of translocation: the entire lipid is accessible to the peptide at time 0 resulting in a fast interaction kinetics. (*B*) MLVs, with peptide translocation: at time 0, only a fraction of the lipid is accessible to the peptide, resulting in a fast, but partial, increase in fluorescence; as the peptide translocates, more lipid becomes accessible, and a full fluorescence increase is eventually reached at a lower rate. (*C*) MLVs, without translocation: there is a fast interaction with the accessible fraction of lipid, but no subsequent increase is expected, as no more lipid becomes accessible. The hatched region indicates the approximate relative measurement dead time for BP100 under our setup.

Cytotoxicity assays

Cell culture

V79 Chinese hamster lung fibroblast cells (MZ subline (60)) were used for the cytotoxicity assays (61). They were routinely cultured in 175 cm^2 tissue flasks in Ham's F-10 medium, supplemented with 10% newborn calf serum and 1% penicillin/streptomycin, in a humidified incubator at 37°C with 5% CO$_2$. Cells were routinely subcultured in the semiconfluent state over a maximum of eight passages and regularly tested negative for *Mycoplasma*. The V79 cells used in this study were kindly obtained from Prof. H. Glatt (German Institute of Human Nutrition, Germany) and were routinely maintained and kindly provided by Dr. Nuno Oliveira (University of Lisbon, Portugal).

Exposure conditions in the assays

V79 cells were suspended in 180 μL culture medium in 96-well plates, at a density of 5×10^3 cells/well, optimized to keep the cultures in optimal growth during the whole experiment. After seeding, the plates were incubated for 24 h before the experiment. BP100 was dissolved in HEPES and added to 20 μL of the medium to obtain final concentrations of 90, 60, 40, 30, and 10 μM. Two replicates for each peptide concentration were used. Each plate contained a negative control (culture medium + 10% HEPES) and a positive control (culture medium + 10 mM H$_2$O$_2$). Cell viability was measured after incubation for 24 h at 37°C with 5% CO$_2$.

Cell viability assays

Three assays were performed to test the cell viability. The MTT assay was used to investigate the effect of BP100 on the mitochondrial dehydrogenase activity, measured as the ability of viable cells to produce formazan crystals (62). The cells were rinsed once with phosphate-buffered saline and then 200 μL MTT solution (5 mg/ml) were added to each well. After 2.5 h incubation at 37°C, 200 μL dimethyl sulfoxide were added to each well to dissolve the purple formazan crystals (63). The absorbance of the resulting dispersion was determined at 595 nm in the multiwell scanning spectrophotometer.

Crystal violet is a dye that accumulates in the cell nucleus and was applied in this study as an indicator for cell viability (62). The fixed dye correlates directly with the nuclear DNA content, and thus also with the cell number. After its application, nonviable, nonadherent cells were washed. The fixed crystal violet was solubilized in 10% SDS for 20 min and the OD of the solution was measured at 595 nm.

The ability of cells to stain with trypan blue was used to investigate the loss of plasma membrane integrity (64). The cells were washed with phosphate-buffered saline, dispersed with 40 μL trypsin EDTA and the resulting cell suspension was diluted in 10 μL of culture medium. 20 μL of the mixed cell suspension were added to 20 μL of 0.4% trypan blue fresh solution, prepared in NaCl 0.9%, to stain nonviable cells. Cell viability was expressed as the percentage of unstained cells (65).

Statistical analysis and regression modeling

To account for the interplate variability, the absolute values of the cell viable parameters were normalized to the average of the negative controls (100% viability) and the positive controls (0% viability, corresponding to 100% cell death) (64). Statistical concentration-response analyses were performed in the same way for all three in vitro tests by fitting a three-parameter nonlinear regression Logit model to the data (66). Dunnett's test ($\alpha = 5\%$) was employed to determine statistical significant differences between the treated groups and the negative controls. IC$_{50}$ values were determined as the midpoint of the fitted curves.

RESULTS

Photophysical characterization in aqueous solution

Both the absorbance and fluorescence intensities of BP100 depended linearly on concentrations up to 140 μM (data not shown). The obtained photophysical parameters were similar to those of free Tyr: the excitation maximum for BP100 was at 275 nm ($\lambda_{em} = 306$ nm), which is coincident with the wavelength of maximal electronic absorption. The calculated absorptivity coefficient (ε) at this wavelength was 1.40×10^3 M^{-1} cm^{-1}. The quenching of BP100 by acrylamide followed a linear Stern-Volmer relationship up to 250 mM of quencher, with a K_{SV} of 15.1 M^{-1} (not shown).

Membrane insertion studies

For all the membrane models tested, an increase of fluorescence intensity was observed upon the partition of BP100 between the aqueous buffered phase and the lipidic membrane studied (Fig. 2). Partition parameters are summarized in Table 1.

For the neutral systems, liquid-crystal POPC and liquid-ordered 2:1 POPC-cholesterol LUVs, the increase of fluorescence followed a hyperbolic-like relationship (Fig. 2 *A*). In contrast, the anionic systems 2:1 POPG/POPC and 4:1 POPG/POPC deviated from this behavior (Fig. 2 *B*). At low lipid concentrations, an overshoot of the fluorescence intensity was detected. This result was assigned to reflect membrane saturation. To confirm this hypothesis, membrane saturation studies were carried out for the 2:1 POPG/POPC system (Fig. 3). Saturation points were identified from the
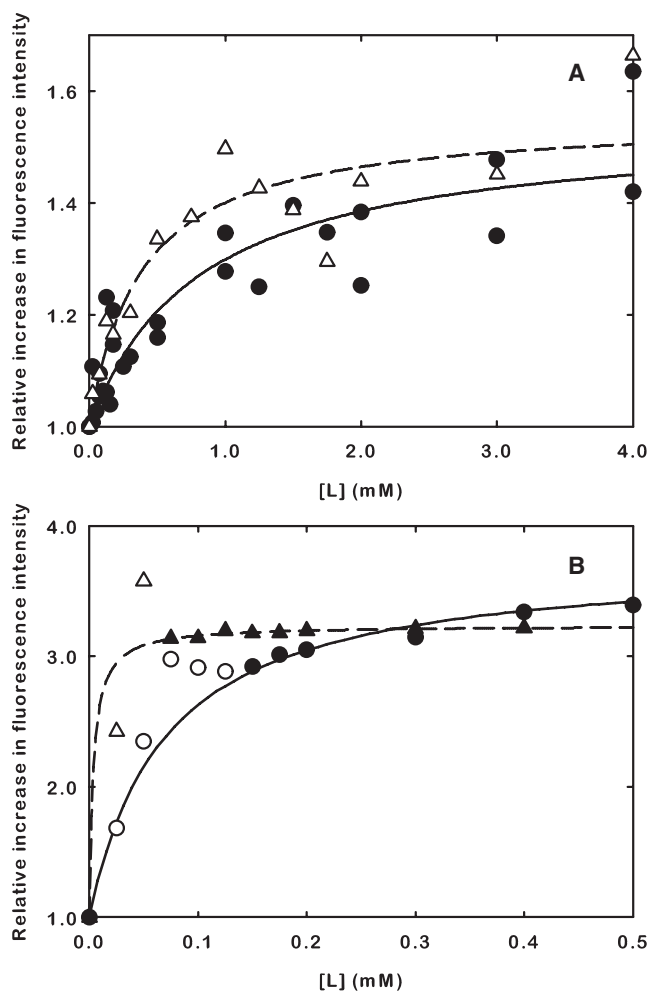
FIGURE 2 Lipid titrations of 15 μM BP100 with different LUV systems. Lines represent the fitting parameters of the data to the partition model in Eq. 1. (*A*) POPC (•, *solid line*) and 2:1 POPC/cholesterol ($\triangle$, *dashed line*) LUVs. (*B*) 4:1 POPG/POPC (•, *solid line*) and 2:1 POPG/POPC (▲, *dashed line*) LUVs; deviations occurred at low lipid concentrations and those data points (*empty*) were removed from the fittings. The difference in the required amounts of lipid for the titrations in panels *A* and *B* indicates a much higher partition toward the anionic models; this is confirmed by the obtained partition constants. Fit parameters are summarized in Table 1.

breaks observed in the curves obtained from titration of vesicles with BP100 and were fitted with Eq. 3 (Fig. 3, *inset*). A K_p value of 8.41×10^4 was obtained and a σ of 0.118 was determined, which corresponds to 8.4 phospholipids per peptide at the saturation of the vesicles.

The depth of membrane internalization was probed using stearic acid molecules labeled at different carbon positions (carbons 5 and 16 for 5- and 16-NS, respectively) with tyrosine quenching nitroxyl groups. With previous knowledge of the in-depth distribution of each quencher, an integrated approach was used to infer the distribution of the tyrosine residue of the peptide from each quencher's quenching profile (based on (55)). These profiles did not change significantly upon saturation (not shown), indicating little change in the in-depth localization of the peptide. This was

TABLE 1 Summary of the characteristics of each studied system: constitution and partition parameters determined using Eq. 1

Modeled system	Constituent phospholipids	$K_p/10^3$	I_L/I_W
Bacterial membrane models			
Outer leaflet	2:1 POPG/POPC	30.8 ± 6.2	3.59 ± 0.06
Inner leaflet	4:1 POPG/POPC	87.6 ± 9.8	3.58 ± 0.02
Mammalian membrane models			
Outer leaflet	100% POPC	1.6 ± 0.5	1.54 ± 0.06
Outer leaflet + cholesterol	2:1 POPC/cholesterol	3.5 ± 1.3	1.55 ± 0.06

confirmed after analysis: in the absence of saturation, the average in-depth localization from the bilayer center was 10.5 Å and the distribution half-width at half maximum was 3.2 Å (a Lorentzian distribution was assumed); under saturation, these parameters were 11.2 Å and 2.4 Å, respectively.

Vesicle permeabilization studies

Fig. 4 displays the leakage kinetics induced by increasing BP100 concentrations. BP100 induced vesicle leakage in a dose-dependent manner. It should be noticed that from 15 μM peptide the kinetics display a markedly sigmoidal rise; this is evident in Fig. 4. A transition at 15 μM of BP100 is also clearly observed in the leakage percentage at 390 s (Fig. 4, *inset*). Thus, for 125 μM lipid, 15 μM is a critical BP100 concentration dictating the transition between two different regimes of peptide-lipid interactions.
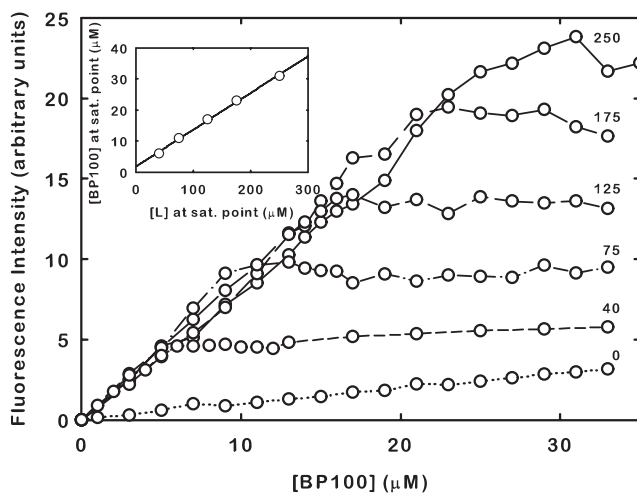
FIGURE 3 Titration of several concentrations of 2:1 POPG/POPC LUVs with BP100 in the presence of 100 mM acrylamide (lipid concentration is indicated in μM for each set of points). Saturation points were identified from the breaks in each curve. (*Inset*) Linear dependence of the global peptide and lipid concentrations at the saturation points, fitted according to Eq. 3, yielding a saturation proportion of 8.4 phospholipids per peptide and a partition constant of 8.41×10^4.
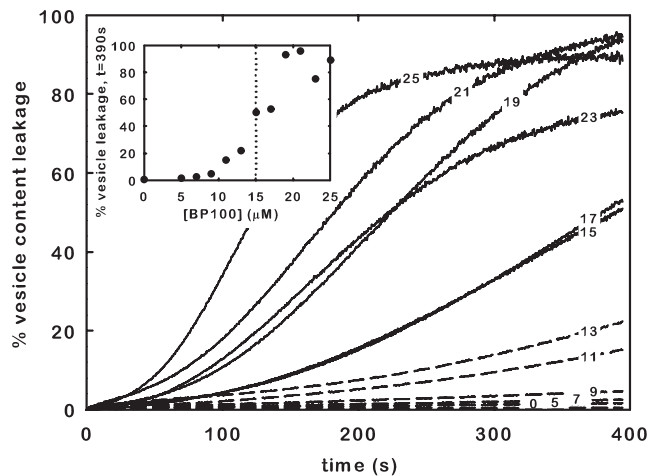
FIGURE 4 Time course of BP100-induced vesicle leakage to Co^{2+} with 125 μM 2:1 POPG/POPC LUVs doped with 1% N-NBD-PE; each curve corresponds to a different BP100 concentration, indicated in the figure in μM. Dashed lines correspond to subsaturation conditions. (*Inset*) Leakage percentage at 390 s in which a transition in behavior with BP100 concentration is evident; this transition occurs close to the expected membrane saturation point for the used lipid concentration, indicated by the dotted line.

The sigmoidal curves could be fitted with the model described by Gregory et al. (59) (not shown), even though in their work only hyperbolic-like kinetics were fit. Both rate constants of pore formation/dissipation needed to be two-to-three orders-of-magnitude lower than those observed by Gregory et al. (59) to generate a sigmoidal behavior comparable to the one observed in Fig. 4. Further quantitative analysis of leakage parameters is, however, not reliable, due to multiple minima in the solution space and some degree of correlation.

Membrane translocation studies

There were marked differences between the peptide-MLV and peptide-LUV interaction kinetics (Fig. 5). Whereas the increase in peptide fluorescence intensity upon LUV addition was almost instantaneous, the MLV-induced increase spanned several minutes. Fluorescence intensity for the MLV additions started out lower than that induced by LUV additions of the same lipid concentration, but rose to approximately the same relative level, as expected for the occurrence of translocation (Fig. 1). To better compare the fluorescence change at both peptide concentrations, Fig. 5 depicts the relative increase in fluorescence upon lipid addition. As a consequence there are small differences in the endpoint of the kinetics at low BP100 concentrations (Fig. 5—MLV1 and LUV1), attributable to error introduced by the low initial Tyr fluorescence signal and further aggravated by the use of acrylamide.

Vesicle aggregation and surface charge studies

Apart from a transient initial increase in turbidity, no significant changes in vesicle OD were observed at peptide

concentrations <15 μM (Fig. 6). For peptide concentrations at or >15 μM, however, there was a remarkable time-dependent increase of the OD due to liposome aggregation induced by BP100 (Fig. 6, *inset*).

A related change was also observed with light scattering measurements where the average particle diameter of the LUV suspension increased by ~10-fold (Fig. 7). Similarly to permeabilization, the BP100-induced increase of vesicle turbidity/aggregation displays a transition between two regimes close to 15 μM, with 125 μM of lipid.

FIGURE 5 Time course of BP100 interaction with 40 μM 2:1 POPG/POPC LUVs and MLVs. LUV1 and MLV1: 4 μM BP100. LUV2 and MLV2: 12 μM BP100. Chosen BP100 concentrations are below and above membrane saturation, as per Eq. 3. Comparison with the expected kinetic profiles (Fig. 1) indicates the occurrence of peptide translocation in both cases.
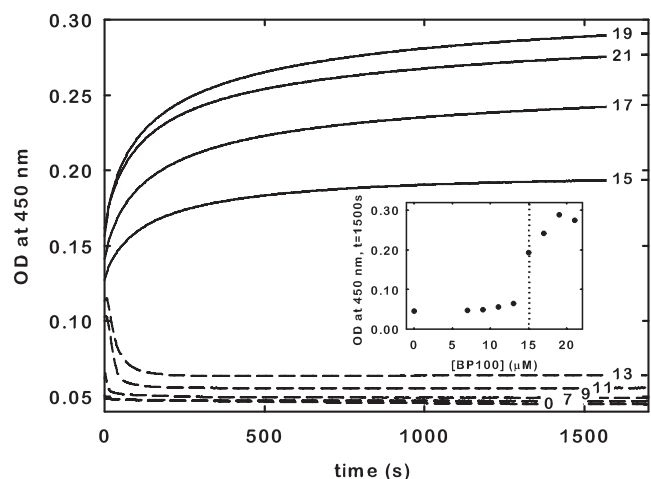
FIGURE 6 Time course of BP100-induced OD change ($\lambda = 450$ nm) of 125 μM 2:1 POPG/POPC LUVs; each curve corresponds to a different BP100 concentration, indicated in the figure in μM. Two different kinetic behaviors are evident. Dashed lines correspond to subsaturation conditions. (*Inset*) OD_{450} at 1500 s. The transition in behavior is evident above 15 μM; as with vesicle leakage (Fig. 4), this transition occurs close to the expected membrane saturation point for the used lipid concentration, indicated by the dotted line.
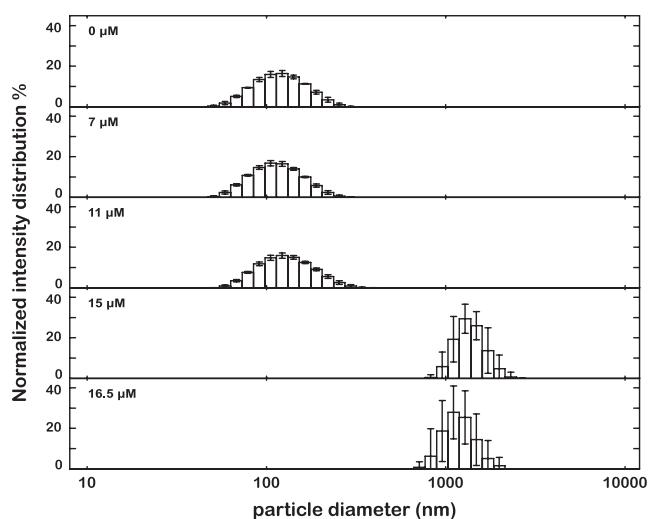
FIGURE 7 Normalized intensity distribution determined by dynamic light scattering of the particle sizes of a 125 μM 2:1 POPG/POPC LUV suspension in the presence of increasing BP100 concentrations (*error bars* represent SD). Above membrane saturation, which is expected at ~15 μM BP100 at this lipid concentration, a significant increase in particle size and heterogeneity is observed, in agreement with the occurrence of vesicle aggregation. This result correlates with the observed distinct behavior of BP100-induced OD change below and above saturation (Fig. 6).

The particles' ζ-potential was -38.3 mV in the absence of peptide but was brought close to zero (-0.1 mV) at saturation (Fig. 8); aggregation and increase in turbidity prevented ζ-potential measurement at higher peptide concentrations.

Effects of BP100 exposure on cell viability

Fig. 9 depicts the effects of BP100 on the mitochondrial activity, cell monolayer adherence, and membrane integrity of cultured hamster fibroblasts. All cell viability parameters responded to the peptide (10–90 μM) in a clear dose-dependent way. At the highest tested concentration (90 μM), low cell viability ($<$10%) was observed. The peptide concentrations, at which 50% inhibition was expected (IC$_{50}$), were interpolated from the regressions for each viability assay, and ranged from 51.1 μM, for the crystal violet stain, to 64.3 μM for the trypan blue assay.

DISCUSSION

The biological activity of small, cationic antimicrobial peptides has been largely associated with their interaction with membranes. It is widely believed that for many of these peptides, membrane disruption is the primary mechanism of cell killing (10–12,15,16,18–20). However, their exact mode of action is still poorly understood. Elucidating their mechanism of action and their specific membrane damaging properties is crucial for the rational design of novel antibiotic peptides with high antibacterial activity and low cytotoxicity. With these observations in mind, and considering
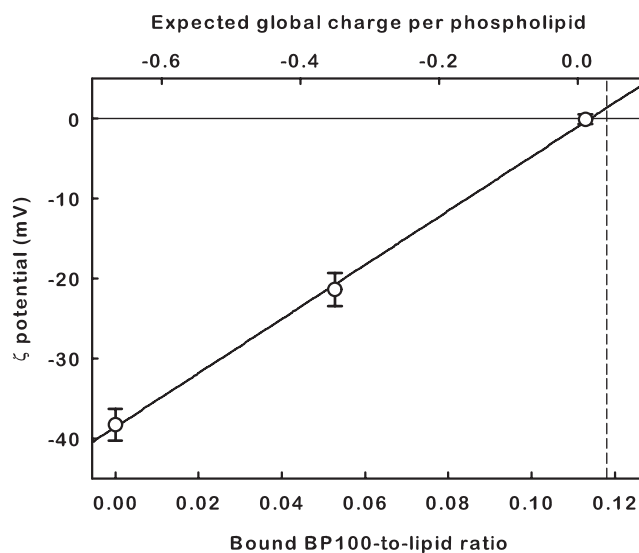
FIGURE 8 The ζ-potential of 250 μM 2:1 POPG/POPC LUV in the presence of different BP100 concentrations (*error bars* represent SD). Peptide concentrations are displayed either as bound peptide/lipid ratios (calculated with the partition constant obtained from Eq. 3) or as the estimated global charge per phospholipid assuming a 6^+ charge on the peptide. A linear regression of the points is displayed as a guide to the eye. The saturation ratio is indicated by the dashed line. A neutralization of the LUV charge at the saturation point was observed, in agreement with what was expected from the saturation proportion (Fig. 3), the peptide charge, and the composition of the system.

that BP100 contains a Tyr residue, which makes it intrinsically fluorescent, we have exploited its photophysical properties to obtain information about its binding affinity and damaging effect on bilayers having a lipid composition
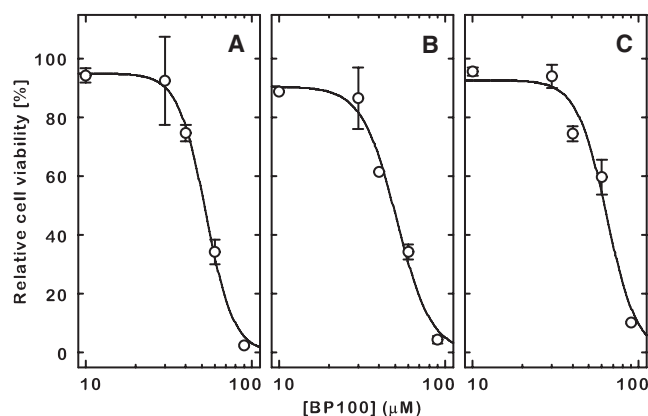
FIGURE 9 Effects of BP100 on the viability of V79 Chinese hamster lung fibroblast cells after 24 h exposure (*error bars* represent SE). (*A*) Mitochondrial activity determined by the MTT assay; IC$_{50}$ = 52.9 μM. (*B*) Loss of monolayer adherence estimated by the crystal violet assay; IC$_{50}$ = 51.1 μM. (*C*) Plasma membrane integrity estimated by the trypan blue assay; IC$_{50}$ = 64.3 μM. Logit curves were fitted to the data and are shown as lines. The IC$_{50}$ values are proportionally greater-than the MIC, by approximately the same factor as the partition constants toward the anionic bacterial models are greater-than toward the neutral mammalian models, suggesting a concentration-dependent disruption mechanism.

similar to that of the bacterial and mammalian cytoplasmic membranes.

Photophysical characterization of BP100 in aqueous solution

The photophysical characterization of peptides in aqueous solution is a prerequisite to understand their interaction with phospholipid model membranes. The observed behavior of BP100 in aqueous solution reflects that peptide aggregation does not occur at the studied peptide concentration range. This is supported by the linear dependencies of fluorescence emission intensity and electronic absorption on concentration and by the obtained λ_{exc}, λ_{em}, and ε-values as they are similar to those of free Tyr (275, 303, and 1400, respectively (47)), indicating that the Tyr in BP100 is exposed to an aqueous environment (47). Moreover, a linear Stern-Volmer plot for the fluorescence quenching of BP100 with acrylamide is observed up to 250 mM (not shown). In addition, there are no significant differences between the obtained K_{SV} and the one for acrylamide quenching of free Tyr, evidencing that Tyr is totally accessible to the aqueous phase. The absence of aggregation observed for BP100, together with its overall positive charge (+6), could account for its high solubility in aqueous solution and facilitates the interpretation of the peptide-membrane interaction results.

Membrane insertion studies

The extent of the partition of BP100 into model membranes was studied using a partition model described by Santos et al. that allows the calculation of the Nernst partition constant (K_p) from fluorescence intensity (I) versus phospholipid concentration ([L]) plots at a constant peptide concentration ([P]) (49). The K_p, defined as the ratio between the equilibrium membrane-bound and aqueous phase peptide concentrations, provides an easy assessment of the extent of peptide-membrane interaction (Eq. 2). For both neutral systems POPC and 2:1 POPC/cholesterol LUVs, used as models of the outer leaflet of mammalian membranes, the fluorescence intensity increased following an hyperbolic-like relationship (Fig. 2 A). The moderate K_p values obtained for vesicles composed of 100% POPC and POPC/cholesterol mixtures (Table 1) could be attributed to the hydrophobic effect and the van der Waals forces that are likely to dominate the interactions between the neutral lipids and the hydrophobic residues of BP100. In this case, no specific interaction with cholesterol was observed, which is an indicator of low toxicity toward mammalian cells. Furthermore, cholesterol seems to play an important role in preventing the intercalation of AMPs into eukaryotic cell membranes (67); its presence and the absence of acidic phospholipids in the eukaryotic membranes could account for the low cytotoxicity displayed by BP100 against erythrocytes (38).

For the anionic liquid-crystalline 2:1 and 4:1 POPG/POPC vesicles, which served as models for bacterial cell membranes, the partition curves deviated from the hyperbolic-like progression at low lipid concentrations (Fig. 2 B). A similar behavior has been recently reported for the antimicrobial peptide omiganan and has been attributed to a membrane saturation process: at low phospholipid concentrations, membrane saturation may occur when the bound peptide concentration, hypothetically dictated by K_p, is higher than what the membrane can accommodate (53); under these conditions, interaction changes may occur, as has also been described for other AMPs upon the crossing of threshold P/L ratios (68,69). Since the model of Santos et al. (49) is not well suited to study these saturated systems, the K_p values were obtained by fitting only the nonsaturated points to the partition model (Fig. 2 B and Table 1). This approach is obviously subject to error because the initial points of the curve, which are important for the accurate calculation of K_p, cannot be used. However, even with great associated errors, the obtained partition constants were one or more orders-of-magnitude higher than those of the neutral systems (Table 1). These results are consistent with the expected preference of cationic peptides for negatively charged membranes as a consequence of the strong electrostatic interaction.

To ensure that the deviation observed in the partition curves of the anionic vesicles was due to a saturation of the system, membrane saturation studies were carried out using 2:1 POPG/POPC LUVs. LUV suspensions were titrated with peptide in the presence of acrylamide while monitoring BP100's fluorescence intensity. Acrylamide is an aqueous quencher that facilitates the identification of alterations in the phase localization of peptides. In a nonsaturation regime, a linear increase of the fluorescence intensity is expected: as per the formalism behind Eq. 1, the fractions of the peptide in each phase are constant with constant [L]; therefore, any variation in peptide concentration will result in a proportional increase in each of these fractions and, also therefore, in a global proportional increase of the fluorescence intensity (53). Conversely, if saturation occurs, the membrane will not be able to accommodate any more peptide, which will then remain in the aqueous phase. Because acrylamide quenches preferentially the fluorescence of the aqueous phase peptide population, a weaker progression of the fluorescence intensity, relatively to a nonsaturation state, should then be detected (53). This behavior was indeed observed in the BP100 titrations (Fig. 3), showing the occurrence of saturation: two different slopes were obtained for each I versus [P] curve. The first slope corresponds to a nonsaturated state while the second one, which is similar to that of the curve in the absence of lipid, can be ascribed to a saturation of the system. The saturation points could be easily obtained from the breaks of the initial slopes of each titration curve. It was observed that the I versus [P] curve with [L] = 125 μM had its saturation point close to [P] = 17 μM (Fig. 3), which is slightly higher than the peptide concentration that yielded an I versus [L] curve

with a deviation maximum close to $[L] = 125\ \mu M$ (Fig. 2 B). This result supports the hypothesis that the deviations observed in the partition curves correspond to a saturation of the membrane.

Further information from the saturation phenomenon was obtained by representing the saturation point $([P],[L])$ pairs for the 2:1 POPG/POPC LUVs (Fig. 3, inset). This system followed Eq. 3, which defines the total amount of peptide at which a saturation point occurs as a linear function of the amount of lipid in the system, and allows the calculation of σ—the P/L ratio at saturation—and the Nernst partition constant K_p. However, it should be noticed that the values for K_p have large associated errors because they are calculated from the reciprocal of a small intercept. Despite that, the obtained K_p (8.41×10^4) had the same order of magnitude as that determined from the partition curve using the model of Santos et al. (49) (3.08×10^4). In addition, the saturation P/L ratio was 0.118, which corresponds to 8.4 phospholipids per peptide directly in contact with the membrane at the saturation. Because there are 2/3 anionic phospholipids in the used system, there will be 5.6 negatively charged phospholipids per peptide at saturation. Interestingly, this number is very close to the expected charge of the peptide (+6) at pH 7.4, which suggests that electroneutrality is reached at the saturation of the system.

There was no significant alteration in the tyrosine in-depth location upon saturation, indicating that most of BP100 molecules maintain their positioning within the membrane. The location of the tyrosine residue, approximately halfway across the membrane leaflet, is coherent with a relatively deep burying of the peptide if it adopts, as expected (40), a horizontally oriented α-helical structure. The lysines have the ability to snorkel and keep their charged amino groups near the headgroup region (70,71) while the hydrophobic side chains could go as far as the bilayer center. This localization within the bilayer is likely responsible, at least in part, for the membrane destabilizing capabilities of BP100.

Vesicle permeabilization studies

Investigations on the mode of action of AMPs, such as cecropins and melittin, have shown that they exert their activity by inducing the formation of transmembrane pores or by causing cell lysis, depending on both the peptide concentration and the membrane composition (41–45). Moreover, it has been reported that cecropin-melittin hybrids are also able to cause membrane permeabilization (72,73). These findings prompted us to test BP100-induced permeabilization of model lipidic membranes.

Results showed that BP100 has an important permeabilizing effect dependant on peptide concentration. The increase in the permeabilization rate with BP100 concentration is, however, not linear (Fig. 4). The clear change of behavior at ~15 μM peptide, toward faster, sigmoidal, and more intense leakage kinetics—visible both in the permeabiliza-

tion kinetics (Fig. 4) and in the leakage percentage profile at 390 s (Fig. 4, inset)—occurs very close to the peptide concentration expected to cause membrane saturation for the 125 μM lipid concentration (Fig. 3). These results show that membrane saturation affects more than just the amount of bound peptide: high P/L ratios at, or close to, membrane saturation are able to induce a change in a functional property of the peptide. The sigmoidal leakage kinetic induced by BP100 is uncommon, as such profiles are usually hyperbolic-like (74). Nevertheless, a similar kinetic was recently observed for an unrelated AMP (74). In both these cases, because the interaction with LUVs is not a limiting step (Fig. 5, LUV traces), the lag involved in the sigmoidal behavior may be related to postbinding events in the membrane (74).

Further information was extracted by fitting the data with the model used by Gregory et al. (59) to describe cecropin A-induced leakage. This model was only used to fit hyperbolic-like kinetics, but, even in those cases (59), close inspection of the model in the first seconds of each kinetics does reveal a brief sigmoidal behavior. Upon fitting, the magnitude of this behavior could only be manipulated to match the timescale of BP100-induced leakage kinetics by lowering the k_1 and k_2 constants of the model two-to-three orders of magnitude, relative to the values obtained in Gregory et al. (59). As these parameters are the rate constants of pore forming/dissipation, this result suggests that, after binding, BP100 becomes disruptive at a slower rate than cecropin A.

The high degree of peptide-induced leakage after saturation may reflect severe membrane damage or lysis, whereas the lower permeabilization before saturation could reflect a lesser destabilization of the membrane upon peptide binding. High P/L ratios close to saturation would then act as the trigger between these two states, and could be the biophysical parallel to the in vivo onset of antibacterial activity. This is supported by the fact that the threshold dependence on peptide concentration (Fig. 4, inset) could not be accounted for with data fitting without assuming some kind of parameter change with increasing BP100 concentration—such as an increase in the mentioned k_1 and k_2 disruption rates. Although hypothetical, this scenario is plausible, and stresses the importance of high local peptide concentrations in the membrane.

Membrane translocation studies

The determination of the occurrence of membrane translocation is an important functional characterization: a nontranslocating peptide can only exert its activity at the extracellular/membrane level, whereas one crossing a membrane may also have cytoplasmic targets. However, detection of translocation can be troublesome, and, although there are several methods available, many require peptide derivatization or have limited applicability (75).

Despite there being other published methods where MLVs are used to enhance an internalization effect (75,76), the method developed in our work is extremely simple and requires only that the peptide has intrinsic fluorescence and that its interaction kinetics with LUVs are significantly faster than its translocation kinetics; quencher enhancement is not an absolute requirement. The results clearly showed a translocation behavior at both high and low P/L ratios (Fig. 5). As predicted in Fig. 1 for a translocating peptide, the interaction with MLVs was slower than with LUVs, but eventually reached the same fluorescence increase. Occurrence of translocation is unequivocal and, together with the permeabilization assays, constitutes a further proof of the membrane activity of the peptide.

Vesicle aggregation and surface charge studies

Turbidity measurements have been described as an useful tool to investigate the affinity of cationic peptides toward charged vesicles (77). The stability of a dispersion of charged vesicles is mainly governed by three types of forces: electrostatic repulsion, van der Waals attraction, and hydration (77). Cationic peptides can alter the charge density of the vesicle surface inducing vesicle aggregation, which can be followed as an increase of the OD. Turbidity results showed two different kinetic patterns depending on BP100 concentration (Fig. 6). For 125 μM lipid (2:1 POPG/POPC LUV) and peptide concentrations <15 μM, which correspond to a nonsaturated state, no significant changes in turbidity were observed. However, when membrane saturation occurs ($\geq$15 μM peptide), the optical density of the solution increased until a plateau was reached, ~30 min after the addition of BP100. This increase is likely due to vesicle aggregation induced under membrane saturation conditions. These results confirm the affinity of BP100 for acidic phospholipids and reinforce the hypothesis that electroneutrality is reached at the membrane saturation point.

These conclusions were confirmed using light scattering methodologies: the change in the LUV suspension OD is related to an increase in the average particle size from 100 nm—in the absence of peptide and up to saturation— to >1 μm upon saturation (Fig. 7). In addition, ζ-potential measurements in this range showed that BP100 brings the LUV charge to approximate electroneutrality at saturation, confirming the prediction based on the saturation proportion (Fig. 8). This effect is certainly favoring vesicle aggregation by canceling the electrostatic repulsion between them.

Partition, saturation, and prediction of MIC

During our recent investigations, we have found that minimum inhibitory concentration, MIC, and saturation can be correlated for peptides, such as omiganan (53). For this peptide, MICs were found to be similar to the peptide concentration needed to reach the saturation state, reflecting the existence of possible saturation-triggered antimicrobial mechanisms.

Since findings from BP100-membrane interaction studies also suggest that membrane saturation is important for the activity of this peptide, we examined whether the results obtained are in agreement with the experimental MIC values.

As previously reported (53), under typical bacterial titers and using the MIC as the total peptide concentration, the membrane-bound peptide concentration ($[P]_L$) is given by $K_p \times$ MIC. On the other hand, σ can be determined as $[P]_L \times \gamma_L$. Combining both expressions, the MIC can be readily calculated as MIC = $\sigma/(K_p \times \gamma_L)$. Using the obtained σ (0.118) and K_p (3.08 $\times$ 10^4 or 8.41 $\times$ 10^4, from the partition and saturation studies, respectively) values, and considering γ_L as 0.763 M^{-1} (50), this equation leads to MIC values of 2 or 5 μM, depending on the selected K_p. These values are consistent with the antibacterial activity displayed by BP100, which inhibited in vitro growth of the bacteria *E. amylovora*, *X. vesicatoria*, and *P. syringae* at 2.5–7.5 μM (38). In addition to validating the obtained values for K_p and σ, these results strongly support the correlation between these constants and the MIC, evidencing the importance of the saturation point in the mode of action of this peptide.

Physiological significance of saturation-induced activity

The obtained results clearly point toward the occurrence of different membrane-disrupting events as saturation is reached. Given the plausible correlation between saturation and the onset of antibacterial activity of BP100, an extrapolation of these events to an in vivo setting was sought.

Surface charge neutralization at saturation was found to be an important occurrence, triggering the observed vesicle aggregation, and probably being responsible for the destabilization that led to an increase in membrane permeabilization, as leakage enhancement correlates with vesicle aggregation. The bacterial metabolism will certainly be sensitive to the neutralization-induced loss of the membrane surface potential, as this will disturb the charge environment of the outer leaflet proteins. The observed coupled permeabilization (if not lysis) entails even further damage to the cell, namely the dissipation of the transmembrane potential which, among other effects, will halt ATP synthesis. Vesicle aggregation may not have a parallel in vivo, as bacterial membranes have additional layers of protection (LPS, peptidoglycan, capsule) preventing direct membrane contact between bacteria; its occurrence in vitro does, however, stress the importance of the surface potential for membrane stability. The observed translocation could be a consequence of the permeabilization or can be an independent event; either way, direct interaction with cytoplasmic targets is yet another possible cause of bacterial death.

Effects of BP100 exposure on cell viability

The experimental results from our studies show cytotoxic effects in the cultured mammalian fibroblast cells at

concentrations of BP100 above 50–60 μM (Fig. 9). This is in good agreement with similar findings in human erythrocytes (38), where an increased release of hemoglobin was observed above 150 μM. Although the membrane integrity in our V79 cells was affected at lower concentrations (IC_{50} = 51.1 μM), it probably just reflects the different cell lines: different sensibilities to antibacterial peptides were also found between human erythrocytes and mammalian COS-7 kidney cells (65), and might indicate a better resistance of the human erythrocytes to this class of peptides (78). Results from the MTT assay (Fig. 9) demonstrated changes in the metabolic activity of mitochondria V79 cells, as the dehydrogenase enzymes started to be less active to convert the yellow water-soluble salt into insoluble formazan crystals at increasing peptide concentrations. Whether this means that there is a direct action on the mitochondria, or indirect loss of mitochondrial activity, cannot be ascertained without further investigation.

A successful application of this peptide as a bactericide demands a high therapeutic index, i.e., a high antimicrobial activity but low cytotoxicity. The high antimicrobial potency (MIC = 2.5–7.5 μM) and relatively low cytotoxicity in human erythrocytes (38) reveals promising values for BP100. Although cytotoxic effects were observed in V79 cells at peptide concentrations above 50–60 μM, this range is still far above the anticipated antimicrobial application levels.

Cytotoxicity against mammalian models is reached at a concentration higher than the MIC by roughly the same proportion that K_p values toward mammalian model bilayers are lower than toward bacterial ones. This observation suggests that cell killing may be dependent on a constant local membrane-bound concentration, independently of the considered lipid system.

CONCLUSION

This work clearly points out a correlation between high membrane concentrations (possibly even saturation) of BP100 and bacterial death. Three different potential causes of activity of AMP, i.e., charge neutralization, permeabilization, and translocation, were identified. In addition, a concentration dependence of the killing phenomena, in bacteria and in mammalian cells, was suggested. While the exact mechanism of action of the peptide may remain elusive in vivo, and depend on the peptide and bacteria species, our findings unravel the bases of the closely coupled occurrence of those causes, as experimentally observed by Friedrich et al. (79).

REFERENCES

1. Brogden, K. A., M. Ackermann, P. B. McCray, Jr., and B. F. Tack. 2003. Antimicrobial peptides in animals and their role in host defenses. *Int. J. Antimicrob. Agents.* 22:465–478.

2. Bulet, P., R. Stocklin, and L. Menin. 2004. Antimicrobial peptides: from invertebrates to vertebrates. *Immunol. Rev.* 198:169–184.

3. Ganz, T., and R. I. Lehrer. 1998. Antimicrobial peptides of vertebrates. *Curr. Opin. Immunol.* 10:41–44.

4. Garcia-Olmedo, F., A. Molina, J. M. Alamillo, and P. Rodriguez-Palenzuela. 1998. Plant defense peptides. *Biopolymers.* 47:479–491.

5. Otvos, L., Jr. 2000. Antibacterial peptides isolated from insects. *J. Pept. Sci.* 6:497–511.

6. Zasloff, M. 2002. Antimicrobial peptides of multicellular organisms. *Nature.* 415:389–395.

7. Broekaert, W. F., B. P. A. Cammue, M. F. C. DeBolle, K. Thevissen, G. W. DeSamblanx, et al. 1997. Antimicrobial peptides from plants. *Crit. Rev. Plant Sci.* 16:297–323.

8. Hancock, R. E., and A. Patrzykat. 2002. Clinical development of cationic antimicrobial peptides: from natural to novel antibiotics. *Curr. Drug Targets Infect. Disord.* 2:79–83.

9. Hancock, R. E., and H. G. Sahl. 2006. Antimicrobial and host-defense peptides as new anti-infective therapeutic strategies. *Nat. Biotechnol.* 24:1551–1557.

10. Boman, H. G. 2003. Antibacterial peptides: basic facts and emerging concepts. *J. Intern. Med.* 254:197–215.

11. Hancock, R. E. 2001. Cationic peptides: effectors in innate immunity and novel antimicrobials. *Lancet Infect. Dis.* 1:156–164.

12. Jenssen, H., P. Hamill, and R. E. Hancock. 2006. Peptide antimicrobial agents. *Clin. Microbiol. Rev.* 19:491–511.

13. Montesinos, E. 2007. Antimicrobial peptides and plant disease control. *FEMS Microbiol. Lett.* 270:1–11.

14. Zhang, L., and T. J. Falla. 2006. Antimicrobial peptides: therapeutic potential. *Expert Opin. Pharmacother.* 7:653–663.

15. Brogden, K. A. 2005. Antimicrobial peptides: pore formers or metabolic inhibitors in bacteria? Nat. Rev. Microbiol. 3:238–250.

16. Yeaman, M. R., and N. Y. Yount. 2003. Mechanisms of antimicrobial peptide action and resistance. *Pharmacol. Rev.* 55:27–55.

17. Perron, G. G., M. Zasloff, and G. Bell. 2006. Experimental evolution of resistance to an antimicrobial peptide. *Proc. Biol. Sci.* 273:251–256.

18. Shai, Y. 2002. Mode of action of membrane active antimicrobial peptides. *Biopolymers.* 66:236–248.

19. Tossi, A., L. Sandri, and A. Giangaspero. 2000. Amphipathic, α-helical antimicrobial peptides. *Biopolymers.* 55:4–30.

20. Bechinger, B. 2004. Structure and function of membrane-lytic peptides. *Crit. Rev. Plant Sci.* 23:271–292.

21. Yang, L., T. A. Harroun, T. M. Weiss, L. Ding, and H. W. Huang. 2001. Barrel-stave model or toroidal model? A case study on melittin pores. *Biophys. J.* 81:1475–1485.

22. Shai, Y. 1999. Mechanism of the binding, insertion and destabilization of phospholipid bilayer membranes by α-helical antimicrobial and cell non-selective membrane-lytic peptides. *Biochim. Biophys. Acta.* 1462:55–70.

23. Kobayashi, S., A. Chikushi, S. Tougu, Y. Imura, M. Nishida, et al. 2004. Membrane translocation mechanism of the antimicrobial peptide buforin 2. *Biochemistry.* 43:15610–15616.

24. Hultmark, D., A. Engstrom, H. Bennich, R. Kapur, and H. G. Boman. 1982. Insect immunity: isolation and structure of cecropin D and four minor antibacterial components from *Cecropia pupae. Eur. J. Biochem.* 127:207–217.

25. Hultmark, D., H. Steiner, T. Rasmuson, and H. G. Boman. 1980. Insect immunity. Purification and properties of three inducible bactericidal proteins from hemolymph of immunized pupae of *Hyalophora cecropia. Eur. J. Biochem.* 106:7–16.

26. Sato, H., and J. B. Feix. 2006. Peptide-membrane interactions and mechanisms of membrane destruction by amphipathic α-helical antimicrobial peptides. *Biochim. Biophys. Acta.* 1758:1245–1256.

27. Andreu, D., R. B. Merrifield, H. Steiner, and H. G. Boman. 1983. Solid-phase synthesis of cecropin A and related peptides. *Proc. Natl. Acad. Sci. USA.* 80:6475–6479.

28. Steiner, H., D. Hultmark, A. Engstrom, H. Bennich, and H. G. Boman. 1981. Sequence and specificity of two antibacterial proteins involved in insect immunity. *Nature.* 292:246–248.

29. Alberola, J., A. Rodriguez, O. Francino, X. Roura, L. Rivas, et al. 2004. Safety and efficacy of antimicrobial peptides against naturally acquired *Leishmaniasis. Antimicrob. Agents Chemother.* 48:641–643.

30. Andreu, D., J. Ubach, A. Boman, B. Wahlin, D. Wade, et al. 1992. Shortened cecropin A-melittin hybrids. Significant size reduction retains potent antibiotic activity. *FEBS Lett.* 296:190–194.

31. Boman, H. G., D. Wade, I. A. Boman, B. Wahlin, and R. B. Merrifield. 1989. Antibacterial and antimalarial properties of peptides that are cecropin-melittin hybrids. *FEBS Lett.* 259:103–106.

32. Cavallarin, L., D. Andreu, and B. San Segundo. 1998. Cecropin A-derived peptides are potent inhibitors of fungal plant pathogens. *Mol. Plant Microbe Interact.* 11:218–227.

33. Chicharro, C., C. Granata, R. Lozano, D. Andreu, and L. Rivas. 2001. N-terminal fatty acid substitution increases the leishmanicidal activity of CA(1–7)M(2–9), a cecropin-melittin hybrid peptide. *Antimicrob. Agents Chemother.* 45:2441–2449.

34. Giacometti, A., O. Cirioni, W. Kamysz, G. D'Amato, C. Silvestri, et al. 2004. In vitro activity and killing effect of the synthetic hybrid cecropin A-melittin peptide CA(1–7)M(2–9)NH$_2$ on methicillin-resistant nosocomial isolates of *Staphylococcus aureus* and interactions with clinically used antibiotics. *Diagn. Microbiol. Infect. Dis.* 49:197–200.

35. Lee, D. G., Y. Park, I. Jin, K. S. Hahm, H. H. Lee, et al. 2004. Structure-antiviral activity relationships of cecropin A-magainin 2 hybrid peptide and its analogues. *J. Pept. Sci.* 10:298–303.

36. Wade, D., D. Andreu, S. A. Mitchell, A. M. Silveira, A. Boman, et al. 1992. Antibacterial peptides designed as analogs or hybrids of cecropins and melittin. *Int. J. Pept. Protein Res.* 40:429–436.

37. Ali, G. S., and A. S. Reddy. 2000. Inhibition of fungal and bacterial plant pathogens by synthetic peptides: in vitro growth inhibition, interaction between peptides and inhibition of disease progression. *Mol. Plant Microbe Interact.* 13:847–859.

38. Badosa, E., R. Ferre, M. Planas, L. Feliu, E. Besalu, et al. 2007. A library of linear undecapeptides with bactericidal activity against phyto-pathogenic bacteria. *Peptides.* 28:2276–2285.

39. Bardají, E., E. Montesinos, E. Badosa, L. Feliu, M. Planas, et al. 2006. Antimicrobial linear peptides. P200601098; priority date: April 28th, 2006; Oficina Española de Patentes y Marcas, Spain.

40. Ferre, R., E. Badosa, L. Feliu, M. Planas, E. Montesinos, et al. 2006. Inhibition of plant-pathogenic bacteria by short synthetic cecropin A-melittin hybrid peptides. *Appl. Environ. Microbiol.* 72:3302–3308.

41. Christensen, B., J. Fink, R. B. Merrifield, and D. Mauzerall. 1988. Channel-forming properties of cecropins and related model compounds incorporated into planar lipid membranes. *Proc. Natl. Acad. Sci. USA.* 85:5072–5076.

42. Ladokhin, A. S., M. E. Selsted, and S. H. White. 1997. Sizing membrane pores in lipid vesicles by leakage of co-encapsulated markers: pore formation by melittin. *Biophys. J.* 72:1762–1766.

43. Ladokhin, A. S., and S. H. White. 2001. "Detergent-like" permeabilization of anionic lipid vesicles by melittin. *Biochim. Biophys. Acta.* 1514:253–260.

44. Silvestro, L., K. Gupta, J. N. Weiser, and P. H. Axelsen. 1997. The concentration-dependent membrane activity of cecropin A. *Biochemistry.* 36:11452–11460.

45. Steiner, H., D. Andreu, and R. B. Merrifield. 1988. Binding and action of cecropin and cecropin analogues: antibacterial peptides from insects. *Biochim. Biophys. Acta.* 939:260–266.

46. Mayer, L. D., M. J. Hope, and P. R. Cullis. 1986. Vesicles of variable sizes produced by a rapid extrusion procedure. *Biochim. Biophys. Acta.* 858:161–168.

47. Santos, N. C., and M. A. Castanho. 2002. Fluorescence spectroscopy methodologies on the study of proteins and peptides. On the 150th anniversary of protein fluorescence. *Trends Appl. Spectrosc.* 4:113–125.

48. Coutinho, A., and M. Prieto. 1993. Ribonuclease-T$_1$ and alcohol-dehydrogenase fluorescence quenching by acrylamide—a laboratory experiment for undergraduate students. *J. Chem. Educ.* 70:425–428.

49. Santos, N. C., M. Prieto, and M. A. Castanho. 2003. Quantifying molecular partition into model systems of biomembranes: an emphasis on optical spectroscopic methods. *Biochim. Biophys. Acta.* 1612:123–135.

50. Nagle, J. F., and M. C. Wiener. 1988. Structure of fully hydrated bilayer dispersions. *Biochim. Biophys. Acta.* 942:1–10.

51. Ladokhin, A. S., S. Jayasinghe, and S. H. White. 2000. How to measure and analyze tryptophan fluorescence in membranes properly, and why bother? Anal. Biochem. 285:235–245.

52. Wenk, M. R., and J. Seelig. 1998. Magainin 2 amide interaction with lipid membranes: calorimetric detection of peptide binding and pore formation. *Biochemistry.* 37:3909–3916.

53. Melo, M. N., and M. A. Castanho. 2007. Omiganan interaction with bacterial membranes and cell wall models. Assigning a biological role to saturation. *Biochim. Biophys. Acta.* 1768:1277–1290.

54. Chalpin, D. B., and A. M. Kleinfeld. 1983. Interaction of fluorescence quenchers with the *n*-(9-anthroyloxy) fatty acid membrane probes. *Biochim. Biophys. Acta.* 731:465–474.

55. Fernandes, M. X., J. Garcia de la Torre, and M. A. Castanho. 2002. Joint determination by Brownian dynamics and fluorescence quenching of the in-depth location profile of biomolecules in membranes. *Anal. Biochem.* 307:1–12.

56. Chattopadhyay, A., and E. London. 1988. Spectroscopic and ionization properties of *N*-(7-nitrobenz-2-oxa-1,3-diazol-4-yl)-labeled lipids in model membranes. *Biochim. Biophys. Acta.* 938:24–34.

57. Pokorny, A., and P. F. Almeida. 2004. Kinetics of dye efflux and lipid flip-flop induced by δ-lysin in phosphatidylcholine vesicles and the mechanism of graded release by amphipathic, α-helical peptides. *Biochemistry.* 43:8846–8857.

58. Lakowicz, J. R. 1999. Quenching of fluorescence. Principles of Fluorescence Spectroscopy, 2nd Ed. Kluwer Academic/Plenum, New York; London.

59. Gregory, S. M., A. Cavenaugh, V. Journigan, A. Pokorny, and P. F. Almeida. 2008. A quantitative model for the all-or-none permeabilization of phospholipid vesicles by the antimicrobial peptide cecropin A. *Biophys. J.* 94:1667–1680.

60. Rueff, J., C. Chiapella, J. K. Chipman, F. Darroudi, I. D. Silva, et al. 1996. Development and validation of alternative metabolic systems for mutagenicity testing in short-term assays. *Mutat. Res.* 353:151–176.

61. Zucco, F., I. De Angelis, and A. Stammati. 1998. Cellular models for in vitro toxicity testing. *In* Animal Cell Culture Techniques. M. Clynes, editor. Springer, Berlin; London.

62. Mickuviene, I., V. Kirveliene, and B. Juodka. 2004. Experimental survey of non-clonogenic viability assays for adherent cells in vitro. *Toxicol. In Vitro.* 18:639–648.

63. Mitchell, J. B. 1988. Potential applicability of nonclonogenic measurements to clinical oncology. *Radiat. Res.* 114:401–414.

64. Brink, C. B., A. Pretorius, B. P. van Niekerk, D. W. Oliver, and D. P. Venter. 2008. Studies on cellular resilience and adaptation following acute and repetitive exposure to ozone in cultured human epithelial (HeLa) cells. *Redox Rep.* 13:87–100.

65. Cudic, M., C. V. Lockatell, D. E. Johnson, and L. Otvos, Jr. 2003. In vitro and in vivo activity of an antibacterial peptide analog against uropathogens. *Peptides.* 24:807–820.

66. Scholze, M., W. Boedeker, M. Faust, T. Backhaus, R. Altenburger, et al. 2001. A general best-fit method for concentration-response curves and the estimation of low-effect concentrations. *Environ. Toxicol. Chem.* 20:448–457.

67. Zhao, H., R. Sood, A. Jutila, S. Bose, G. Fimland, et al. 2006. Interaction of the antimicrobial peptide pheromone Plantaricin A with model membranes: implications for a novel mechanism of action. *Biochim. Biophys. Acta.* 1758:1461–1474.

68. Huang, H. W. 2000. Action of antimicrobial peptides: two-state model. *Biochemistry.* 39:8347–8352.

69. Huang, H. W. 2006. Molecular mechanism of antimicrobial peptides: the origin of cooperativity. *Biochim. Biophys. Acta.* 1758:1292–1302.

70. Segrest, J. P., H. De Loof, J. G. Dohlman, C. G. Brouillette, and G. M. Anantharamaiah. 1990. Amphipathic helix motif: classes and properties. *Proteins.* 8:103–117.

71. Kandasamy, S. K., and R. G. Larson. 2006. Molecular dynamics simulations of model trans-membrane peptides in lipid bilayers: a systematic investigation of hydrophobic mismatch. *Biophys. J.* 90:2326–2343.

72. Abrunhosa, F., S. Faria, P. Gomes, I. Tomaz, J. C. Pessoa, et al. 2005. Interaction and lipid-induced conformation of two cecropin-melittin hybrid peptides depend on peptide and membrane composition. *J. Phys. Chem. B.* 109:17311–17319.

73. Juvvadi, P., S. Vunnam, E. L. Merrifield, H. G. Boman, and R. B. Merrifield. 1996. Hydrophobic effects on antibacterial and channel-forming properties of cecropin A-melittin hybrids. *J. Pept. Sci.* 2:223–232.

74. Rathinakumar, R., and W. C. Wimley. 2008. Biomolecular engineering by combinatorial design and high-throughput screening: small, soluble peptides that permeabilize membranes. *J. Am. Chem. Soc.* 130:9849–9858.

75. Henriques, S. T., M. N. Melo, and M. A. Castanho. 2007. How to address CPP and AMP translocation? Methods to detect and quantify peptide internalization in vitro and in vivo. (Review). *Mol. Membr. Biol.* 24:173–184.

76. Matsuzaki, K., S. Yoneyama, O. Murase, and K. Miyajima. 1996. Transbilayer transport of ions and lipids coupled with mastoparan X translocation. *Biochemistry.* 35:8450–8456.

77. Persson, D., P. E. Thoren, and B. Norden. 2001. Penetratin-induced aggregation and subsequent dissociation of negatively charged phospholipid vesicles. *FEBS Lett.* 505:307–312.

78. Otvos, L., Jr., K. Bokonyi, I. Varga, B. I. Otvos, R. Hoffmann, et al. 2000. Insect peptides with improved protease-resistance protect mice against bacterial infection. *Protein Sci.* 9:742–749.

79. Friedrich, C. L., D. Moyles, T. J. Beveridge, and R. E. Hancock. 2000. Antibacterial action of structurally diverse cationic peptides on Gram-positive bacteria. *Antimicrob. Agents Chemother.* 44:2086–2092.

Chapter V. General results and discussion

Since their discovery, AMPs have drawn attention due to their potential application to control important diseases caused by microbes in areas such as agroscience, veterinary and human health. Despite the existence of natural potent AMPs (e.g. cecropins, mellitin and magainins), the search for more active and shorter peptides with a broader spectrum of activity has led to the identification of synthetic AMPs highly active against plant pathogens (Montesinos 2007, Marcos 2008, Montesinos and Bardají 2008). Among the several strategies to design AMPs, the hybridization of two fragments of diverse natural AMPs has resulted in new short synthetic peptides with better antimicrobial spectra than the parent peptides and exhibiting less hemolytic activity. This is the case of the cecropin A-melittin hybrid undecapeptide Pep3 which has been reported to display activity against the phytopathogenic bacteria *Erwinia carotovora* and fungicidal activity against few fungal strains (Cavallarin 1998, Ali 2000).

V.1 Synthesis of Pep 3 analogues and evaluation of their biological activity.

V.1.1 Antimicrobial acitivity of Pep 3

The short size of Pep3 together with its reported biological activity profile attracted our attention to study its application as an antibiotic active against economically important plant pathogens (Table V.1). Thus, Pep3 was prepared and evaluated for its antimicrobial activity towards the bacteria *E. amylovora*, *P. syringae*, and *X. vesicatoria*, and the fungi *F. oxysporum*, *A. niger*, *R. stolonifer*, and *P. expansum*. Moreover, its hemolytic activity was also evaluated towards human red blood cells.

Interestingly, Pep3 inhibited the growth of all tested bacteria and fungi with minimal inhibitory concentrations (MICs) in the range of 7 to 10 μM and 2.5 to 20 μM, respectively. Pep3 showed moderate cytotoxicity, with a percent hemolysis of 56% at 150 μM (Table V.2). These results together with the ones previously reported were indicative of the wide spectrum of activity displayed by Pep3. These observations prompted us to design and synthesize new Pep3 analogues with the aim of improving its biological properties.

V.1.2 Design and synthesis of Pep3 analogues

Using Pep3 as template (Figure V.1), 22 analogues were designed by modifying some fundamental parameters that have been described to modulate the activity of AMPs, such as the positive charge, the overall hydrophobicity and amphipathicity (Yeaman and Yount 2003, Melo 2009).
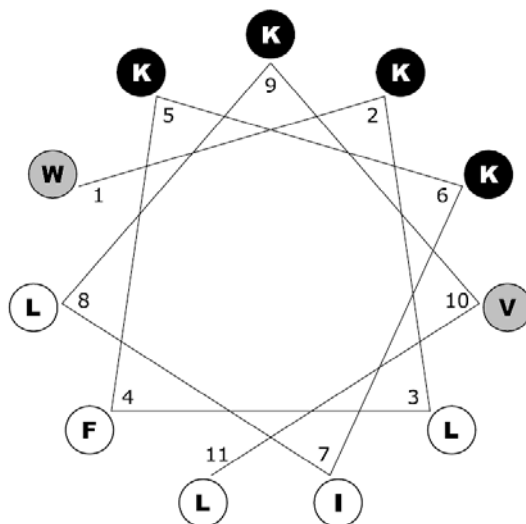
Figure V.1 Edmundson wheel projection of Pep3. Black background, hydrophilic amino acids; white background, hydrophobic amino acids; gray background, residues that were substituted for either hydrophilic (Lys) or hydrophobic (Leu, Trp, Tyr, and Phe) residues depending on the sequence as shown in Table V.1.

Primary structures of the designed Pep3 analogues are shown in Table V.1. All peptides were synthesized by the solid-phase method using Fmoc-type chemistry and were prepared as C-terminal amides except for BP01, BP05, and BP07 which were C-terminal carboxylic acid derivatives. All of them showed purity by high pressure liquid chromatography (HPLC) >90% and their identity was confirmed by electrospray ionization mass spectrometry (ESI-MS).

Analogues BP08-BP12 were blocked at the N-termini with an acetyl (Ac), tosyl (Ts), benzoyl (Bz), benzyl (Bn) or palmitoyl (Pam) group, respectively. To examine whether the entire sequence of Pep3 is necessary for its full antibacterial activity, N- and C-terminal deletion analogues (BP02-BP07) were synthesized. Peptides BP13-BP20, BP33, and BP76 were designed based on the ideal α-helical wheel diagram of Pep3 (Figure V.1). Trp and Val were substituted for amino acids possessing various degrees of hydrophobicity and hydrophilicity. Thus, Trp was replaced with Phe (BP13),

Tyr (BP14), Lys (BP15) or Leu (BP33). Val was replaced with Lys (BP17), Trp (BP18), Phe (BP19) or Tyr (BP20). Both, Trp and Val were replaced with Lys and Phe, respectively (BP76). The hydrophilic surface area and the charge of Pep3 was further increased by replacing both Trp and Val with Lys (BP16).

Table V.1 Sequences and α-helicity of Pep3 and analogues.

Peptide	Sequence[a]	$[\theta]_{222}$[b]	α-helix (%)
Pep3	W K L F K K I L K V L-NH$_2$	−9048	23.5
BP01	W K L F K K I L K V L-**OH**	-[c]	-
BP02	K L F K K I L K **K** L-NH$_2$	-	-
BP03	K L F K K I L K-NH$_2$	-	-
BP04	W K L F K-NH$_2$	-	-
BP05	W K L F K-**OH**	-	-
BP06	K I L K V L-NH$_2$	-	-
BP07	K I L K V L-**OH**	-	-
BP08	**Ac**-W K L F K K I L K V L-NH$_2$	−10851	29.5
BP09	**Ts**-W K L F K K I L K V L-NH$_2$	−13341	37.8
BP10	**Bz**-W K L F K K I L K V L-NH$_2$	−13119	37.1
BP11	**Bn**-W K L F K K I L K V L-NH$_2$	−10665	28.9
BP12	**Pam**-W K L F K K I L K V L-NH$_2$	-	-
BP13	**F** K L F K K I L K V L-NH$_2$	-	-
BP14	**Y** K L F K K I L K V L-NH$_2$	-	-
BP33	**L** K L F K K I L K V L-NH$_2$	−8918	23.1
BP15	**K** K L F K K I L K V L-NH$_2$	−9892	26.3
BP16	**K** K L F K K I L K **K** L-NH$_2$	-	-
BP76	**K** K L F K K I L K **F** L-NH$_2$	−9188	24.0
BP17	W K L F K K I L K **K** L-NH$_2$	-	-
BP18	W K L F K K I L K **W** L-NH$_2$	−8922	23.1
BP19	W K L F K K I L K **F** L-NH$_2$	−9950	26.5
BP20	W K L F K K I L K **Y** L-NH$_2$	−10316	27.7

[a] Bold letters indicate the modifications introduced into the Pep3 sequence.
[b] Determined in 50% TFE in 10 mM sodium phosphate buffer (pH = 7.4).
[c] Not determined.

V.1.3 Antimicrobial and cytotoxic activity of Pep 3 analogues

Peptides synthesized were tested for their antimicrobial activity against the bacteria *E. amylovora*, *P. syringae*, and *X. vesicatoria*, and the fungi *F. oxysporum*, *A. niger*, *R. stolonifer*, and *P. expansum*. Antimicrobial activities were evaluated at peptide concentrations ranging from 0.3 to 100 μM. Peptides which did not inhibit the growth

of the pathogens below 100 μM were considered inactive. Peptide toxicity to eukaryotic cells was determined as the ability to lyse erythrocytes as compared to melittin and was analyzed at 150 μM peptide concentration. Red blood cells instead of plant cells were used because of the highly standardized methods available and allowed to compared straightforwardly our data with previous reports. The obtained biological activity results are shown in Table V.2.

Table V.2 Antibacterial, antifungal and hemolytic activities of Pep3 and selected analogues.

Peptide	Bacteria (MIC, μM)			Fungi (MIC, μM)				Hemolysis[a] (%)
	Ea^b	Pss^b	Xav^b	Fo^b	Pe^b	An^b	Rs^b	
Pep3	7-10	7-10	7-10	2.5-5.0	15-20	5.0-7.5	10-12.5	56 ± 4.7
BP01	12-25	25-50	>100	20-25	>100	20-25	>100	0.0
BP08	10-12	7-10	2-5	1.2-2.5	7.5-10	15-20	>100	96 ± 5.2
BP09	12-15	12-15	<2	1.2-2.5	15-20	20-25	50-100	76 ± 3.5
BP10	15-20	15-20	<2	5.0-7.5	20-25	20-25	>100	73 ± 3.4
BP11	7-10	5-7	2-5	1.2-2.5	25-50	20-25	>100	90 ± 1.8
BP12	50-100	50-100	25-50	20-25	20-25	>100	>100	98 ± 4.1
BP13	25-50	12-25	50-100	1.2-2.5	25-50	20-25	50-100	15 ± 3.9
BP14	25-50	12-25	50-100	1.2-2.5	25-50	15-20	50-100	30 ± 3.0
BP15	5-7	2-5	12-15	0.6-1.2	12.5-15	5.0-7.5	7.5-10	16 ± 2.9
BP16	>100	>100	>100	0.6-1.2	>100	20-25	50-100	0
BP17	50-100	25-50	50-100	1.2-2.5	50-100	20-25	25-50	25 ± 2.2
BP18	5-7	5-7	<2	1.2-2.5	20-25	20-25	25-50	68 ± 6.3
BP19	5-7	5-7	<2	1.2-2.5	20-25	20-25	25-50	95 ± 3.3
BP20	2-5	2-5	2-5	0.6-1.2	20-25	15-20	25-50	77 ± 1.3
BP33	5-7	5-7	10-12	0.3-0.6	25-50	20-25	25-50	37 ± 2.7
BP76	2-5	2-5	2-5	0.6-1.2	25-50	20-25	25-50	34 ± 2.1

[a] Percent hemolysis at 150 μM. The confidence interval for the mean is included.
[b] *Pss, Pseudomonas syringae* pv. *syringae*; *Xav, Xanthomonas axonopodis* pv. *vesicatoria*; *Ea, Erwinia amylovora; Fo, Fusarium oxysporum; Pe, Penicillium expansum; An, Aspergillus niger; Rs, Rhizopus stolonifer.*

Despite being the fungus *F. oxysporum* the most susceptible pathogen, all peptides displayed, in general, a higher antibacterial than antifungal activity. Except for

X. vesicatoria was the most sensitive bacteria, result that is in agreement with previous reports, which showed that this bacteria was more susceptible than *P. syringae* and *E. carotovora* to peptides such as MII, MSI-99, and cecropin B (Alan and Earle 2002). Moreover, in a parallel study performed in our group during the development of

this thesis, *X. vesicatoria* also resulted to be more sensitive than *E. amylovora* and *P. syringae* to cyclic cationic antimicrobial decapeptides (Monroc 2006). This different level of susceptibility of pathogens to the same AMP has been attributed to variation in the components of the plasma membrane of the target microorganism, e.g., charge and lipid composition, which would influence the rates of binding of cationic peptides to the membranes (Yeaman and Yount 2003).

Moreover, peptides with high antimicrobial activity and low hemolysis were identified. This selectivity could be ascribed to the absence of acidic phospholipids and the presence of sterols which reduce the susceptibility of eukaryotic cells to lytic peptides (Matsuzaki 2009).

The influence of modifications introduced in Pep3 on the antimicrobial and hemolytic activity is described below:

(i) The C-terminal peptide acid derivative BP01 was significantly less active than Pep3, fact that can be ascribed to the repulsion between the C-terminal carboxylate and the negatively charged phospholipids that constitute the microbial surfaces. This repulsion may difficult the peptide-membrane internalization limiting the peptide disrupting effect.

(ii) The N- and C-terminal deletion analogues (BP02 to BP07) were inactive against the tested pathogens and they were not further tested for their hemolysis. The inactivity could be attributed to the size of their sequence which is too short to stabilize an α-helical structure.

(iii) The N-terminal derivatization of Pep3 led to analogues BP08 to BP11 with significant antimicrobial activity, except for the N-palmitoylated peptide BP12. Among them, the N-benzylated analogue BP11 was the most antibacterial peptide while the N-acetylated derivative BP08 was the most antifungal, being both peptides slightly more effective than Pep3 against some of the tested pathogens (Table V.2).

However, the N-terminal derivatization (BP08 to BP12) caused a significant increase of the hemolytic activity (ranging from 70 to 100% at 150 μM) compared to Pep3 (56%). This higher toxicity could be ascribed to the increase of the peptide hydrophobicity, and to the reduction of the cationic charge due to the blockage of N-terminal amino group. In fact, the less hemolytic peptide of this group is BP11 (by

comparing the 50% effective dose (HD_{50}) (see Ferre 2006)), in which the derivatization does not modify the charge.

(iv) The replacement of the amino acids located at the interface (Trp and Val) with residues with various degrees of hydrophobicity (Figure V.1, Table V.2), resulted in great changes in antimicrobial activity. These substitutions led to analogues with significant less antifungal activity than Pep3 against *A. niger*, *R. stolonifer*, and *P. expansum*. Only the analogue BP15, which incorporates a Lys residue at the N-terminus, displayed a slightly higher antifungal activity against *P. expansum* and *R. stolonifer* compared to the parent petide. Against *F. oxysporum*, all the analogues displayed a higher activity than Pep3.

Regarding the antibacterial and hemolytic activities, the replacement of Trp with Lys (BP15) or Leu (BP33) induced a slight increase of the overall activity, and a significant reduction of the hemolytic activity (from 2- to 3-fold). In contrast, replacement of Trp with Phe (BP13) or Tyr (BP14) resulted in analogues with poor antibacterial activity and less hemolytic than Pep3. The reduction of the toxicity of BP15 may be associated to an increase of the overall cationic charge and a reduction of the hydrophobicity compared to Pep3. For peptides BP13, BP14 and BP33, the reduction of the toxicity could be due to the absence of Trp residue. It has been reported that Trp can assume a defined orientation when binding to the cholesterol present in mammalian cell membranes leading high hemolysis (Blondelle and Lohner 2000).

On the other hand, the replacement of Val with hydrophobic aromatic residues such as Trp (BP18), Phe (BP19) or Tyr (BP20) resulted in analogues with a considerably higher antibacterial activity than Pep3 (MICs of <2 to 7 μM), but were also more hemolytic. In contrast, BP17, which has a Lys instead of a Val, did not show antibacterial activity.

A double replacement of both Trp and Val with Lys and Phe (BP76), respectively, led to a significant increase of the antibacterial activity (MICs ranging from 2 to 5 μM), and to a twofold decrease of the hemolytic activity compared to Pep 3. Moreover, when Trp and Val were both replaced with two Lys (BP16), which increased the peptide charge from +5 to +7, resulted in an analogue with no antibacterial and hemolytic activity.

Therefore, these results confirm previous data on how subtle changes in AMP sequences influence antimicrobial and hemolytic activity (López-Garcia 2002, Monroc 2006). For Pep3 analogues, structural features that seem to be important for the antimicrobial activity are a basic N-terminus and a hydrophobic C-terminus. In particular, an aromatic amino acid residue at the C-teminus is preferable for a high antibacterial activity. Moreover, the most active peptides had a net charge of +5 or +6. In contrast to antimicrobial and hemolytic activities that were dramatically influenced by single- or double-residue replacement, the α-helical content of peptides was not significantly affected, as shown in Table V.1. Notably, peptides BP33 and BP76 should be praised for their good balance between antibacterial and hemolytic activities, as well as BP15 for its wide spectrum of antimicrobial activity against both bacteria and fungi, and for its low toxicity towards mammalian cells.

V.1.4 Microbicidal activity of Pep 3 analogues

Since some of the peptides showed similar activity against some of the tested strains, their microbicidal activity was evaluated to compare their efficacy. A microbicidal effect is preferable as the compounds kill the cells, in contrast to a microbiostatic effect in which the inhibition persists after releasing the treatment. Different biological assays were carried out for bacteria and fungi.

Bactericidal activity of selected peptides (Pep 3, BP11, BP15, BP33, and BP76) was assessed by comparing the time course to kill mid-logarithmic-phase culture suspensions of *E. amylovora*, *P. syringae*, and *X. vesicatoria*. As previously described with other cationic peptides and unlike conventional antibiotics that in many cases are bacteriostatic (Hanckok 2001, Hanckok and Rozek 2002), all peptides showed a bactericidal effect against the three bacteria at concentrations around the MIC (5 μM), except for BP11 which had no effect against *E. amylovora* (Fig V.2). The bactericidal effect of these peptides was slower against *P. syringae* compared to the other two bacteria. Notably, BP76 was the most bactericidal against *X. vesicatoria* and *E. amylovora* inhibiting completely their growth after 90- and 120-min exposure period, respectively. These results stress the efficacy of these compounds against such pathogens and are indicative of their potential applicability to control severe bacterial diseases.
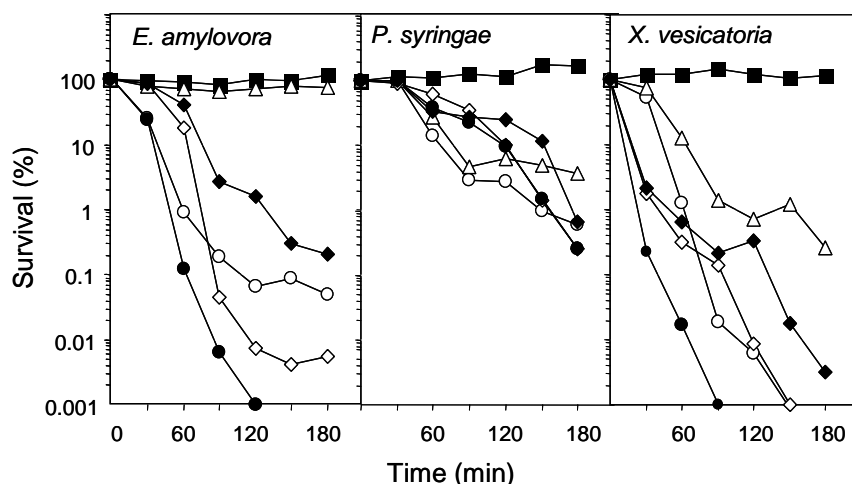
Figure V.2 Kinetics of survival of *P. syringae*, *X. vesicatoria* and *E. amylovora* in the presence of Pep3 (○) or selected analogues. Bacterial suspensions were untreated (■) or treated with 5 μM BP11 (△), BP15 (◇), BP33 (◆), or BP76 (●), and viable cells were determined at different time intervals.

On the other hand, the sporicidal activity of the most antifungal peptides, Pep3, BP15, BP20, BP33, and BP76, was evaluated against *F. oxysporum* by comparing the survival of conidia after 35 min of exposure at different peptide concentrations (Figure V.3). Spores are resting structures of fungi with high survival capacity under adverse conditions and are the most difficult stages to control (Russell 1982). Therefore, the sporicidal activity of antifungal peptides is critical for efficient control of fungal diseases. At concentrations around the MIC (<5.0 μM), all peptides exhibited a similar behaviour, whereas an increase of peptide concentration led to a different logarithmic pattern for each peptide making evident in all cases a fungicidal effect. Except for BP15, all peptides were more potent than Pep 3, being BP33 the most sporicidal killing 99 to 99.9% of the *F. oxysporum* spores in 35 min at 15 μM. This fungicidal activity is comparable with the activities reported for currently used fungicide agents (Mazzola 2003).

In order to further understand the damaging effects of peptides Pep3, BP15, BP20, BP33, and BP76 on *F. oxysporum* conidia, Sytox green uptake experiments were carried out and were correlated with the sporicidal activity (See Figure 2 in Badosa 2009). Sytox green, a cationic nucleic acid probe, increases its fluorescence after binding DNA chains, which is indicative of membrane leakage, and allows the assessment of the peptide capability to permeabilize the membrane. Results showed a clear increase of the Sytox green fluorescence upon the treatment of *F. oxysporum*

conidia with different peptide concentrations, suggesting that membrane permeabilization may be crucial for their mode of action.
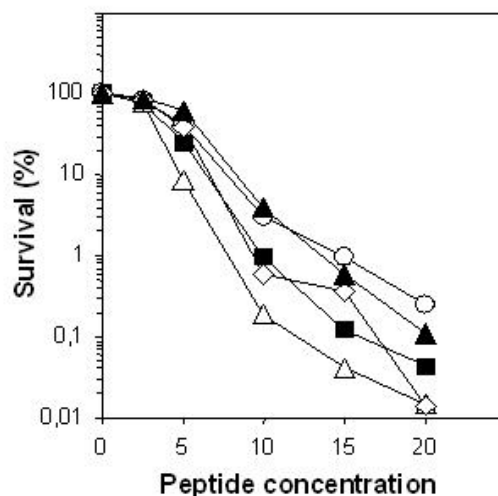

Figure V.3 Sporicidal activity of selected peptides on *F. oxysporum* conidia. Conidial suspensions were treated with peptides Pep3 (▲), BP20 (■), BP33 (△), BP15 (○) or BP76 (◇), and incubated at 25 ºC for 35 min. Viable spores were counted after dilution and plating in PDA agar. Values are expressed as percentage of survival from the start of the experiment.

V.1.5 Susceptibility to proteolysis of Pep 3 analogues

In order to use these peptides for plant protection, protease digestion stability is a desired property to assure a reasonable half-life of the molecules in the plant environment. Proteases from epiphytic microorganisms or intrinsic to the plant internal tissues may degrade AMPs (Cavallarin 1998, Ali and Reddy 2000). However, it must be taken into account that a certain level of biodegradability is necessary to avoid peptide accumulation in the natural environment which could entail negative effects.

The susceptibility of the most active peptides to proteolysis was studied by exposure to proteinase K and degradation was monitored by HPLC over time (Figure V.4). Proteinase K is a broad spectrum serine protease commonly used for the digestion of peptides and proteins. Interestingly, BP76 turned out to be twofold more stable than Pep3 and than the rest of the analogues. While Pep3 was completely degraded after 45 min of incubation with the enzyme, BP76 underwent only 50% degradation. The higher protease stability of BP76 compared to Pep3 could be associated to the double amino acid replacement, which resulted to be equivalent to methods commonly used to increase peptide stability, such as replacement of a natural amino acid with a D-amino acid or by peptide cyclization (Hong 1999, Rozek 2003).
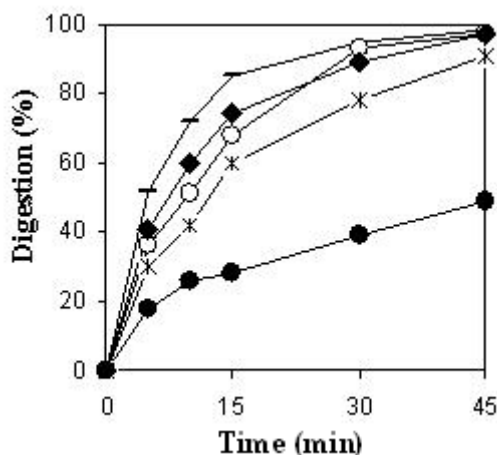
Figure V.4 Digestion kinetics of Pep3 (○) and selected analogues BP08 (─), BP20 (✕), BP33 (◆), and BP76 (●) by proteinase K.

V.2 Improvement of the biological properties of BP76 through a combinatorial chemistry approach

Since *in vitro* results do not necessary reflect the efficacy of peptides *in vivo*, a large number of peptides with potential *in vitro* activity must be prepared in order to successfully find *in vivo* active compounds. Thus, the promising results obtained for BP76 prompted us to design a combinatorial library to improve the antimicrobial activity of this peptide and minimize its cytotoxicity, with the aim of testing the best peptides in *in vivo* experiments.

V.2.1 Design and synthesis of the library

The peptide library was designed based on the ideal α-helical wheel diagram of H-K^{1}KLFKKILKF^{10}L-NH$_2$ (BP76) and comprised 125 peptides (Figure V.5). Similarly to the previous studies on Pep3, the library was designed by incorporating at positions 1 and 10 amino acids possessing various degrees of hydrophobicity and hydrophilicity. Thus, Lys, Tyr, Leu, Phe or Trp were incorporated at position 1, and Lys, Tyr, Val, Phe or Trp were introduced at position 10. Moreover, blocking of the N-terminus with an acetyl (Ac), tosyl (Ts), benzoyl (Bz) or benzyl (Bn) group was also studied.
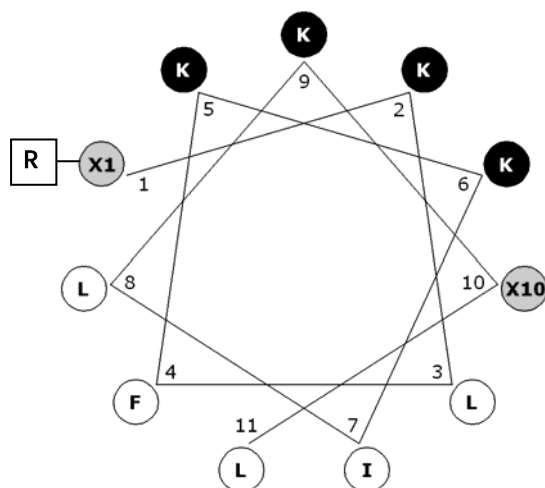
Figure V.5 Edmunson wheel projection of the 11-mer peptides of the 125-member library. Black background stands for hydrophilic amino acids (Lys) and white background for hydrophobic amino acids. The library was designed by combining 5 variations at each R, X1 and X10 positions: R= H, Ac, Ts, Bz or Bn; X1= Lys, Leu, Trp, Tyr or Phe; X10= Lys, Val, Trp, Tyr or Phe.

In order to facilitate the representation of the library members, they are denoted using brace numbers as {R, X1, X10}, which define the variations at each R, X1 and X10 positions.

Peptides were prepared by the solid-phase method using Fmoc-type chemistry, in a parallel approach. Due to the size of the library, this strategy was chosen because it provides pure samples of individual compounds which facilitates interpretation of the biological results. Except for the N-terminal benzylated peptides, which were obtained as a mixture of mono and dibenzylated derivatives, all peptides showed >90% HPLC purity, and their identity was confirmed by ESI-MS.

V.2.2 Antibacterial activity of the peptide library

The antibacterial activity of the peptide library was tested for the *in vitro* growth inhibition of *E. amylovora*, *X. vesicatoria*, and *P. syringae*. Most peptides (94.4% of the 125-member library) exhibited potent antibacterial activity against at least one pathogen, except for {H,K,K} (BP16), {H,Y,V} (BP14), {H,L,K}, {Ac,L,K}, {H,F,K}, {H,F,V} (BP13), and {H,W,V}(Pep 3) (Figure V.6). MIC values below 7.5 μM were obtained for 113, 40 and 27 peptides against *X. vesicatoria*, *P. syringae* and *E. amylovora*, respectively. Interestingly, while 84 peptides were as potent as the parent peptide BP76 against *X. vesicatoria* (MIC of 2.5-5 μM), 18 peptides improved its antimicrobial activity (MIC < 2.5 μM). Complete inhibition of *P. syringae* and *E.*

amylovora was observed at the same MIC range than BP76 (2.5 to 5 µM) for 8 and 6 peptides, respectively. Moreover, 32 and 21 peptides exhibited remarkable MIC values of 5.0 to 7.5 µM against *P. syringae* and *E. amylovora*, respectively.
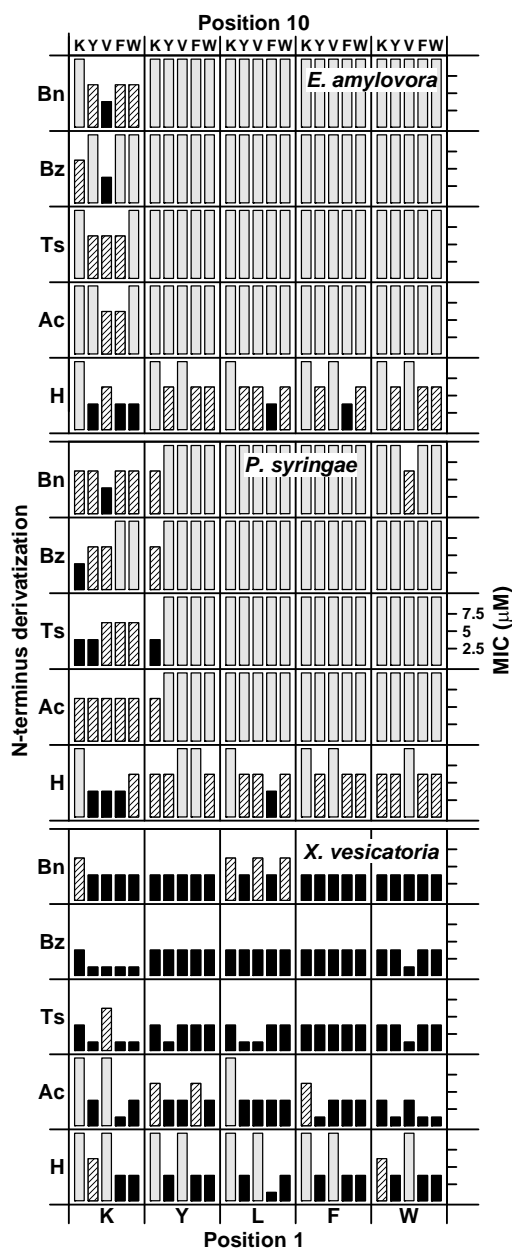
Figure V.6 MICs of the 125-member peptide library against *E. amylovora*, *P. syringae* pv. *syringae* and *X. axonopodis* pv. *vesicatoria*. Amino acids of different degree of hydrophilicity and hydrophobicity (X) at positions 1 and 10, and N-terminal derivatizations (R) were introduced in R-X^{1}KLFKKILKX^{10}L-NH$_2$. Derivatization corresponds to acetylation (Ac), tosylation (Ts), benzoylation (Bz) and benzylation (Bn). Solid black bars stand for MIC<5.0 µM, striped bars for MIC of 5.0 to 7.5 µM, and shaded bars for MIC>7.5 µM.

This study confirms our preliminary results obtained for the first set of Pep3 analogues. A basic N-terminus and a hydrophobic C-terminus are important for the antimicrobial activity (Ferre 2006). The most active peptides had a net charge of +5 to +6. Moreover, activity was favoured when position 10 incorporated an aromatic residue. N-terminal derivatization led to an important decrease of the antibacterial activity

against *P. syringae* and *E. amylovora*, but afforded peptides with identical or improved MIC values against *X. vesicatoria*. For non-derivatized peptides accommodating residues other than Lys at position 1, best activities were observed when position 10 was occupied by an aromatic residue. The most active peptides against the three plant pathogenic bacteria followed these general structural requirements, i.e. BP31, BP32, BP52, BP66, BP76, BP77, BP78, BP81, BP100, BP102, BP103, BP105, BP121, BP125, and BP126 (Table V.3).

Table V.3 Antibacterial activity (MIC) and cytotoxicity of the most active peptides of the library.

Peptide			MIC intervals (µM)			Hemolysis (%)[a]
Code	Notation[b]	Sequence	*Pss*[c]	*Xav*[c]	*Ea*[c]	150 µM
BP76	{H,K,F}	H-KKLFKKILKFL-NH$_2$	2.5-5.0	2.5-5.0	2.5-5.0	34 ± 2.1
BP31	{Bz,K,V}	Bz-KKLFKKILKVL-NH$_2$	5.0-7.5	<2.5	2.5-5.0	71 ± 2.3
BP32	{Bn,K,V}	Bn-KKLFKKILKVL-NH$_2$	2.5-5.0	2.5-5.0	2.5-5.0	-[d]
BP52	{H,K,W}	H-KKLFKKILKWL-NH$_2$	5.0-7.5	2.5-5.0	2.5-5.0	84 ± 6.5
BP66	{H,F,F}	H-FKLFKKILKFL-NH$_2$	5.0-7.5	2.5-5.0	2.5-5.0	63 ± 5.9
BP77	{Ac,K,F}	Ac-KKLFKKILKFL-NH$_2$	5.0-7.5	<2.5	5.0-7.5	40 ± 3.8
BP78	{Ts,K,F}	Ts-KKLFKKILKFL-NH$_2$	5.0-7.5	<2.5	5.0-7.5	85 ± 7.4
BP81	{H,L,F}	H-LKLFKKILKFL-NH$_2$	2.5-5.0	<2.5	2.5-5.0	65 ± 1.5
BP100	{H,K,Y}	H-KKLFKKILKYL-NH$_2$	2.5-5.0	5.0-7.5	2.5-5.0	22 ± 2.8
BP102	{Ts,K,Y}	Ts-KKLFKKILKYL-NH$_2$	2.5-5.0	<2.5	5.0-7.5	79 ± 6.5
BP103	{Bz,K,Y}	Bz-KKLFKKILKYL-NH$_2$	5.0-7.5	<2.5	>7.5	83 ± 13.5
BP105	{H,L,Y}	H-LKLFKKILKYL-NH$_2$	5.0-7.5	2.5-5.0	5.0-7.5	91 ± 6.2
BP121	{Ts,Y,K}	Ts-YKLFKKILKKL-NH$_2$	2.5-5.0	2.5-5.0	>7.5	81 ± 3.7
BP125	{Ts,K,K}	Ts-KKLFKKILKKL-NH$_2$	2.5-5.0	2.5-5.0	>7.5	8 ± 1.6
BP126	{Bz,K,K}	Bz-KKLFKKILKKL-NH$_2$	2.5-5.0	2.5-5.0	5.0-7.5	14 ± 2.9

[a]Percent hemolysis at 150 µM plus confidence interval (α = 0.05)
[b]Letters included in the braces define variations at each R, X1 and X10 positions for the sequence R-X^{1}KLFKKILKX^{10}L-NH$_2$. Derivatization of R corresponds to acetylation (Ac), tosylation (Ts), benzoylation (Bz) and benzylation (Bn)
[c]*Pss, Pseudomonas syringae* pv. *syringae; Xav, Xanthomonas axonopodis* pv. *vesicatoria*; *Ea, Erwinia amylovora*
[d]Not determined

The bactericidal activity of peptides BP76, BP77, BP100, BP125, and BP126 against *E. amylovora* was evaluated, and results showed that all of them behaved as bactericides, being BP100 slightly more bactericidal than BP76 (Badosa 2007).

V.2.3 Antifungal activity of the peptide library

The antifungal activity of the peptide library was evaluated against the fungus *P. expansum* (Figure V.7). Fifty-four sequences displayed antifungal activity below 25 μM against *P. expansum*. Thirty-nine peptides displayed MICs of 12.5 to 25 μM and 13 sequences showed moderate activity (MICs of 6.25 to 12.5 μM). Peptides BP21 {Ac,F,V} and BP34 {Ac,L,V} were the most active with MICs below 6.25 μM. Difficulties were encountered in order to set general peptide features that are related to antifungal activity. Nevertheless, the best peptides bear a charge of +4 to +5, a Val at position 10 and were N-terminal acetylated (Figure V.7 and Table V.4). On the other hand, peptides bearing a Lys at position 10 did not show antifungal activity at the higher tested concentration (25 μM). The latter is concurrent with our previous observation that a hydrophobic C-terminus was crucial for the antimicrobial activity.
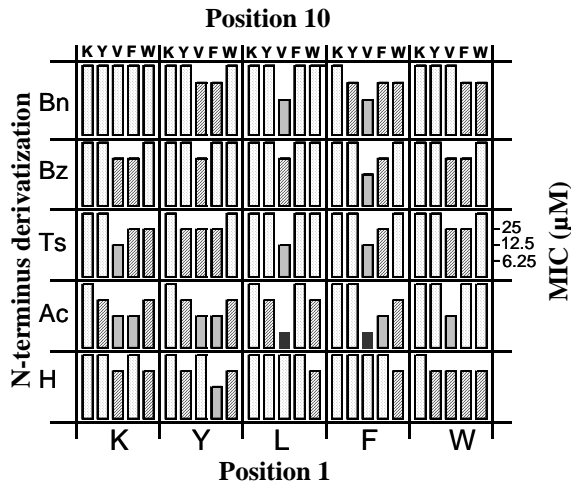
Figure V.7 MICs of the 125-member peptide library against *P. expansum*. Amino acids with various degree of hydrophilicity and hydrophobicity (X^1 and X^{10}) and N-terminal derivatizations (R) were introduced in the sequence R-X^1KLFKKILKX^{10}L-NH$_2$. Derivatization corresponds to acetylation (Ac), tosylation (Ts), benzoylation (Bz) and benzylation (Bn). Solid black bars stand for MIC <6.5 μM, shaded bars for MIC = 6.25-12.5 μM, striped bars for MIC = 12.5-25 μM, and dotted bars for MIC >25 μM.

Table V.4 Antifungal activity (MIC) and cytotoxicity of the most active peptides of the library.

Peptide			MIC (μM)	Hemolysis (%)[a]
Code	Notation[b]	Sequence	*P. expansum*	150 μM
BP08	{Ac,W,V}	Ac-WKLFKKILKVL-NH$_2$	6.25-12.5	96 ± 5.2
BP21	{Ac,F,V}	Ac-FKLFKKILKVL-NH$_2$	<6.5	85 ± 1.4
BP22	{Ts,F,V}	Ts-FKLFKKILKVL-NH$_2$	6.25-12.5	73 ± 1.5
BP23	{Bz,F,V}	Bz-FKLFKKILKVL-NH$_2$	6.25-12.5	81 ± 9.8
BP24	{Bn,F,V}	Bn-FKLFKKILKVL-NH$_2$	6.25-12.5	96 ± 2.8
BP25	{Ac,Y,V}	Ac-YKLFKKILKVL-NH$_2$	6.25-12.5	54 ± 7.6
BP29	{Ac,K,V}	Ac-KKLFKKILKVL-NH$_2$	6.25-12.5	70 ± 4.0
BP30	{Ts,K,V}	Ts-KKLFKKILKVL-NH$_2$	6.25-12.5	70 ± 5.9
BP34	{Ac,L,V}	Ac-LKLFKKILKVL-NH$_2$	<6.5	45 ± 2.8
BP35	{Ts,L,V}	Ts-LKLFKKILKVL-NH$_2$	6.25-12.5	80 ± 1.1
BP37	{Bn,L,V}	Bn-LKLFKKILKVL-NH$_2$	6.25-12.5	87 ± 7.9
BP67	{Ac,F,F}	Ac-FKLFKKILKFL-NH$_2$	6.25-12.5	86 ± 2.4
BP71	{H,Y,F}	H-YKLFKKILKFL-NH$_2$	6.25-12.5	69 ± 7.1
BP72	{Ac,Y,F}	Ac-YKLFKKILKFL-NH$_2$	6.25-12.5	63 ± 1.0
BP77	{Ac,K,F}	Ac-KKLFKKILKFL-NH$_2$	6.25-12.5	40 ± 2.3

[a]Percent hemolysis at 150 μM plus confidence interval ($\alpha = 0.05$)
[b]Letters included in the braces define variations at each R, X1 and X10 positions for the sequence R-X^{1}KLFKKILKX^{10}L-NH$_2$. Derivatization of R corresponds to acetylation (Ac), tosylation (Ts), benzoylation (Bz) and benzylation (Bn).

The fungicidal activity of peptides BP21 {Ac,F,V} and BP22 {Ts,F,V} against *P. expansum* was evaluated, and results showed that they were sporicidal, but a longer exposure (180 min) was necessary to kill the conidia, compared to that for *F. oxysporum* (35 min) (See Figure 1 in Badosa 2009).

V.2.4 Toxicity of the peptide library

The toxicity of the peptide library was first evaluated as the ability to lyse human erythrocytes. The percent hemolysis of peptides with the best antibacterial or antifungal activities are shown in Tables V.3 and V.4. Several studies have shown that an increase of the hydrophobicity is related to an increase of cytotoxicity (Blondelle and Lohner 2000, Oh 2000). Moreover, the absence of acidic phospholipids and the presence of sterols reduce the susceptibility of eukaryotic cells to cationic peptides

(Matsuzaki 2009). Accordingly, we have found that the N-terminal derivatization and the substitution of the Lys at position 1 by hydrophobic amino acids led to an important increase of the hemolytic activity, being those that incorporate Trp among the most hemolytic. In contrast, peptides bearing Lys at positions 1 and/or 10 resulted to be the less hemolytic. Thus, the hemolytic activity was clearly related to the overall peptide charge, being the most cationic peptides the less hemolytic. This trend was observed for the most active antifungal peptides which were less cationic and more hemolytic that the peptides with the highest antibacterial activity. Despite the hemolytic activity of the antifungal peptides was significant at 150 μM, this concentration is around 20-30 times the MIC, and it is of the same order than that of current fungicides, such as imazalil.

To further study the toxicity of these peptides, BP100, one of the most active antibacterial analogues of the library, was tested *in vitro* on V79 hamster lung fibroblast cells (Ferre 2009). The effect of BP100 on the mitochondrial activity, cell monolayer adherence, and membrane integrity of these cells was evaluated. Results showed that BP100 was cytotoxic, with IC_{50} ranging from 51.1 to 64.3 μM. Despite cytotoxicity in V79 cells was observed at a lower peptide concentration range than for human erythrocytes, this range is still far above the anticipated antimicrobial application levels.

Although *in vitro* tests give valuable information of toxicity, *in vivo* studies have to be performed to assess the potential application of these compounds in crop protection. Toxicity studies of AMPs on animals are scarce and few information has been reported (Marr 2006). However, since both animals and humans are in contact with pesticides through food ingestion, toxicity tests on animals are essential for safety reasons. Thus, we submitted three of the best peptides (BP15, BP21, and BP100) to acute oral toxicology testing in mice of both sexes. No mortality was recorded in animals of either sex for peptides BP15 and BP21 at the highest tested concentration, showing a maximum nonlethal dose (NLD) higher than 2000 mg/kg and 900 mg/kg of body weight, respectively. Peptide BP100 showed a NLD in the range of 1000-2000 mg/kg of body weight (Montesinos and Bardají 2008). These results clearly point out the safety profile of these antimicrobial peptides.

V.2.5 Modulating antibacterial and/or antifungal activity

Antimicrobial peptides derived from natural compounds or *de novo* designed have been reported to be antibacterial, antifungal, or both (Marcos 2008, Montesinos and Bardají 2008). The screening of the present AMP library against plant pathogenic bacteria and fungi led to the identification of peptides covering all possibilities. As a matter of example, peptides BP76, BP100, BP125 and BP126 were strongly antibacterial but poorly antifungal, BP21 and BP34 displayed a strong antifungal activity but a poor antibacterial activity, and peptide BP77 showed a broad-spectrum of activity being both antibacterial and antifungal.

The selectivity of these peptides towards a specific microorganism has been associated to structural differences, such as the overall peptide charge, the nature of the amino acids located at position 1 or 10, and the N-terminal derivatization. Thus, based on this study, it is tempting to speculate that the antimicrobial activity of these peptides may be modulated by tailoring them with the above mentioned structural modifications.

V.2.6 *Ex vivo* antimicrobial activity in plant model systems

In vitro tests can not predict the efficacy of compounds on the plant host tissue environment. On the other hand, *in vivo* plant experiments are complex and time-consuming limiting the number of compounds to be evaluated. In this context, *ex vivo* experiments have evolved as good testing methods as they are closer to the real plant environment and allow the screening of a large number of compounds. Moreover, *ex vivo* methods are crucial when involving plant quarantine pathogens that require biosafety containment levels in the laboratory greenhouse (e.g., *E. amyolvora* in the EU) (Montesinos and Bardají 2008).

In order to evaluate the anti-infective efficacy of the peptides that showed a good balance between antimicrobial and cytotoxic activity, we used *ex vivo* assays based on detached flowers and fruits. Unlike other reports (Alan and Earle 2002), a more realistic preventive strategy was used in order to mimic preventive treatments used for field or post-harvest disease control. In contrast to reported methods where the peptides are mixed and/or preincubated with the pathogens before being applied to the plant, in our strategy, peptides were first applied to the plant model system to be adsorbed by the plant tissue, and then the pathogen was inoculated into the treated site. The antibacterial

activity of selected peptides was evaluated as the reduction of the severity of infection caused by *E. amylovora* in apple and pear flowers after 5 days of exposure. We used flowers as plant model systems because they are the main entrance sites on susceptible plants for fire blight infections (Thompson 1986, Vanneste 2000). On the other hand, the antifungal activity of selected peptides was assessed as the reduction of rot lesion diameter caused by *P. expansum* on immature apple fruits after 11 days of exposure.

All the peptides tested, BP76, BP77, BP100, BP125, and BP126, significantly reduced the severity of infections caused by *E. amylovora* in apple and pear flowers at 100 and 200 μM, except for the peptide BP77 at 100 μM (Figure V.8). BP100 resulted to be the most potent with a disease reduction of 63% in apple and 74% in pear flowers. The effective concentration observed for BP100 is comparable to the dose of streptomycin (50 to 200 μM) currently used in field sprays for control of fire blight and other bacterial diseases of plants (McManus 2002, Vidaver 2002). Moreover, no visible signs of phytotoxicicity in flowers were observed at the peptide concentration assayed indicating their feasibility for their application in plant protection.
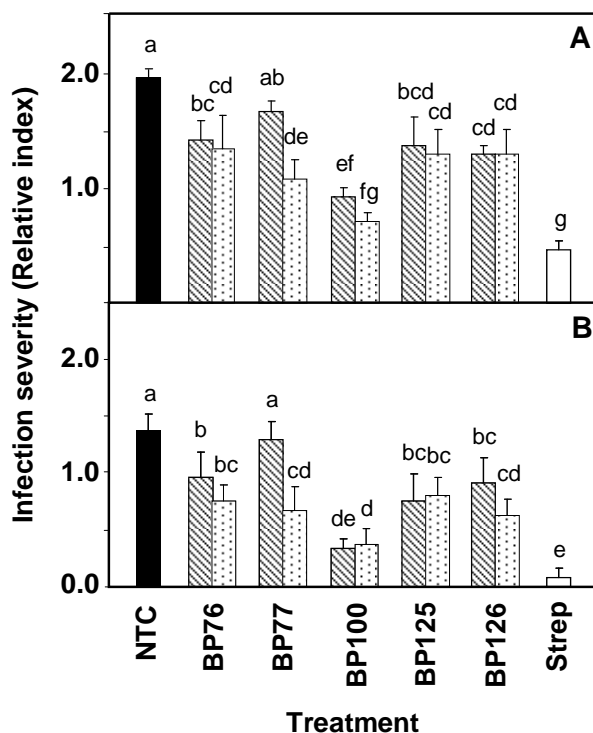

Figure V.8 Effect of the preventive application of linear undecapeptides at 100 μM (hatched bars) or 200 μM (dotted bars) on *E. amylovora* infections in detached apple (A) and pear (B) flowers. A non-treated control (black bars) and a reference treatment with streptomycin (white bars) were used. The confidence interval for the mean is indicated on the top of the bars.

The antifungal preventive effect of peptides BP21, BP22, BP23, BP29, BP34 and BP71, was evaluated against infections caused by *P. expansum* in wounds of apple fruits, and was compared with the commercial fungicide imazalil (Figure V.9). All peptides tested significantly decreased apple rot lesion size at 300 μM compared to the non-treated control, except for BP71 in the first experiment. The most active peptide was BP22 with an average efficacy of 56% disease reduction, being only slightly lower than that of the commercial formulation of the fungicide imazalil. Moreover, the obtained results stress the importance of the *ex vivo* experiments on the finding of active pesticides. For example BP22, which was less active than BP21 and BP34 when was evaluated *in vitro*, resulted to be the most active in *ex vivo* plant model experiments.
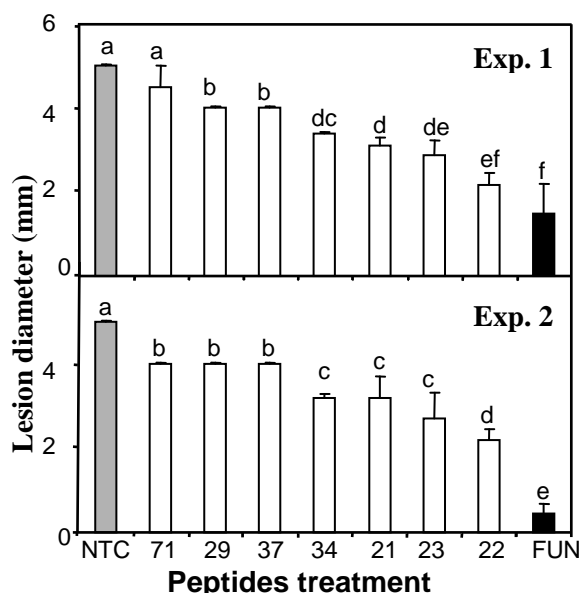

Figure V.9 Effect of the preventive application of peptides in wounds of apple fruits on *P. expansum* infection. Wounds were treated with peptides at 300 μM, inoculated with conidia and rot lesion diameter determined after 11 days of incubation at 20 ºC. Two experiments were performed. A non-treated control (NTC) and a reference treatment with the fungicide imazalil (FUN) (375 μM) were used. The confidence interval for the mean is indicated on the top of the bars.

It should be noticed that formulation can greatly improve the antimicrobial activity of pesticides. In our case peptides were applied as aqueous solutions, therefore their effective concentration could be reduced after an appropriate formulation.

V.3 Study of the mode of action of BP100 using spectroscopic methodologies

With the aim of better understanding the biological activities displayed by our designed antimicrobial peptides, we investigated the interaction of one of the most representative peptides from the library (BP100) with different model membranes using spectroscopic methodologies. Considering that BP100 contains a Tyr residue, which makes the peptide intrinsically fluorescent, we exploited its photophysical properties to obtain information about its binding affinity and damaging effect on LUVs having a lipid composition similar to that of the bacterial and mammalian cytoplasmatic membranes.

V.3.1 Photophysical characterization of BP100 in aqueous solution

Since peptide aggregation in solution makes difficult the interpretation of the peptide-membrane interaction data, we first ensured that BP100 did not aggregate at those concentrations in which the biophysical studies should be carried out. Linear dependencies were observed for both absorbance and fluorescence intensities of BP100 at concentrations up to 140 μM reflecting the absence of aggregation below this concentration. This observation was reinforced by the obtained λ_{exc}, λ_{em} and ε values which resulted to be similar to those of free Tyr (275 nm, 303 nm and 1400 $M^{-1}cm^{-1}$, respectively) (Santos and Castanho 2002b) pointing out its accessibility to the polar environment. Moreover, a Stern-Volmer quenching constant (K_{SV}) of 15.1 M^{-1} was obtained by fluorescence quenching of BP100 with the aqueous quencher acrylamide. This value was similar to the one observed for the free Tyr, supporting that this residue in BP100 is accessible to the aqueous media. The high cationic charge of BP100 (+6) together with its unability to adopt a α-helical structure in aqueous solution (data not shown) account for its high solubility and the absence of aggregation in aqueous solution.

V.3.2 Membrane insertion studies

In order to study at the molecular level the selectivity observed for BP100 towards microbial cells, we evaluated the partition extent of this peptide into bacterial and mammalian model membranes using the partition model adapted from the described by Santos et al. that allows the calculation of the Nernst partition constant (K_p) from the fluorescence intensity of a peptide-lipid system (*I*) versus phospholipid concentration

([L]) plots at a constant peptide concentration (Equation V.1) (Santos 2003). I_W and I_L are the fluorescence intensities that the mixture would display if all the peptide is in the aqueous or the lipidic phase, respectively; γ_L is the phospholipid molar volume, which is considered to be 0.763 M^{-1}, corresponding to the typical value for liquid crystalline lipid bilayers (Nagle and Wiener 1988).

$$\frac{I}{I_W} = \frac{1 + K_p \gamma_L \dfrac{I_L}{I_W}[L]}{1 + K_p \gamma_L [L]} \quad \textbf{Equation V.1}$$

The partition parameters obtained for each model system as well as their phospholipid constitution are shown in Table V.5. The neutral systems palmitoyl oleoyl phosphatidyl choline (POPC) and 2:1 POPC/cholesterol LUVs were used as models of the outer leaflet of mammalian membranes. The anionic systems consisting on 2:1 and 4:1 palmitoyl oleoyl phosphatidyl glycerol (POPG)/POPC LUVs served as models for the outer and the inner leaflet of bacterial membranes, respectively. The K_p values obtained for BP100 in bacterial and mammalian membrane models differed in one order of magnitude (Table V.5). These results are in good agreement with the potent antibacterial activity and the low cytotoxicity displayed by BP100 (Badosa 2007, Montesinos and Bardají 2008), and are consistent with the expected preference of cationic peptides for negatively charged membranes as a consequence of a strong electrostatic interaction. The high K_p values obtained upon partition with bacterial model systems are also indicative of a high peptide concentration in the membrane, which is expected to be more than 30000 times higher than in the aqueous phase.

Table V.5 Summary of the characteristics of each studied system: constitution and partition parameters determined using Equation V.1

Modeled system	Constituent phospholipids	$K_p / 10^3$	I_L/I_W
Bacterial membrane models			
Outer leaflet	2:1 POPG:POPC	30.8 ± 6.2	3.59 ± 0.06
Inner leaflet	4:1 POPG:POPC	87.6 ± 9.8	3.58 ± 0.02
Mammalian membrane models			
Outer leaflet	100 % POPC	1.6 ± 0.5	1.54 ± 0.06
Outer leaflet + cholesterol	2:1 POPC:cholesterol	3.5 ± 1.3	1.55 ± 0.06

Interestingly, while for the neutral systems the increase of fluorescence followed a hyperbolic-like relationship, the partition curves for the anionic systems deviated from this behaviour (Figure V.10). For the latter, an overshoot of the fluorescence was detected at low lipid concentrations (high P:L ratio) (FIG V.10B). A similar behaviour has been recently reported for the antimicrobial peptide omiganan and has been attributed to a membrane saturation process: at low phospholipid concentration, membrane saturation may occur when the bound peptide concentration, hypothetically dictated by K_p, is higher than what the membrane can accommodate (Melo 2007); under these conditions, interaction changes may occur, as has also been described for other AMPs upon the crossing threshold P/L ratios (Huang 2000 and 2006).
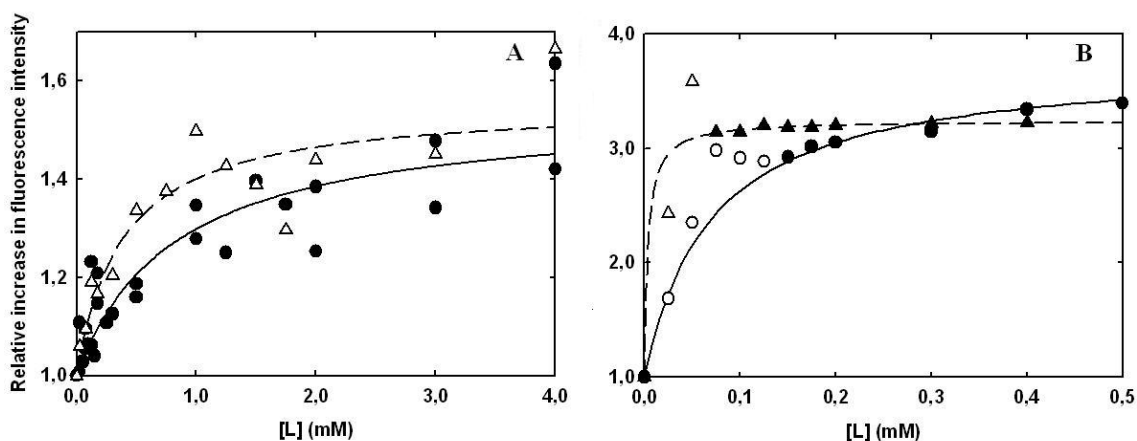

Figure V.10 Lipid titrations of 15 μM BP100 with different LUV systems. Lines represent the fitting parameters of the data to the partition model in Eq. V.1. (*A*) Neutral systems; POPC (●, *solid line*) and 2:1 POPC:cholesterol (△, *dashed line*) LUVs. (*B*) Anionic systems; 2:1 POPG:POPC (●, *solid line*) and 4:1 POPG:POPC (▲, *dashed line*) LUVs; deviations occurred at low lipid concentrations and those data points (*empty*) were removed from the fittings. The difference in the required amounts of lipid for the titrations in A and B indicates a much higher partition towards the anionic models; this is confirmed by the obtained partition constants. Fit parameters are summarized in Table V.5.

Membrane saturation was confirmed by titrating 2:1 POPG/POPC LUVs with BP100 in the presence of acrylamide while monitoring its fluorescence intensity (Figure V.11). Two different slopes were obtained for each *I* vs [*P*] curve. The first slope corresponds to a non-saturated state while the second one, which is similar to that of the curve in the absence of lipid, can be ascribed to a saturation of the system. The saturation points could be easily obtained from the breaks of the initial slopes of each titration curve. It was observed that the *I* vs [*P*] curve with [*L*]=125 μM had its saturation point close to [*P*]=17 μM (Figure V.11), which is slightly higher than the

peptide concentration that yielded an *I* vs [*L*] curve with a deviation maximum close to [*L*]=125 µM (Figure V.10B). This results supports the hypothesis that the deviations observed in the partition curves correspond to a saturation of the membrane.
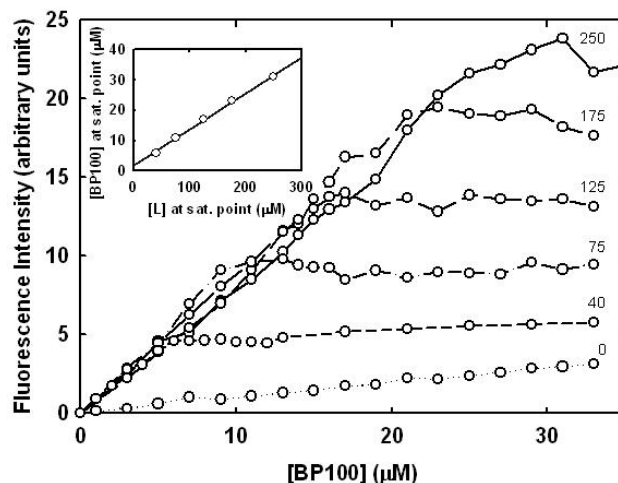

FIGURE V.11 Titration of several concentrations of 2:1 POPG:POPC LUVs with BP100 in the presence of 100 mM acrylamide (lipid concentration is indicated in µM for each set of points). Saturation points were identified from the breaks in each curve. Inset: linear dependence of the global peptide and lipid concentrations at the saturation points, fitted according to Equation V.2.

Further information from the saturation phenomenon was obtained by representing the saturation point ([*P*],[*L*]) pairs for the 2:1 POPG:POPC LUVs (Figure V.11 inset). This system followed Equation V.2 (Melo 2007), from which a K_p of 8.41 × 10^4 was obtained, being of the same order of magnitude than that determined from the partition curve using the model of Santos et al (Santos 2003) (3.08 × 10^4). In addition, the saturation P:L ratio (σ) was 0.118, which corresponds to 8.4 phospholipids per peptide directly in contact with the membrane at the saturation. Because there are 2/3 anionic phospholipids in the used system, there will be 5.6 negatively charged phospholipids per peptide at saturation. Interestingly, this number is very close to the expected charge of the peptide (+6) at pH 7.4, which suggests that electroneutrality is reached at the saturation of the system. The obtained value of σ is indicative of a high membrane coverage, stressing that a high peptide concentration in the membrane can be expected, and thus supporting the high value of K_p (8.41 × 10^4) obtained.

$$[P] = \frac{\sigma}{K_p \gamma_L} + \sigma[L] \quad \textbf{Equation V.2}$$

In order to study if BP100 concentration influences its interaction with the membrane, in-depth location studies were carried out at both saturated and non-saturated regimes. Stearic acid molecules labelled at different carbon positions (carbons 5 and 16 for 5- and 16-NS, respectively) with tyrosine quenching nitroxyl groups were used to probe the internalization of BP100 (Ferre 2007). There was no significant alteration in the tyrosine in-depth location upon saturation, indicating that most of BP100 molecules maintain their positioning within the membrane. The location of the tyrosine residue, approximately halfway across the membrane leaflet, is coherent with a relatively deep burying of the peptide if it adopts, as expected, a horizontally oriented α-helical structure (Badosa 2007). The lysines have the ability to snorkel and keep their charged amino groups near the headgroup region (Segrest 1990, Kandasamy and Larson 2006) while the hydrophobic side chains could go as far as the bilayer centre. This localization within the bilayer is likely responsible, at least in part, for the membrane destabilizing capabilities of BP100.

V.3.3 Membrane permeabilization studies

The BP100-induced permeabilization of model lipidic membranes was studied. Results showed that BP100 induced vesicle leakage in a dose-dependent manner (Figure V.12). Interestingly, a clear change of the permeabilization behaviour at ~15 μM petide concentration, toward a faster, sigmoidal, and more intense leakage kinetics—visible both in the permeabilization kinetics (Figure V.12) and in the leakage percentage profile at 390 s (Figure V.12 inset)—occurs very close to the peptide concentration expected to cause membrane saturation for the 125 μM lipid concentration. These results point out a clear change in a functional property of BP100 to induced leakage at high P:L ratios at, or close to, saturation. The high degree of peptide-induced leakage after saturation may reflect severe membrane damage or lysis, whereas the lower permeabilization before saturation could reflect a lesser destabilization of the membrane upon binding. Therefore, high P:L ratios close to saturation would then act as the trigger between these two states, and could be the biophysical parallel to the *in vivo* onset of antibacterial activity.
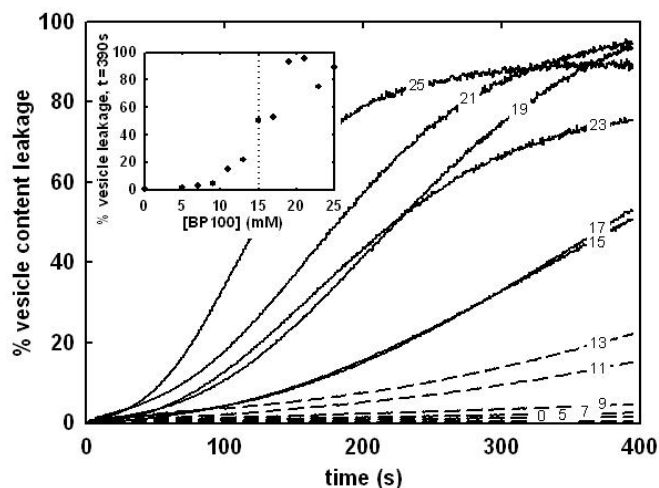
Figure V.12 Time course of BP100 induced vesicle leakage to Co^{2+} with 125 μM 2:1 POPG:POPC LUVs doped with 1% N-NBD-PE; each curve corresponds to a different BP100 concentration, indicated in the figure in μM. Dashed lines correspond to sub-saturation conditions. Inset: leakage percentage at 390 s in which a transition in behavior with BP100 concentration is evident; this transition occurs close to the expected membrane saturation point for the used lipid concentration, indicated by the dotted line.

V.3.4 Vesicle aggregation and surface charge studies

The net positive charge of BP100 together with its strong affinity toward negatively charged membranes suggests that bacterial charge neutralization could be expected at high P:L ratios. If charge neutralization occurs, the electrostatic repulsions are suppressed leading to vesicle aggregation, which can be followed by turbidity and light scattering measurements, as an increase of the optical density (OD) or as an increase of the average particle size, respectively.

Turbidity and light scattering results showed two different patterns depending on BP100 concentration and, similarly to the vesicle leakage studies, were associated to saturated and non-saturated states (Figure V.13 and Figure V.14). For 125 μM lipid (2:1 POPG/POPC LUV) and peptide concentration <15 μM, which correspond to a non-saturated state, no significant changes in turbidity and in the average particle size were observed. However, when membrane saturation occurs ($\geq$ 15μM) the OD of the solution increased until a plateau was reached, ~30 min after the addition of BP100, and the average particle size increases from 100 nm to > 1 μm. This increase of the OD and of the average particle size is likely due to vesicle aggregation induced under membrane saturation conditions. These results confirm the affinity of BP100 for negatively

charged membranes and reinforce the hypothesis that electroneutrality is reached at the membrane saturation point. This was further confirmed through ζ-potential measurements which showed that BP100 brings the LUV charge to approximate electroneutrality at saturation (Ferre 2009), confirming the prediction based on the saturation proportion. Indeed, we have recently reviewed that membrane neutralization can also be expected for several AMPs, taking into account the reported thershold ratios together with the global charge of the peptide and the used membrane model (Melo 2009).
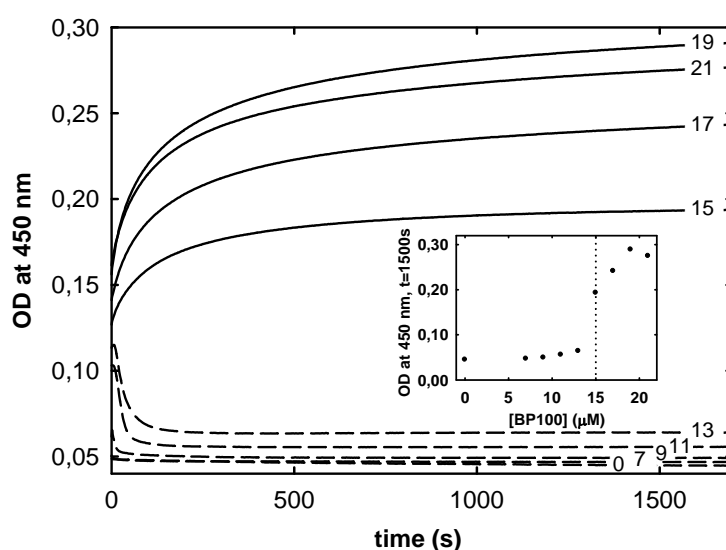
Figure V.13 Time course of BP100 induced OD change (λ=450 nm) of 125 μM 2:1 POPG:POPC LUVs; each curve corresponds to a different BP100 concentration, indicated in the figure in μM. Two different kinetic behaviors are evident. Dashed lines correspond to sub-saturation conditions. Inset: OD_{450} at 1500s. The transition in behavior is evident above 15 μM; as with vesicle leakage (Figure V.12) this transition occurs close to the expected membrane saturation point for the used lipid concentration, indicated by the dotted line.

Figure V.14 Normalized intensity distribution determined by dynamic light scattering of the particle sizes of a 125 μM 2:1 POPG:POPC LUV suspension in the presence of increasing BP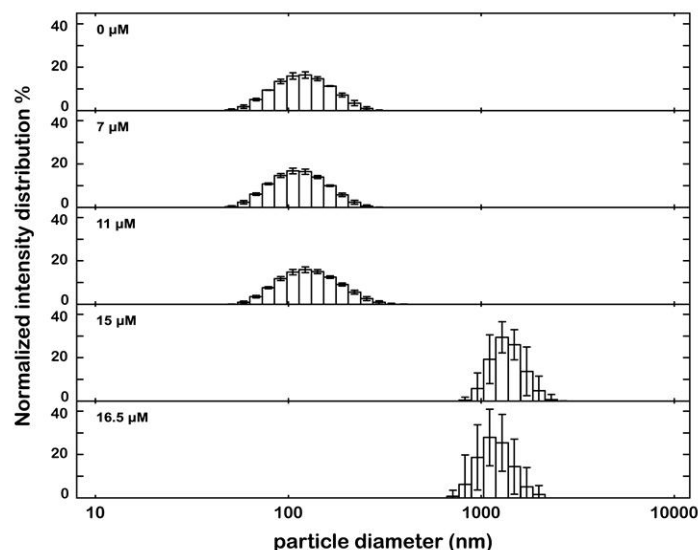100 concentrations (*error bars* represent SD). Above membrane saturation, which is expected around 15 μM BP100 at this lipid concentration, a significant increase in particle size and heterogeneity is observed, in agreement with the occurrence of vesicle aggregation. This result correlates with the observed distinct behavior of BP100 induced OD change below and above saturation (Figure V.12).

Despite these results, it must be taken into account that vesicle aggregation may not have a parallel *in vivo*, as bacterial membranes are protected by additional layers, such as LPS and peptidoglycan coats, preventing direct cytoplasmatic membrane contact between bacteria. However, membrane electroneutrality at saturation may be parallel *in vivo*, as the onset of antibacterial activity of BP100 could be correlated, among other disrupting effects, to the dissipation of the transmembrane potential essential for a thriving cell (Yeaman and Yount 2003).

V.3.5 Membrane translocation studies

Apart from membrane damage, intracellular targets have been reported to be involved in the killing mechanism of some AMPs (Yeaman and Yount 2003, Brodgen 2005, Hancock and Sahl 2006, Jenssen 2006, Nicolas 20099). In that context, the membrane translocation or penetration capability of AMPs has been demonstrated for an increasing number of AMPs (Henriques 2007). This observation has generated a recent controversy about which is the frontier between cell-penetratin peptides (CPPs) and AMPs, and if they belong to a unique class of compounds that has been proposed to

be termed either as membrane active peptides (MAP)s or cell-penetrating antimicrobial peptides (CP-AMP)s (Henriques 2006, Marcos 2008). In order to know if BP100 is able to penetrate bacterial cytoplasmatic membranes, translocation studies were carried out We devised a novel extremely simple method using MLVs which requires only that the peptide has intrinsic fluorescence and that its interaction kinetics with LUVs are significantly faster than its translocation kinetics (Ferre 2009).

Using this new method described in Ferre 2009, we determined the occurrence of translocation of BP100 at both high and low P:L ratios (saturated and nonsaturated states). Results clearly showed that BP100 unequivocally translocates at both tested P:L ratios (See Figure 5 in Ferre 2009).

The occurrence of translocation together with the permeabilization and membrane aggregation/neutralization assays constitutes a further proof of the membrane activity of BP100. Moreover, the ability of this peptide to translocate bacterial membrane systems suggests the possibility that its antimicrobial activity could also be exerted by the disruption of essential intracellular processes.

V.3.6 Partition, saturation, and prediction of MIC

The findings from the BP100-membrane interaction studies clearly stress the relevance of the membrane saturation phenomena therefore suggest that membrane saturation could also be highly related with its *in vivo* onset bactericidal activity. Therefore, the key question is: Is there a parallellsim between the threshold concentration to reach membrane saturation at the molecular level and the macroscopically observed MIC?. An excellent previous report about the membrane actions of omiganan gave some light on that question: A relation between saturation and MIC was deduced which reported the existence of a possible saturation-triggered antimicrobial mechanism (Melo 2007). For this peptide, MICs were found to be similar to the peptide threshold concentration needed to reach the saturation state. With these observations in mind, we further examined whether the biophysical results obtained were in also agreement with the experimental MIC values.

As previously reported by Melo et al., under typical bacterial titers and using the MIC as the total peptide concentration, the membrane-bound peptide concentration

([P]$_L$) is given by $K_P \times$ MIC. On the other hand, σ can be determined as [P]$_L \times \gamma_L$. Combining both expressions, the MIC can be readily calculated as:

$$MIC = \frac{\sigma}{K_P \gamma_L}$$ **Equation V.3**

This equation provides a correlation between the macroscopic parameter MIC with the molecular parameters K_P and the threshold concentration in the membrane (σ). Therefore, from Equation V.3 we can calculated the MIC values of BP100 from the obtained biophysical parameters and compare them with the obtained from the biological studies. Using the obtained σ (0.118) and K_P (3.08 $\times$ 10^4 or 8.41 $\times$ 10^4, from the partition and saturation studies, respectively) values, and considering γ_L as 0.763 M^{-1}, this equation leads to MIC values of 2 or 5 μM, depending on the selected K_P. These values are certaintly consistent with the antibacterial activity displayed by BP100, which inhibited *in vitro* growth of *E. amylovora*, *X. vesicatoria*, and *P. syringae* at 2.5-7.5 μM. In addition to validating the obtained values of K_P and σ, these results strongly support the correlation between these constants and the MIC, evidencing the importance of the saturation point in the mode of action of this peptide. It is important to stress that this equation provides molecular fundations to MIC which up to now has been used in a rather empirical way.

Moreover, in a recent review, we have surveyed reports of threshold events of AMPs and correlated them with properties such as bactericidal concentration and membrane binding. This supports our point of view that a high peptide membrane-bound concentration at, or close to, bilayer saturation is required for the mode of action of AMPs (Melo 2009).

Chapter VI. General conclusions

The present PhD dissertation has been devoted to: (i) the design and synthesis of short synthetic cecropin-melittin hybrid antimicrobial undecapeptides derived from Pep3 to be used as pesticides for the control of plant diseases caused by the economically important plant pathogenic bacteria *Erwinia amylovora*, *Pseudomonas syringae* pv. *syringae*, *Xanthomonas axonopodis* pv. *vesicatoria*, and the phytopathogenic fungi *Fusarium oxysporum*, *Aspergillus niger*, *Rhizopus stolonifer*, and *Penicillium expansum*; (ii) the study of the mode of action of the peptide with the best biological profile to understand its biological properties for its further improvement.

From the results of the first part the following conclusions can be derived:

Short antimicrobial undecapeptides with better biological properties than Pep3 can be tailored by modifying some fundamental parameters such as the charge, the overall hydrophobicity and amphipathicity. The modifications that resulted to influence the biological properties of Pep3 include the N-terminal derivatization, and the replacement of the residues located at positions 1 and 10 by amino acids with various degrees of hydrophilicity and hydrophobicity.

Combinatorial chemistry resulted to be an useful tool for lead optimization to identify peptides with an optimal biological profile in terms of antimicrobial and cytotoxictiy activities, and stability to protease degradation.

In general, peptides were more antibacterial than antifungal. *X. vesicatoria* resulted to be the most susceptible bacteria while *F. oxysporum* was the most sensitive fungi.

A basic N-terminus and a hydrophobic C-terminus are crucial to obtain peptides with high *in vitro* antibacterial activity and low cytotoxicity. Thus, the introduction of a Lys residue at postion 1 and an aromatic residue at position 10 provided antibacterial peptides with MIC values below 7.5 µM against the bacteria tested, while displaying low cytotoxicity.

Reduction of the cationic charge of Pep3 by derivatization of the N-terminus together with the introduction of hydrophobic residues at both the N- and the C-terminus provided peptides with high antifungal activity (MIC<12.5 µM)

The above structural modifications also led to peptides with a higher microbicidal effect and more stable to protease degradation than Pep3.

BP100 and BP22 resulted to be the best peptides preventing infections of *E. amylovora* in deatached flowers and of *P. expansum* in immature fruits, respectively. BP100 was only slightly less effective in flowers than streptomycin, which is the antibiotic currently used in fire blight control. Therefore, the application of this peptide during the bloom period of trees may offer a good perspective in future management of this disease. On the other hand, BP22 displayed an average efficacy of 56% disease reduction, being not significantly different than that of a commercial formulation of the reference fungicide imazalil.

The use of these peptides as pesticides can be considered safetey in terms of toxicity. BP15, BP21, and BP100 showed very low toxicity on acute oral toxicology in mice.

The second part led to the following conclusions:

Biophysical studies using model membranes are useful to rationalize the biological properties displayed by BP100.

The higher preference of this peptide to the bacterial model systems compared to the mammalian ones, shown by the obtained partition constants, was in agreement with its potent antibacterial activity and low cytotoxicity.

High membrane concentration of BP100 (possibly membrane saturation) correlated with bacterial death.

Three different potential causes of activity of AMP, i.e., Charge neutralization, permeabilization, and translocation were identified to be involved in AMP activity, being the first two dependent on peptide concentration. Peptide concentrations on the range of the observed MICs are required to membrane saturation which resulted to be crucial for membrane neutralization and high permeabilization. Clearly, these closely coupled events provide some insight into the antimicrobial mechanism adopted by BP100.

An equation which correlates the MIC of AMPs with partition constants and threshold concentrations in the membrane was deduced. This equation provides

molecular fundation of MIC and stresses the fact that a high peptide membrane-bound concentration is required for the mode of action of membrane active AMPs.

In summary, some of the peptides can be considered as potential agents for use in plant protection either as pesticide ingredients or expressed in transgenic plants. Moreover, these compounds represent a sustainable alternative to conventional antibiotics, especially for the treatment of drug-resistant infections in the fields of human, veterinary and plant disease control. The major challenge for their use as pesticide ingredients in food and agriculture is to minimize their cost production. In that sense, molecular farming of these peptides is currrently under development and evaluation.

References

Agrios, G.N. 2005. Plant Pathology, 5th ed., Elsevier Academic Press, London.

Alan, A.R., E.D. Earle. 2002. Sensitivity of bacterial and fungal plant pathogens to the lytic peptides, MSI-99, magainin II, and cecropin B. *Mol. Plant-Microbe Interact.* 15:701-708.

Ali, G.S., A.S. Reddy. 2000. Inhibition of fungal and bacterial plant pathogens by synthetic peptides: *in vitro* growth inhibition, interaction between peptides and inhibition of disease progression. *Mol. Plant-Microbe Interact.* 13:847-859.

Andreu, D., R.B. Merrifield, H. Steiner, H.G. Boman. 1983. Solid-phase synthesis of cecropin A and related peptides. *Proc. Natl. Acad. Sci. USA*. 80:6475-6479.

Andreu, D., J. Ubach, A. Boman, B. Wahlin, D. Wade, R.B. Merrifield, H.G. Boman. 1992. Shortened cecropin A-melittin hybrids. Significant size reduction retains potent antibiotic activity. *FEBS Lett.* 296:190-194.

Andreu, D. 2008. Bruce Merrifield's contribution to antimicrobial peptide research. *Biopolymers (Peptide Sci.)* 90:236-239.

Auvynet, C., Y. Rosentein. 2009. Multifunctional host defense peptides: Antimicrobial peptides, the small yet big players in innate and adaptive immunity. *FEBS J.* 276:6407-6508.

Badosa, E., R. Ferre, M. Planas, L. Feliu, E. Besalú, J. Cabrefiga, E. Bardají, E. Montesinos. 2007. A library of linear undecapeptides with bactericidal activity against phytopathogenic bacteria. *Peptides* 28:2276-2285.

Badosa, E., R. Ferre, J. Francés, E. Bardají, L. Feliu, M. Planas, E. Montesinos. 2009. Sporicidal activity of synthetic antifungal undecapeptides and control of Penicillium rot of apples. *Appl. Environ.Microbiol.* 75:5563-5569.

Bangham, A.D., M.M. Standish, J.C. Watkins. 1965. Diffusion of univalent ions across lamellae of swollen phospholipids. *J. Mol. Biol*. 13:238-252.

Bannwarth, W., B. Hinzen. 2006. Combinatorial chemistry: from theory to application, 2on Ed., Wiley-VCH, Weinheim.

Bechinger, B. 2004. Structure and function of membrane-lytic peptides. *Crit. Rev. Plant. Sci*. 23:271-92.

Blondelle, S.E., K. Lohner. 2000. Combinatorial libraries: a tool to design antimicrobial and antifungal peptide analogues having lytic specificities for structure-activity relationship studies. *Biopolymers* 55:74-87.

Bhargava, A., M. Osusky, R.E.W. Hancock, B.S. Forward, W.W. Kay, S. Misra. 2007. Antiviral indolicidin variant peptides: evaluation for broad-spectrum disease resistance in transgenic *Nicotiana tabacum*. *Plant Sci.* 172:515-523.

Bonaterra, A., M. Mari, L. Casalini, E. Montesinos. 2003. Biological control of *Monilinia laxa* and *Rhizopus stolonifer* in postharvest of stone fruit by *Pantoea agglomerans* EPS125 and putative mechanisms of antagonism. *Int. J. Food Microbiol.* 84:93-104.

Boman, H.G., D. Wade, I.A. Boman, B. Wahlin, R.B. Merrifield. 1989. Antibacterial and antimalarial properties of peptides that are cecropin-melittin hybrids. *FEBS Lett.* 259:103-106.

Boman, H.G. 2003. Antibacterial peptides: basic facts and emerging concepts. *J. Intern. Med.* 254:197-215.

Brodgen, K.A., M. Ackermann, P.B. McCray Jr., B.F. Tack. 2003. Antimicrobial peptides in animals and their role in host defences. *Int. J. Antimicrob. Agents* 22:465-478.

Brodgen, K.A. 2005. Antimicrobial peptides: pore formers or metabolic inhibitors in bacteria? *Nat. Rev. Microbiol.* 3:238-250.

Broekaert, W.F., B.P.A. Cammue, M.F.C. DeBolle, K. Thevissen, G.W. De Samblanx, R.W. Osborn. 1997. Antimicrobial peptides from plants. *Crit. Rev. Plant Sci.* 16:297-323.

Bulet, P., C. Hetru, J-L. Dimarcq, D. Hoffmann. 1999. Antimicrobial peptides in insects; structure and function. *Devel. Com. Immunol.* 23:329-344.

Bulet, P., R. Stöcklin, L. Menin. 2004. Antimicrobial peptides: from invertebrates to vertebrates. *Immunol. Rev.* 198:169-184.

Cabrefiga, J., E. Montesinos. 2005. Analysis of aggressiveness of *Erwinia amyolovora* using disease-dose and time relationships. *Phytopathology* 95:1430-1437.

Campbell, C.L., L.V. Madden. 1990. Introduction to plant disease epidemiology. Wiley & Sons, New York.

Carpino, L.A., G.Y. Han. 1970. 9-Fluorenylmethoxycarbonyl function, a new base-sensitive amino-protecting group. *J. Am. Chem. Soc.* 92:5748-5749.

Cavallarin, L., D. Andreu, B. San Segundo. 1998. Cecropin A-derived peptides are potent inhibitors of fungal plant pathogens. *Mol. Plant-Microbe Interact.* 11:218-227.

Cooter, P.D., C. Hill, P. Ross. 2005. Bacterial lantibiotics: strategies to improve therapeutic potential. *Curr. Prot. Pept. Sci.* 6:61-75.

DeLucca A.J., T.J. Walsh. 1999. Antifungal peptides: novel therapeutic compounds against emerging pathogens. *Antimicrob. Agents Chemother*. 43:1-11.

Denning, W. 1974. On the decay of apple trees. *New York Society for the Promotion of Agricultural Arts and Manufactures Transaction 2*:219-222.

Epand, R.M., H.J. Vogel. 1999. Diversity of antimicrobial peptides and their mechanisms of action. *Biochim. Biophys. Acta* 1462:11-28.

Epple, P., K. Apel, H. Bohlmann. 1997. Overexpression of an endogenous thionin enhances resistance of Arabidopsis against *Fusarium oxysporum. Plant Cell* 9:509-520.

Falla, T.J., R.E.W. Hancock. 1997. Improved activity of a synthetic indolicidin analog. *Antimicrob. Agents. Chemother*. 41:771-775.

FAO. 2009. The State of Food Insecurity in the World. Economic crises – impacts and lessons learned. *Food and Agricultural Organization of the United Nations*. Rome

Ferre, R., E. Badosa, L. Feliu, M. Planas, E. Montesinos, E. Bardají. 2006. Inhibition of plant-pathogenic bacteria by short synthetic cecropin A-melittin hybrid peptides. *Appl. Environ. Microbiol*. 72:3302-3308.

Ferre, R., M.N. Melo, A.D. Correia, L. Feliu, E. Bardají, M. Planas, M. Castanho. 2009. Synergistic effects of the membrane actions of cecropin-melittin antimicrobial hybrid peptide BP100. *Biophys. J*. 96:1815-1827.

Fleming, A. 1929. On the antibacterial action of cultures of *Penicillium* with special reference to their use in the isolation of *B. influenzae. British J. of Exper. Pathol*. 10:226-236.

Ganz, T., R.I. Lehrer. 1998. Antimicrobial peptides of vertebrates. *Curr. Opin. Immunol.* 10:41-44

García-Olmedo, F., A. Molina, J.M. Alamillo, P. Rodríguez-Palenzuela. 1998. Plant defense peptides. *Biopolymers* 47:479-491.

Gonzalez, C.F., E.M. Provin, L. Zhu, D.J. Ebbole. 2002. Independent and synergistic acdtivity of synthetic peptides against thiabendazole-resistant *Fusarium sambucinum. Phytopathology* 92:917-924.

Habermann, E. 1972. Bee and wasp venoms. *Science* 177:314-322.

Hancock, R.E.W. 2001. Cationic peptides: effectors in innate immunity and novel antimicrobials. *Lancet Infect. Dis*. 1:156-164.

Hancock, R.E.W., A. Patrzykat. 2002. Clinical development of cationic antimicrobial peptides: from natural to novel antibiotics. *Curr. Drug Targets Infect. Disord*. 2:79-83.

Hancock R.E.W., A. Rozek. 2002. Role of membrane in the activities of antimicrobial cationic peptides. *FEMS Microbiol. Lett*. 206:143-149.

Hancock, R.E.W., K.L. Brown, N. Mookherjee. 2006. Host defence peptides from invertebrates – emerging antimicrobial strategies. *Immunobiology* 211:315-322.

Hancock, R.E.W., H.G. Sahl. 2006. Antimicrobial and host-defense peptides as new anti-infective therapeutic strategies. *Nat. Biotechnol.* 24:1551-1557.

Henriques, S.T., M.A.R.B. Castanho. 2004. Consequences of nonlytic membrane perturbation to the translocation of the cell penetrating peptide Pep-1 in lipidic vesicles. *Biochemistry* 43:9716-9724.

Henriques, S.T., M.N. Melo, M.A.R.B. Castanho. 2006. Cell-penetrating peptides and antimicrobial peptides: how different are they? *Biochem. J.* 399:1-7.

Henriques, S.T., M.N. Melo, M.A.R.B. Castanho. 2007. How to address CPP and AMP translocation? Methods to detect and quantify peptide internalization *in vit*ro and *in vivo. Mol. Membr. Biol*. 24:173-184.

Hong, S.Y., J.E. Oh, K-H. Lee. 1999. Effect of D-amino acid substitution on the stability, the secondary structure and the activity of membrane-active peptide. *Biochim. Pharmacol*. 58:1775-1780.

Hoskin, D.W., A. Ramamoorthy. 2008. Studies on anticancer activities of antimicrobial peptides. *Biochim. Biophys. Acta*. 1778:357-375.

Huang, H.W. 2000. Action of antimicrobial peptides: two-state model. *Biochemistry* 39:8347-8352.

Huang, H.W. 2006. Molecular mechanism of antimicrobial peptides: The origin of cooperativity. *Biochim. Biophys. Acta* 1758:1292-1302.

Hutlmark, D. H. Steiner, T. Rasmunson, H.G. Boman. 1980. Insect immunity. Purification and properties of three inducible bactericidal proteins from hemolymph of immunized pupae of *Hyalophora cecropia. Eur. J. Biochem*. 106:7-16.

Hultmark, D., A. Engstrom, H. Bennich, R. Kapur, H.G. Boman. 1982. Insect immunity: isolation and structure of cecropin D and four minor antibacterial components from *cecropia pupue. Eur. J. Biochem*. 106:7-16.

Isidro-Llobet, A., M. Alvarez, F. Albericio. 2009. Amino acid-protecting groups. *Chem. Rev.* 109:2455-2504.

Iwanaga, S., B.L. Lee. 2005. Recent advances in the innate immunity of invertebrate animals. *J. Biochem. Mol. Biol.* 38:128-150

Jaynes, J.M. et al. 1993. Expression of a cecropin-B lytic peptide analog in transgenic tobacco confers enhanced resistance to bacterial wilt caused by *Pseudomonas solanacearum*. *Plant Sci.* 89:43-53.

Jenssen, H., P. Hamill, R.E.W. Hancock. 2006. Peptide antimicrobial agents. *Clin. Microbiol. Rev.* 19:491-511.

Kamysz, W., A. Krolicka, K. Bogucka, T. Ossowski, J. Lukasiak, E. Lojkowska. 2005. Antibacterial activity of synthetic peptides against plant pathogenic *Pectobacterium* species. *J. Phytopathol.* 153:313-317.

Kandasamy, S.K., R.G. Larson. 2006. Molecular dynamics simulations of model trans-membrane peptides in lipid bilayers: a systematic investigation of hydrophobic mismatch. *Biophys. J.* 90:2326-2343.

Karabelas, A.J., K.V. Plakas, E.S. Solomou, V. Drossou, D.A. Sarigiannis. 2009. Impact of European legislation on marketed pesticides – A view from the standpoint of health impact assessment studies. *Environ. Int.*. 35:1096-1107.

Kates, S.A., F. Albericio. 2000. Solid-phase synthesis a practical guide. Marcel Dekker, Inc. New York.

Kruszewska, D., H.G. Sahl, G. Bierbaum, U. Pag, S.O. Heynes, A. Ljungh. 2004. Mersacidin eradicates methicillin-resistant *Staphylococcus aureus* (MRSA) in a mouse rhinitis model. *J. Antimicrob. Chemother.* 54:648-653.

Lai, Y., R.L. Gallo. 2009. AMPed up immunity: how antimicrobial peptides have multiple roles in immune defense. *Trends. Immunol.* 30:131-141.

Lazo, J.S., P. Wipf. 2000. Combinatorial chemistry and contemporary pharmacology. *J. Pharmacol. Exp. Ther.* 293:705-709.

Lee, D.G., J.H. Park, S.Y. Shin, S.G. Lee, M.K. Lee, K.S. Hahm. 1997. Design of novel analogue peptides with potent fungicidal but low hemolytic activity based on the cecropin A-melittin hybrid structure. *Biochem. Mol. Biol. Int.* 43:489-498.

Lee, D.G., K.S. Hahm, S.Y. Shin. 2004. Structure and fungicidal activity of a synthetic antimicrobial peptide, P18, and its truncated peptides. *Biotechnol. Lett.* 26:337-341.

Leontiadou, H., A.E. Mark, S.J. Marrink. 2006. Antimicrobial peptides in action. *J. Am. Chem. Soc.* 128:12156-12161.

Leyns, F., M. De Cleene, J. Swings, J. De Ley. 1984. The host range of the genus *Xanthomonas*. *Bot. Rev.* 50:305-355.

Li, Q.S., C.B. Lawrence, H.M. Davies, N.P.Everett. 2002. A tridecapeptide possesses both antimicrobial and protease-inhibitory activities. *Peptides* 23:1-6.

Loper, J.E., M.D. Henkels, R.G. Roberts, G.G. Grove, M.J. Willet, T.J. Smith. 1991. Evaluation of streptomycin, oxytetracycline and copper resistance of *Erwinia amylovora* isolated from pear orchards in Washington state. *Plant Dis*. 75:287-290.

López-García, B., E. Perez-Payá, J.F. Marcos. 2002. Identification of novel hexapeptides bioactive against phytopathogenic fungi through screening of synthetic peptide combinatorial libray. *Appl. Environ. Microbiol*. 68:2453-2460.

Ludtke, S.J. et al. 1996. Membrane pores induced by magainin. *Biochemistry*. 35:13723-13728.

Marcos J.F., A. Muñoz, E. Perez-Payá, S. Misra, B. López-García. 2008. Identification and Rational design of novel antimicrobial peptides for plant protection. *Annu. Rev. Phytopathol*. 46:273-301.

Margni, M., D. Rossier, P. Crettaz, O. Jolliet. 2002. Life cycle impact assessment of pesticides on human health and ecosystems. *Agric. Ecosyst. Environ*. 93:379-392.

Marr, A.K.; W.J. Gooderham, R.E.W. Hancock. 2006. Antibacterial peptides for therapeutic use: obstacles and realistic outlook. *Current Opin. Phamacol*. 6:468-472.

Mason, A.J., A. Marquette, B. Bechinger. 2007. Zwitterionic phopholipids and sterols modulate antimicrobial peptide-induced membrane destabilization. *Biophys. J*. 93:4289-4299.

Matsuyama K., S. Natori. 1988. Purification of 3 antibacterial proteins from the culture-medium of NIH-SAPE-4, an embryonic-cell line of *Sarcophaga-peregrina*. *J. Biol. Chem*. 263:17112-17116

Matsuzaki, K. 2009. Control of cell selectivity of antimicrobial peptides. *Biochim. Biophys. Acta* 1788:1687-1692.

Mattick, A.T., A. Hirsch. 1947. Further observations on an inhibitory substance (nisin) from lactic streptococci. *Lancet* ii:5-7.

Mazzola, P.G., T.C. Vessoni, A.M. Martins. 2003. Determination of decimal reduction time (D value) of chemical agents used in hospitals for desinfection purposes. *BMC Infect. Dis*. 3:24.

McManus, P.S., V.O. Stockwell, G.W. Sundin, A.L. Jones. 2002. Antibiotic use in plant agriculture. *Annu. Rev. Phytopathol*. 40:443-465.

Melo, M.N., M.A.R.B. Castanho. 2007. Omiganan interaction with bacterial membranas and cell wall models. Assigning a biological role to saturation. *Biochim. Biophys. Acta* 1768:1277-1290.

Melo, M.N., R. Ferre, M.A.R.B. Castanho. 2009. Antimicrobial peptides: linking partition, activity and high membrane-bound concentrations. *Nat. Rev. Microbiol*. 7:245-250.

Merrifield, R.B. 1963. Solid phase peptide synthesis 1. Synthesis of a tetrapeptide. *J. Am. Chem. Soc*. 85:2149-2154.

Merrifield, R.B. 1986. Solid phase synthesis. *Science* 232:341-347.

Mills, D., F.A. Hammerschlag, R.O. Nordeen, L.D. Owens. 1994. Evidence for breakdown of cecropin-B by proteinases in the intercellular fluid of peach leaves. *Plant Sci.* 104:17-22.

Miranda, L.P., P.F. Alewood. 2000. Challenges for protein chemical synthesis in the 21st century: bridging genomics and proteomics. *Biopolymers* 55:217-226.

Monroc, S., E. Badosa, E. Besalú, M. Planas, E. Bardaji, E. Montesinos, L. Feliu. 2006. Improvement of cyclic decapeptides against plant pathogenic bacteria using a combinatorial chemistry approach. *Peptides* 27:2575-2584.

Moragrega, C., I. Llorente, C. Manceau, E. Montesinos. 2003. Susceptibility of European pear cultivars to *Pseudomonas syringae* pv. *syringae* using immature fruit and deatached leag assays. *Eur. J. Plant Pathol*. 109:319-326.

Montesinos, E., P. Malgarejo, M.A. Cambra, J. Pinochet. 2000. Enfermedades de los frutales de pepita y hueso. Ediciones Mundi Prensa, Barcelona.

Montesinos, E. 2007. Antimicrobial peptides and plant disease control. *FEMS Microbiol. Lett.* 270:1-11.

Montesinos, E., E. Bardají. 2008. Synthetic antimicrobial peptides as agricultural pesticides for plant-disease control. *Chem. Biodivers*. 5:1225-1237.

Muñoz, A., B. López-Gárcia, E. Pérez-Payá, J.F. Marcos. 2007. Antimicrobial properties of derivatives of the cationic tryptophan-rich hexapeptide PAF26. *Biochim. Biophys. Res. Commun.* 354:172-177.

Nagle, J.F., M.C. Wiener. 1988. Structure of fully hydrated bilayer dispersions. *Biochim. Biophys. Acta* 942:1-10.

Ng, T.B. 2004. Peptides and proteins from fungi. *Peptides* 25:1055-1073.

Nicolas, P. 2009. Multifunctional host defense peptides: intracellular-targeting antimicrobial peptides. *FEBS J.* 276:6483-6496.

Nordeen, R.O, S.L. Sinden, J.M. Jaynes, L.D. Owens. 1992. Activity of Cecropin SB37 against protoplasts from several plant-species and their bacterial pathogens. *Plant Sci.* 82:101-107.

Oh, D., et al. 2000. Role of the hinge region and the tryptophan residue in the synthetic antimicrobial peptides, cecropin A(1-8)-magainin 2(1-12) and its analogues, on their antibiotic activities and structures. *Biochemistry* 39:11855-11864.

Osusky M., L. Osuska, R.E.W. Hancock, W. Kay, S. Misra. 2004. Transgenic potatoes expressing a novel cationic peptide are resistant to late blight and pink rot. *Transgenic Res*. 13:181-90.

Osusky M., L. Osuska, W. Kay, S. Misra. 2005. Genetic modification of potato against microbial diseases: *in vitro* and *in planta* activity of a dermaseptin B1 derivate, MsrA2. *Theor. Appl. Genet.* 111:711-722.

Otvos Jr., L. 2000. Antibacterial peptides isolated from insects. *J. Peptide Sci.* 6:497-511.

Peschel A, H.G. Sahl. 2006. The co-evolution of host cationic antimicrobial peptides and microbial resistance. *Nat. Rev. Microbiol*. 4:529-36.

Piers, K.L., R.E. Hancock. 1994. The interaction of a recombinant cecropin/meittin hybrid peptide with the outer membrane of Pseudomonas aeruginosa. *Mol. Microbiol*. 12:951-958.

Pouny, Y., D. Rapaport, A. Mor, P. Nicolas, Y. Shai. 1992. Interaction of antimicrobial dermaseptin and its fluorescently labeled analogues with phopholipid membranes. *Biochemistry* 31:12461-12423.

Raghuramann, H., A. Chattopadhyay. 2007. Melittin: a membrane-active peptide with diverse functions. *Biosci. Rep.* 27:189-223.

Rao, A.G. 1999. Conformation and antimicrobial activity of linear derivates of tachyplesin lacking disulfide bonds. *Arch. Biochem. Biophys*. 361:127-134.

Reed, J.D., D.L. Edwards, C.F. Gonzalez. 1997. Synthetic peptide combinatorial libraries: a method for the identification of bioactive peptides against phytopathogenic fungi. *Mol. Plant-Microbe Interact*. 10:537-549.

Rozek, A., J.-P.S. Powers, C.L. Friedrich, R.E.W. Hancock. 2003. Structure-based design of an indolicidin peptide analogue with increased protease stability. *Biochemistry* 42:14130-14138.

Russell, A.D., W.D. Hugo, G.A.J. Ayliffe. 1982. Principles and practice of desinfection, preservation and sterilization. Blackwell Science, Oxford, United Kingdom.

Santos, N.C., M.A.R.B. Castanho. 2002a. Lipossomas: a bala magica acertou?. *Quim. Nova*. 25:1-5.

Santos, N.C., M.A.R.B. Castanho. 2002b. Fluorescence spectroscopy methodologies on the study of proteins and peptides. On the 150th anniversary of protein fluorescence. *Trends Appl. Spectrosc*. 4:113-125.

Santos, N.C., M. Prieto, M.A.R.B. Castanho. 2003. Quantifying molecular partition into model systems of biomembranes: an emphasis on optical spectroscopic methods. *Biochim. Biophys. Acta* 942:1-10.

Sanzani, S.M., A. De Girolamo, L. Schena, M. Solfrizzo, A. Ippolito, A. Visconti. 2009. Control of *Penicillium expansum* and patulin accumulation on apples by quercetin and umbelliferone. *Eur. Food Res. Technol*. 228:381-389.

Sato, H., J.B. Feix. 2006. Peptide-membrane interactions and mechanisms of membrane destruction by amphipathic α-helical antimicrobial peptides. *Biochim. Biophys. Acta* 1758:1245-1256.

Segrest, J.P., H. De Loof, J.G. Dohlman, C.G. Brouillete, G.M. Anantharamaiah. 1990. Amphipathic helix motif: classes and properties. *Proteins* 8:103-117.

Sengupta, D., H. Leontiadou, A.E. Mark, S.J. Marrink. 2008. Toroidal pores formed by antimicrobial peptides show significant disorder. *Biochim. Biophys. Acta* 10:2308-2317.

Shai Y. 2002. Mode of action of membrane active antimicrobial peptides. *Biopolymers*. 66:236-48.

Steiner, H., D. Hultmark, A. Engstrom, H. Bennich, H.G. Boman. 1981. Sequence and specificity of two antibacterial proteins involved in insect immunity. *Nature* 292:246-248.

Strange, R.N, P.R. Scott. 2005. Plant disease: a threat to global food security. *Annu. Rev. Phytopathol.* 43:83-116.

Sundin, G.W., C.L. Bender. 1993. Ecological and genetic analysis of copper and streptomycin resistance in *Pseudomonas syringae* pv. *syringae*. *Appl. Environ. Microbiol*. 59:1018-1024.

Thompson, S.V. 1986. The role of stigma in fire blight infection. *Phytopathology* 76:476-482.

Tincu, J.A., S.W. Taylor. 2004. Antimicrobial peptides from marine invertebrates. *Antimicrob. Agents Chemother*. 48:3645-3654.

Tossi, A., L. Sandri, A. Giangaspero. 2000. Amphipathic, α-helical antimicrobial peptides. *Biopolymers* 55:4-30

Valeur, E., M. Bradley. 2009. Amide bond formation: beyond the myth of coupling reagents. *Chem. Soc. Rev*. 38:606-631.

Van der Zwet, T., H.L. Keil. 1979. Fire blight, a bacterial disease of rosaceous plants. USDA *Agricultural Handbook*. 510. Washington, DC: Science and Education Administration USDA.

Van der Zwet, T. 2002. Present worldwide distribution of fire blight. *Acta Hortic*. 590:33:34.

Van't Hof, W., E.C.I. Veerman, E.J. Helmerhorst, A.V.N. Amerongen. 2001. Antimicrobial peptides: properties and applicability. *Biol. Chem*. 382:597-619.

Vanneste, J. 2000. Fire blight: the disease and its causative agent *Erwinia amylovora*. CABI Publishing. New York.

Vidaver, A.K. 2002. Uses of antimicrobials in plant agriculture. *Clin. Infect. Dis*. 34:S107-S110.

Wade, D. et al. 1990. All D-amino acids-containing channel-forming antibiotic peptides. *Proc. Natl. Acad. Sci. USA* 87:4761-4765.

Wade, D., D. Andreu, S.A. Mitchell, A.M. Silveira, A. Boman. H.G. Boman, R.B. Merrifield. 1992. Antibacterial peptides designed as analogs or hybrids of cecropin and melittin. *Int. J. Pept. Protein Res*. 40:429-436.

Weidenbörner, M. 2001. Encyclopedia of food mycotoxins. Springer. Berlin, Germany.

Yang, L., T.A. Harroun, T.M. Weiss, L. Ding, H.W. Wang. 2001. Barrel-stave model or toroidal model? A case study on melittin pores. *Biophys. J*. 81:1475-1485.

Yeaman, M.R., N.Y. Yount. 2003. Mechanisms of antimicrobial peptide action and resistance. *Pharmacol. Rev*. 55:27-55.

Zaiou, Z., 2007. Multifunctional antimicrobial peptides: therapeutic targets in several human diseases. *J. Mol. Med.* 85:317-329.

Zasloff, M. 1987. Magainins, a class of antimicrobial peptides from Xenopus skin: isolation, characterization of two actives forms, and partial cDNA sequence of a precursor. *Proc. Natl. Acad. Sci. USA* 84:5449-5453.

Zasloff, M. 2002. Antimicrobial peptides of multicellular organisms. *Nature* 415:389-395.

Zhang, L., A. Rozek, R.E.W. Hancock. 2001. Interaction of cationic antimicrobial peptides with model membranes. *J. Biol. Chem*. 276:35714-35722.

Zhang, L., T.J. Falla. 2006. Antimicrobial peptides: therapeutic potential. *Expert Opin. Pharmacother.*7:653-66